PB95-212320

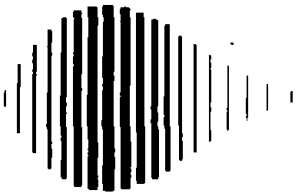

NATIONAL CENTER FOR EARTHQUAKE ENGINEERING RESEARCH
State University of New York at Buffalo

Experimental Verification of Acceleration Feedback Control Strategies for an Active Tendon System

by

S.J. Dyke, B.F. Spencer, Jr., P. Quast, M.K. Sain and D.C. Kaspari, Jr.
University of Notre Dame
Department of Civil Engineering and Geological Sciences
Notre Dame, Indiana 46556

and

T.T. Soong
State University of New York at Buffalo
Department of Civil Engineering
Buffalo, New York 14260

Technical Report NCEER-94-0024

August 29, 1994

This research was conducted at the University of Notre Dame and the State University of New York at Buffalo and was partially supported by the National Science Foundation under Grant No. BCS 90-25010 and the New York State Science and Technology Foundation under Grant No. NEC-91029.

REPRODUCED BY:
U.S. Department of Commerce
National Technical Information Service
Springfield, Virginia 22161

NOTICE

This report was prepared by the University of Notre Dame and the State University of New York at Buffalo as a result of research sponsored by the National Center for Earthquake Engineering Research (NCEER) through grants from the National Science Foundation, the New York State Science and Technology Foundation, and other sponsors. Neither NCEER, associates of NCEER, its sponsors, the University of Notre Dame and the State University of New York at Buffalo, nor any person acting on their behalf:

a. makes any warranty, express or implied, with respect to the use of any information, apparatus, method, or process disclosed in this report or that such use may not infringe upon privately owned rights; or

b. assumes any liabilities of whatsoever kind with respect to the use of, or the damage resulting from the use of, any information, apparatus, method or process disclosed in this report.

Any opinions, findings, and conclusions or recommendations expressed in this publication are those of the author(s) and do not necessarily reflect the views of the National Science Foundation, the New York State Science and Technology Foundation, or other sponsors.

50272-101

REPORT DOCUMENTATION PAGE	1. REPORT NO. NCEER-94-0024	2.	3. Re PB95-212320

4. Title and Subtitle
Experimental Verification of Acceleration Feedback Control Strategies for an Active Tendon System

5. Report Date
August 29, 1994

6.

7. Author(s) S.J. Dyke, B.F. Spencer, Jr., P. Quast
M.K. Sain, D.C. Kaspari, Jr. and T.T. Soong

8. Performing Organization Rept. No.

9. Performing Organization Name and Address
University of Notre Dame, Dept. of Civil Engineering and Geological Sciences, Notre Dame, Indiana 46556
State University of New York at Buffalo, Department of Civil Engineering, Buffalo, New York 14260

10. Project/Task/Work Unit No.

11. Contract(C) or Grant(G) No.
(C) BCS 90-25010
(G) NEC-91029

12. Sponsoring Organization Name and Address
National Center for Earthquake Engineering Research
State University of New York at Buffalo
Red Jacket Quadrangle
Buffalo, New York 14261

13. Type of Report & Period Covered
Technical Report

14.

15. Supplementary Notes This research was conducted at the University of Notre Dame and the State University of New York at Buffalo and was partially supported by the National Science Foundation under Grant No. BCS 90-25010 and the New York State Science and Technology Foundation under Grant No. NEC-91029.

16. Abstract (Limit: 200 words)

Most of the current active structural control strategies for aseismic protection have been based on either full-state feedback (i.e., structural displacements and velocities) or velocity feedback. However, accurate measurement of the displacements and velocities is difficult to achieve directly, particularly during seismic activity, since the foundation of the structure is moving with the ground. Because accelerometers can readily provide reliable and inexpensive measurements of the structural accelerations at strategic points on the structure, development of control methods based on acceleration feedback is an ideal solution to this problem. The purpose of this report is to demonstrate experimentally that stochastic control methods based on absolute acceleration measurements are viable and robust, and that they can achieve performance levels comparable to full-state feedback controllers.

17. Document Analysis a. Descriptors

b. Identifiers/Open-Ended Terms

Earthquake engineering. Active control systems. Acceleration feedback control.
Active tendon systems. Stochastic control. Absolute acceleration.

c. COSATI Field/Group

18. Availability Statement	19. Security Class (This Report)	21. No. of Pages
Release Unlimited	Unclassified	102
	20. Security Class (This Page) Unclassified	22. Price

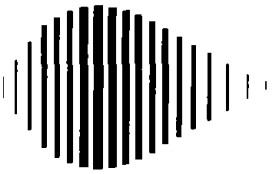

Experimental Verification of Acceleration Feedback Control Strategies for an Active Tendon System

by

S.J. Dyke[1], B.F. Spencer, Jr.[2], P. Quast[3], M.K. Sain[4], D.C. Kaspari, Jr.[1] and T.T. Soong[5]

August 29, 1994

Technical Report NCEER-94-0024

NCEER Task Number 93-5121

NSF Master Contract Number BCS 90-25010
and
NYSSTF Grant Number NEC-91029

1 Graduate Research Assistant, Department of Civil Engineering and Geological Sciences, University of Notre Dame
2 Associate Professor, Department of Civil Engineering and Geological Sciences, University of Notre Dame
3 Graduate Research Assistant, Department of Electrical Engineering, University of Notre Dame
4 Freimann Professor, Department of Electrical Engineering, University of Notre Dame
5 Samuel P. Capen Professor, Department of Civil Engineering, State University of New York at Buffalo

NATIONAL CENTER FOR EARTHQUAKE ENGINEERING RESEARCH
State University of New York at Buffalo
Red Jacket Quadrangle, Buffalo, NY 14261

PREFACE

The National Center for Earthquake Engineering Research (NCEER) was established to expand and disseminate knowledge about earthquakes, improve earthquake-resistant design, and implement seismic hazard mitigation procedures to minimize loss of lives and property. The emphasis is on structures in the eastern and central United States and lifelines throughout the country that are found in zones of low, moderate, and high seismicity.

NCEER's research and implementation plan in years six through ten (1991-1996) comprises four interlocked elements, as shown in the figure below. Element I, Basic Research, is carried out to support projects in the Applied Research area. Element II, Applied Research, is the major focus of work for years six through ten. Element III, Demonstration Projects, have been planned to support Applied Research projects, and will be either case studies or regional studies. Element IV, Implementation, will result from activity in the four Applied Research projects, and from Demonstration Projects.

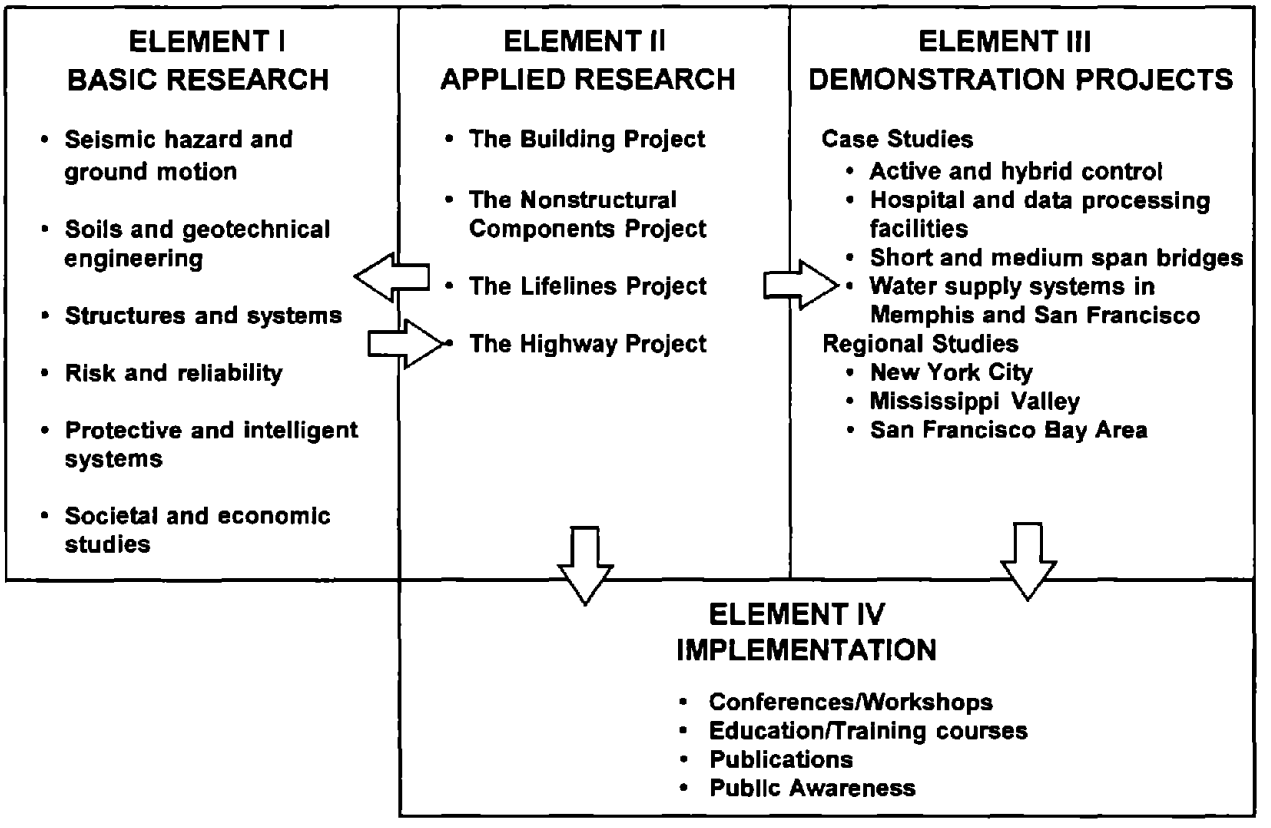

Research in the **Building Project** focuses on the evaluation and retrofit of buildings in regions of moderate seismicity. Emphasis is on lightly reinforced concrete buildings, steel semi-rigid frames, and masonry walls or infills. The research involves small- and medium-scale shake table tests and full-scale component tests at several institutions. In a parallel effort, analytical models and computer programs are being developed to aid in the prediction of the response of these buildings to various types of ground motion.

Two of the short-term products of the **Building Project** will be a monograph on the evaluation of lightly reinforced concrete buildings and a state-of-the-art report on unreinforced masonry.

The **protective and intelligent systems program** constitutes one of the important areas of research in the **Building Project**. Current tasks include the following:

1. Evaluate the performance of full-scale active bracing and active mass dampers already in place in terms of performance, power requirements, maintenance, reliability and cost.
2. Compare passive and active control strategies in terms of structural type, degree of effectiveness, cost and long-term reliability.
3. Perform fundamental studies of hybrid control.
4. Develop and test hybrid control systems.

This report details experimental verification of a class of active control strategies based on absolute acceleration feedback. Since accelerometers can provide inexpensive and reliable response measurements, control strategies based on these measurements are more practical and more easily implementable in comparison with full-state or velocity feedback strategies. The experiments were performed on a 1/4-scale tendon-controlled test structure using the shaking table facility at the University at Buffalo. Frequency domain optimal control strategies were employed to achieve the control objectives. The experimental results reported for the various control designs indicate that the acceleration-feedback controllers are robust and they can achieve performance levels comparable to full-state feedback controllers.

ABSTRACT

Most of the current active structural control strategies for aseismic protection have been based on either full-state feedback (i.e., structural displacements and velocities) or velocity feedback. However, accurate measurement of the displacements and velocities is difficult to achieve directly, particularly during seismic activity, since the foundation of the structure is moving with the ground. Because accelerometers can readily provide reliable and inexpensive measurements of the structural accelerations at strategic points on the structure, development of control methods based on acceleration feedback is an ideal solution to this problem. The purpose of this report is to demonstrate experimentally that stochastic control methods based on absolute acceleration measurements are viable and robust, and that they can achieve performance levels comparable to full-state feedback controllers.

ACKNOWLEDGMENT

This research is partially supported by National Science Foundation Grant No. BCS 93-01584 and by the Nationl Center for Earthquake Engineering Research Grant No. NCEER-93-5121. The experiments reported herein were conducted at the shaking table facility of the National Center for Earthquake Engineering Research. The assistance of Professor A.M. Reinhorn, Dr. R.C. Lin, Mr. M.A. Riley and Mr. M. Pitman in conducting the experiments is appreciated.

TABLE OF CONTENTS

LIST OF FIGURES

LIST OF TABLES

SECTION 1
INTRODUCTION

Recent trends toward building taller, more flexible structures have resulted in designs which are more vulnerable to severe dynamic loadings such as strong winds and earthquakes. At some point it may no longer be prudent to rely entirely on the strength of the structure and its ability to dissipate energy to withstand these extreme loads. Active control strategies for structural systems have been developed as one means by which to minimize the effects of these environmental loads (see Soong, 1990; Housner and Masri, 1990, 1993).

Most of the current active structural control strategies for aseismic protection have been based either on full-state feedback (*i.e.*, displacement and velocity measurements of the structure) or velocity feedback. Because displacements and velocities are not absolute, but dependent upon the inertial reference frame in which they are taken, their direct measurement at arbitrary locations on large-scale structures is difficult to achieve. Moreover, the ground and the foundation to which the structure is attached are moving during an earthquake, making control algorithms that are dependent on direct measurement of structural displacements and velocities impracticable. Alternatively, accelerometers can provide inexpensive and reliable measurements of the accelerations at strategic points on the structure, making the use of absolute structural acceleration measurements for determination of the control force an ideal way to avoid this problem.

In this report, the acceleration feedback control strategies previously developed by Spencer, *et al.* (1991, 1994a) for seismically excited structures are experimentally verified on a 1:4 scale, tendon-controlled, three-story, test structure at the National Center for Earthquake Engineering Research, SUNY-Buffalo. The system identification procedure employed to develop the mathematical models used in the control design is discussed herein, with particular emphasis placed on the incorporation of control-structure interaction effects. The resulting model is provided in the Appendix. Frequency domain optimal control strategies are employed to achieve the control objectives. A description of the hardware and software employed for the controller implementation is provided, including a discussion of the supervisory features designed to monitor operation of

the control system. The experimental results reported for the various control designs indicate that the controllers are robust and that full-state feedback performance can be effectively recovered using acceleration feedback control strategies.

SECTION 2
EXPERIMENTAL SETUP

Experimental verification of the acceleration feedback control strategies was performed on the 12 ft. × 12 ft. earthquake simulator at the National Center for Earthquake Engineering Research at SUNY-Buffalo. The test structure was the 1:4 scale model of a three-story building previously used by Chung, *et. al.* (1989) in state feedback experiments. The structural system consisted of the test structure, a hydraulic control actuator and a tendon/pulley system, as shown in Figures 2.1 and 2.2. The test structure had a weight of 6,250 lbs., distributed evenly among the three floors, and was 100 in. in height.

The hydraulic control actuator, four pretensioned tendons, and a stiff frame connecting the actuator to the cables were provided to apply control forces to the test structure. The four diagonal tendons transmitted the force from the control actuator to the first floor of the structure, and the steel frame connected the actuator to the tendons. Because hydraulic actuators are inherently open-loop unstable, a feedback control system was employed to stabilize the control actuator and improve its performance. This feedback signal included a combination of the position, velocity and pressure measurements. For this actuator, an LVDT (linear variable differential transformer), rigidly mounted to the piston, provided the displacement measurement, which was the primary feedback signal. This measurement was also sent through an analog differentiator to determine the velocity measurement, and a pressure transducer across the actuator piston provided the pressure measurement.

The structure was fully instrumented to provide for a complete record of the motions undergone by the structure during testing. Accelerometers positioned on each floor of the structure measured the absolute accelerations of the model, and an accelerometer located on the base measured the ground excitation, as shown in Fig. 2.1. The displacement of the actuator was measured using the LVDT mentioned above. Additional measurements were taken to evaluate the performance of the control system. Force transducers were located on each of the four tendons and their individual outputs were combined to determine the total force applied to the structure. Displace-

ment transducers on the base and on each floor were attached to a fixed frame (*i.e.*, not attached to the earthquake simulator) as shown in Fig. 2.1 to measure the absolute displacement of the structure and of the base. The relative displacements were determined by subtracting the base displacement from the absolute displacement of each floor.

Note that only acceleration measurements and the displacement of the actuator were employed in the control algorithms presented herein (see Fig. 2.1).

Implementation of the discrete controller was performed using the Spectrum Signal Processing Real-Time Digital Signal Processor (DSP) System. It is configured on a board that plugs into a 16-bit slot in a PC's expansion bus and features a Texas Instruments TMS320C30 Digital Signal Processor chip, RAM memory and on board A/D and D/A systems. An expansion I/O daughter board, which connects directly to the DSP board, provides an additional four channels of input and two channels of output. Thus, the computer controller employed herein can accommodate up to 6 inputs and 4 outputs. Additional daughter cards may be added to expand the system's I/O capabilities. With the high computation rates of the DSP chip and the extremely fast sampling and output capability of the associated I/O system, high overall sampling rates are achieved for the digital control system. Further discussion of the control implementation is provided in Spencer, *et al.*, 1994b; Quast, *et al.*, 1994 and in Section 5.

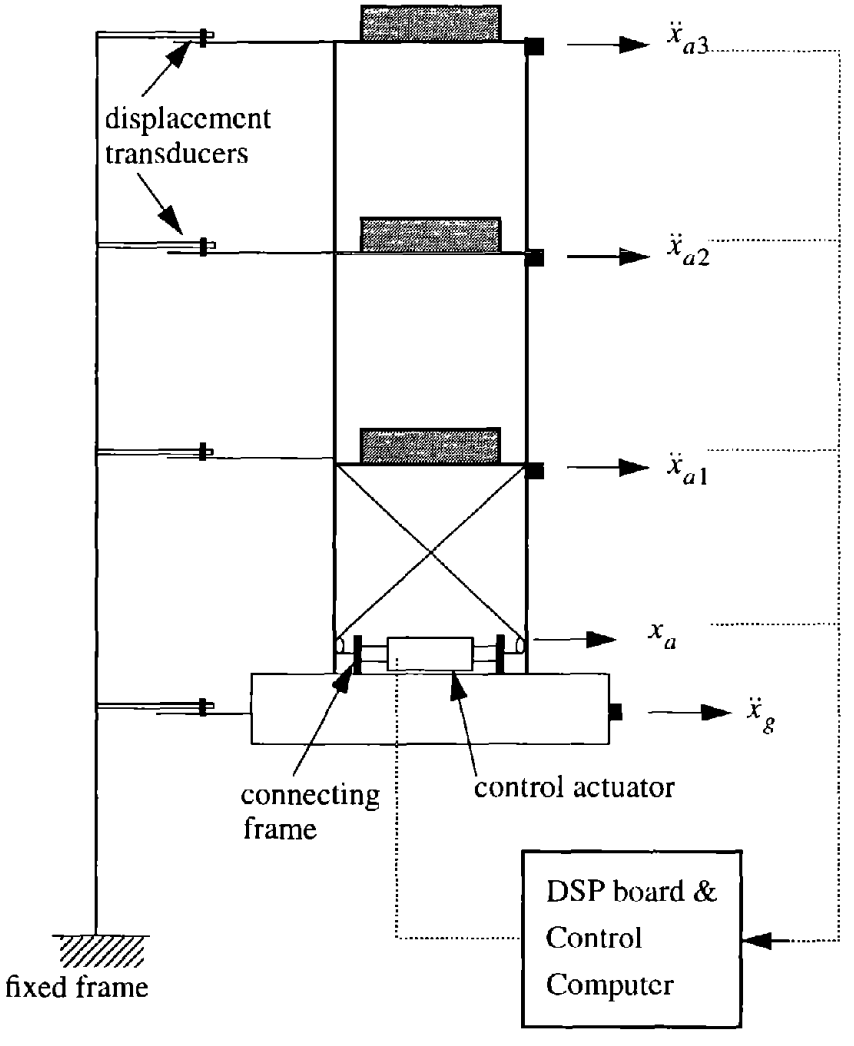

Figure 2.1 Schematic of Experimental Setup.

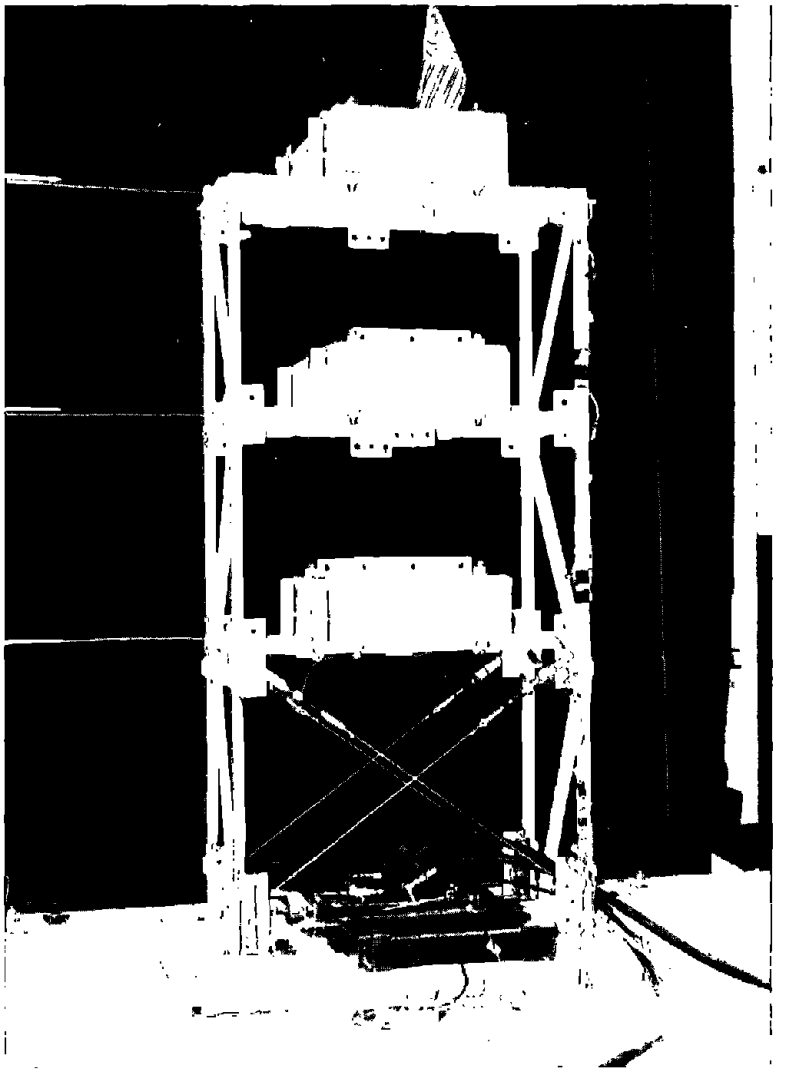

Figure 2.2 Three-Degree-of-Freedom Test Structure.

SECTION 3
SYSTEM IDENTIFICATION AND VALIDATION

One of the most important and challenging components of control design is the development of an accurate mathematical model of the structural system. There are several methods by which to accomplish this task. One approach is to analytically derive the system input/output characteristics by physically modeling the plant. Often this technique results in complex models that do not correlate well with the observed response of the physical system.

An alternative approach to developing the necessary dynamical model of the structural system is to measure the input/output relationships of the system and construct a mathematical model that can replicate this behavior. This approach is termed system identification in the control systems literature. The steps in this process are as follows: (i) collect high-quality input/output data (the quality of the model is tightly linked to the quality of the data on which it is based), (ii) compute the best model within the class of systems considered, and (iii) evaluate the adequacy of the model's properties.

System identification techniques fall into two categories: time domain and frequency domain. Time domain techniques such as the recursive least squares (RLS) system identification method (Friedlander, 1982) are superior when limited measurement time is available. Frequency domain techniques are generally preferred when significant noise is present in the measurements and the system is assumed to be linear and time invariant.

In the frequency domain approach to system identification, the first step is to experimentally determine the transfer functions (also termed frequency response functions) from each of the system inputs to each of the outputs. Subsequently, each of the experimental transfer functions is modeled as a ratio of two polynomials in the Laplace variable s and then used to determine a state space representation for the structural system. The frequency domain system identification approach will be employed herein for the development of a mathematical model of the structural system.

A block diagram of the structural system to be identified (*i.e.*, in Figs. 2.1 and 2.2) is shown in Fig. 3.1. The two inputs are the ground excitation $\ddot{x}_g$ and the command signal to the actuator u. The four measured system outputs include the actuator displacement x_a and the absolute accelerations, $\ddot{x}_{a1}$, $\ddot{x}_{a2}$, $\ddot{x}_{a3}$, of the three floors of the test structure. Thus, a 4×2 transfer function matrix (*i.e.*, eight input/output relations) must be identified to describe the characteristics of the system in Fig. 3.1.

3.1 Experimental Determination of Transfer Functions

Methods for experimental determination of transfer functions break down into two fundamental types: (i) swept-sine, and (ii) the broadband approaches using fast Fourier transforms (FFT). While both methods can produce accurate transfer function estimates, the swept-sine approach is rather time consuming, because it analyzes the system one frequency at a time.

The second approach estimates the transfer function simultaneously over a band of frequencies. The first step in the frequency domain approach is to independently excite each of the system inputs over the frequency range of interest. Exciting the system at frequencies outside this range is typically counter-productive; thus, the excitation should be band-limited (*e.g.*, pseudo-random, chirps, *etc.*). Assuming the two continuous signals (input, u, and output, y) are stationary, the transfer function is determined by dividing the cross-spectral density of the two signals by the autospectral density of the input signal (Bendat and Piersol, 1980) as in

$$H_{yu}(j\omega) = \frac{S_{uy}(\omega)}{S_{uu}(\omega)}. \tag{3.1}$$

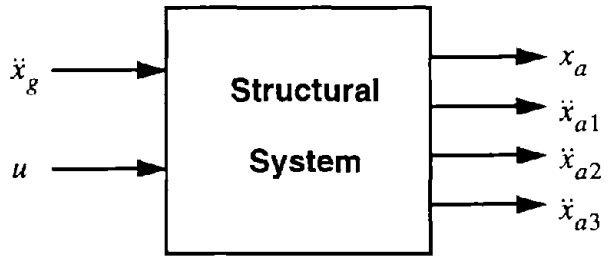

Figure 3.1 System Identification Block Diagram.

Experimental transfer functions are determined in a discrete sense. The continuous time records of the specified system input and the resulting responses are sampled at N discrete time intervals using an A/D converter, yielding the finite duration, discrete-time representations of each signal, $u(nT)$ and $y(nT)$, where T is the sampling period and $n = 0, 1 \ldots N$ is an integer representing the discrete time variable. A periodic representation of this signal (with period NT) is then formed as

$$u_p(nT) = \sum_{r=-\infty}^{\infty} u(nT + rNT). \tag{3.2}$$

An N-point FFT is performed on the periodic discrete-time signal to compute the discrete Fourier transform given by

$$U(jk\Omega) = \sum_{n=0}^{N-1} u_p(nT)\, W^{-nk}, \qquad k = 0, \ldots, N-1, \tag{3.3}$$

where $W = e^{2\pi j/N}$, $\Omega = \omega_s/N$, and ω_s is the sampling frequency (Antoniou, 1993). The discrete form of the autospectral density of each input signal and of the cross-spectral density of each pair of input and output signals are then determined by

$$S_{uu}(k\Omega) = cU^*(jk\Omega)\, U(jk\Omega) \tag{3.4}$$

$$S_{uy}(k\Omega) = cU^*(jk\Omega)\, Y(jk\Omega) \tag{3.5}$$

where c is a normalization constant defined as $c = T/N$, and '*' indicates the complex conjugate. For the discrete case, Eq. (3.1) can be written as

$$H_{yu}(jk\Omega) = \frac{S_{uy}(k\Omega)}{S_{uu}(k\Omega)}. \tag{3.6}$$

This discrete frequency transfer function can be thought of as a frequency sampled version of the continuous transfer function in Eq. (3.1).

In practice, one collection of samples of length N does not produce very accurate results. Better results are obtained by averaging the spectral densities of a number of collections of samples of the same length (Bendat and Piersol, 1980). Given that the number of collections of samples is M, the equations corresponding to (3.4) through (3.6) are

$$\bar{S}_{uu}(k\Omega) = \frac{1}{M}\sum_{i=1}^{M} S_{uu}^{i}(k\Omega) \tag{3.7}$$

$$\bar{S}_{uy}(k\Omega) = \frac{1}{M}\sum_{i=1}^{M} S_{uy}^{i}(k\Omega) \tag{3.8}$$

$$\bar{H}_{yu}(jk\Omega) = \frac{\bar{S}_{uy}(k\Omega)}{\bar{S}_{uu}(k\Omega)} \tag{3.9}$$

where S^i denotes the spectral density of the ith collection of samples and the overbar represents the ensemble average.

The quality of the resulting transfer functions is heavily dependent upon the specific manner in which the data are obtained and the subsequent processing. Three important phenomena associated with data acquisition and digital signal processing are aliasing, quantization error, and spectral leakage.

Aliasing

One way of eperimentally determining the frequency domain representation of a continuous signal is to sample the signal at discrete time intervals and perform an FFT on the resulting samples. According to Nyquist sampling theory, the sampling rate must be at least twice the largest significant frequency component present in the signal to obtain an accurate discrete representation of the signal (Bergland, 1969). If this condition is not satisfied, the frequency components above the Nyquist frequency ($f_c = 1/(2T)$, where T is the sampling period) are *aliased* to lower frequencies.

In reality, no signal is ideally bandlimited, and a certain amount of aliasing will occur in the sampling of any physical signal. To reduce the effect of this phenomenon, analog lowpass filters can be introduced prior to sampling to attenuate the high frequency components of the signal that would be aliased to lower frequencies. Since a transfer function is the ratio of the frequency domain representations of an output signal of a system to an input signal, it is important to use anti-aliasing filters with identical phase and amplitude characteristics for measuring both signals. Such phase/amplitude matched filters prevent incorrect information due to the filtering process from being present in the resulting transfer functions.

Quantization Error

Another effect which must be considered when measuring signals digitally is quantization error. An A/D converter can be viewed as being composed of a sampler and a quantizer. In sampling a continuous signal, the quantizer must truncate, or round, the value of the continuous signal to a digital representation in terms of a finite number of bits. The difference between the actual value of the signal and the quantized value is considered to be a noise which increases uncertainty in the resulting transfer functions. To minimize the effect of this noise, the truncated portion of the signal should be small relative to the actual signal. Thus, the maximum value of the signal should be as close as possible to, but not exceed, the full scale voltage of the A/D converter. If the maximum amplitude of the signal is known, an input amplifier can be incorporated before the A/D converter to accomplish this and thus reduce the effect of quantization. Once the signal is processed by the A/D system, it can be divided numerically in the data analysis program by the same ratio that it was amplified by at the input to the A/D converter to restore the original scale of the signal.

Spectral Leakage

To determine the frequency domain characteristics of a signal, a finite number of samples is acquired and an FFT is performed. This process introduces a phenomenon associated with Fourier analysis known as *spectral leakage* (Bergland, 1969; Harris, 1978). There are two approaches to

explain the source of spectral leakage. To describe the first, more intuitive approach, notice from Eq. (3.3) that the discrete Fourier transform is defined only at frequencies which are integer multiples of ω_s/N. If the signal contains frequencies which are not exactly on these spectral lines, the periodic representation of the signal in Eq. (3.2) will have discontinuities and the frequency domain representation of the signal is distorted. In the second description of spectral leakage, the finite duration discrete signal is considered be an infinite duration signal which has been multiplied by a rectangular window. This multiplication in the time domain is equivalent to a convolution of the frequency domain representations of the signal and the rectangular window. The Fourier transform of the rectangular window has a magnitude described by the function $\mathrm{Sinc}\,(fT)$ (where $\mathrm{Sinc}\,(fT) = \mathrm{Sin}\,(\pi fT) / (\pi fT)$). The result of this convolution is a distorted version of the Fourier transform of the original infinite signal.

A technique known as *windowing* is applied to minimize the amount of distortion due to spectral leakage. The sampled finite duration signal is multiplied by a function before the FFT is performed. This function, or window, is chosen with certain frequency domain characteristics to reduce the amount of distortion in the frequency domain.

A Tektronix 2630 Fourier Analyzer was used to determine the eight experimental transfer functions for the system shown in Fig. 3.1. This instrument greatly simplifies the tasks of obtaining and processing experimental data. Both analog and digital anti-aliasing filters are included in this instrument and adjustable input amplifiers for the A/D converters are provided to minimize the errors due to quantization. Various windowing options are available, including a Hanning window, which is recommended when a broadband excitation is used. Accurate experimental data are easily obtained if these features are understood and used properly.

The transfer functions from the ground acceleration to each of the measured responses were obtained by exciting the structure with a band-limited white noise ground acceleration (0-50 Hz) with the actuator and tendons in place and the actuator command set to zero. Similarly, the experimental transfer functions from the actuator command signal to each of the measured outputs

were determined by applying a bandlimited white noise (0-50 Hz) to the actuator command while the ground was held fixed.

Figures 3.2–3.4 show representative magnitude and phase plots for the experimentally determined transfer functions. All transfer functions were obtained using twenty averages. Figure 3.2 presents the transfer function from the ground acceleration $\ddot{x}_g$ to the first floor acceleration $\ddot{x}_{a1}$ (with the input to the control actuator set to zero). Note the three distinct, lightly-damped modes occurring in each of the transfer functions. These peaks occur at 2.33 Hz, 7.37 Hz, and 12.24 Hz and correspond to the first three modes of the structural system. Similarly, the experimental transfer function from the control command u to the first floor acceleration $\ddot{x}_{a1}$ (setting the input to the earthquake simulator to zero) is depicted in Fig. 3.3. Note the significant high frequency dynamics present; the magnitude of the transfer function at 40 Hz is as great as that corresponding to the building's primary modes. Clearly, these dynamic effects must be considered in the control design.

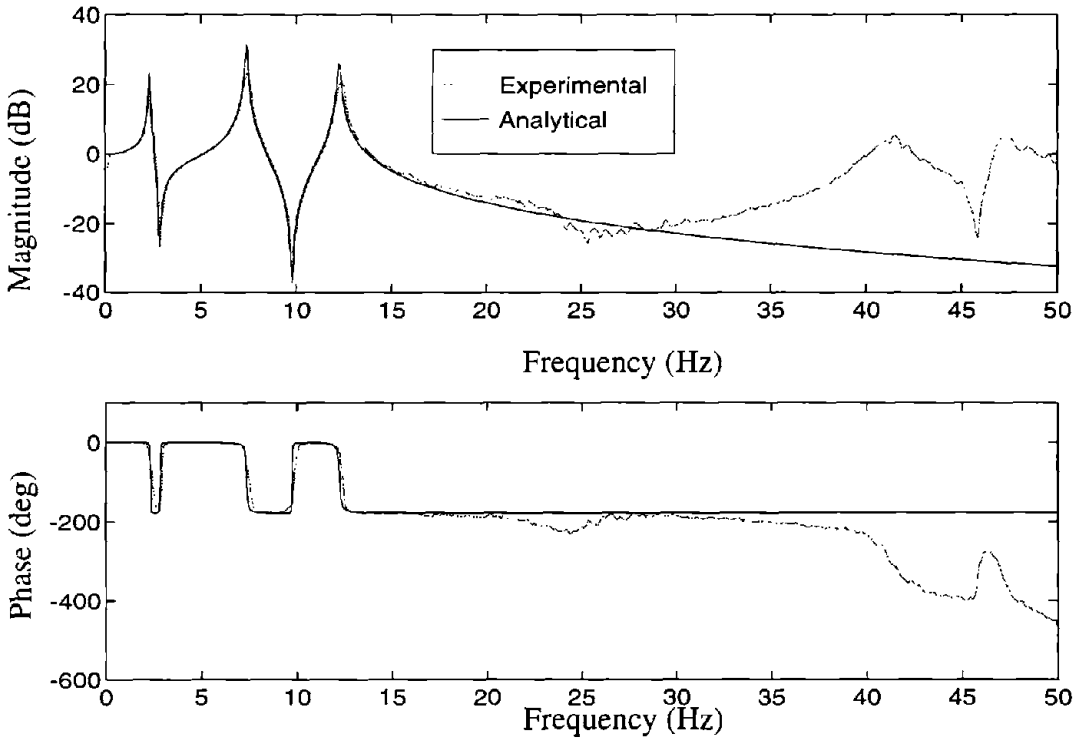

Figure 3.2 Transfer Function from Ground Acceleration to First Floor Acceleration.

Figure 3.4 shows the transfer function from the actuator command u to the actuator displacement x_a (*i.e.*, the actuator transfer function). As expected, this transfer function has the same three lightly damped modes of the structural system that are seen in Figs. 3.2 and 3.3. In addition, there are significant modes at high frequencies that correspond to actuator dynamics. These actuator dynamics are the primary source of the high frequency dynamics seen in the transfer functions in Figs. 3.2 and 3.3. If the gain on the stabilization loop of the hydraulic actuator is reduced, these high frequency dynamics are greatly reduced, although at the expense of a more slowly responding actuator. To observe this effect, the actuator transfer function was experimentally determined for two different feedback gains. The two transfer functions are compared in Fig. 3.5. Notice that reducing the feedback gain causes the actuator transfer function to roll off at a lower frequency and the actuator dynamics to be highly damped.

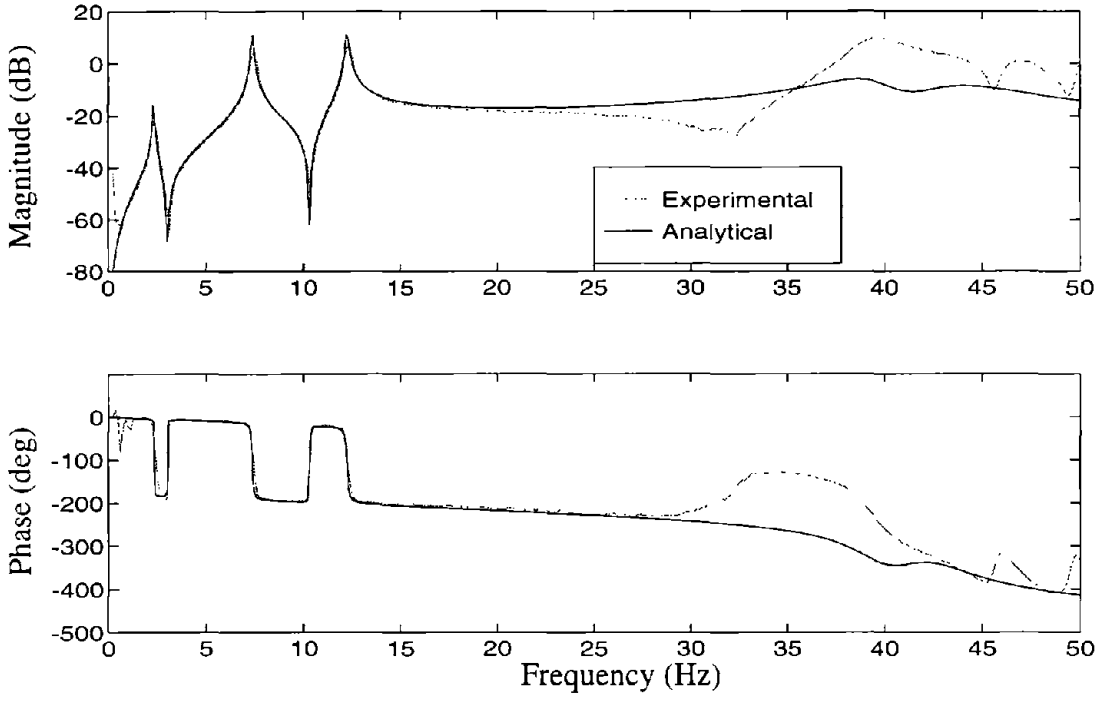

Figure 3.3 Transfer Function from Actuator Command to First Floor Acceleration.

3.2 Mathematical Modeling of Transfer Functions

Once the experimental transfer functions have been obtained, the next step in the system identification procedure is to model the transfer functions as a ratio of two polynomials in the Laplace variable s. This task was accomplished via a least squares fit of the ratio of numerator and denominator polynomials, evaluated on the $j\omega$ axis, to the experimentally obtained transfer functions (Schoukens and Pintelon, 1991). The algorithm requires the user to input the number of poles and zeros to use in estimating the transfer function, and then determines the location for the poles/zeros and the gain of the transfer function for a best fit. This algorithm was used to fit each of the eight transfer functions.

To effectively identify a structural model, a thorough understanding of the significant dynamics of the structural system is required. For example, because the transfer functions represent the input/output relationships for a single physical system, a common denominator was assumed for the elements of each column of the transfer function matrix. The curve fitting routine, howev-

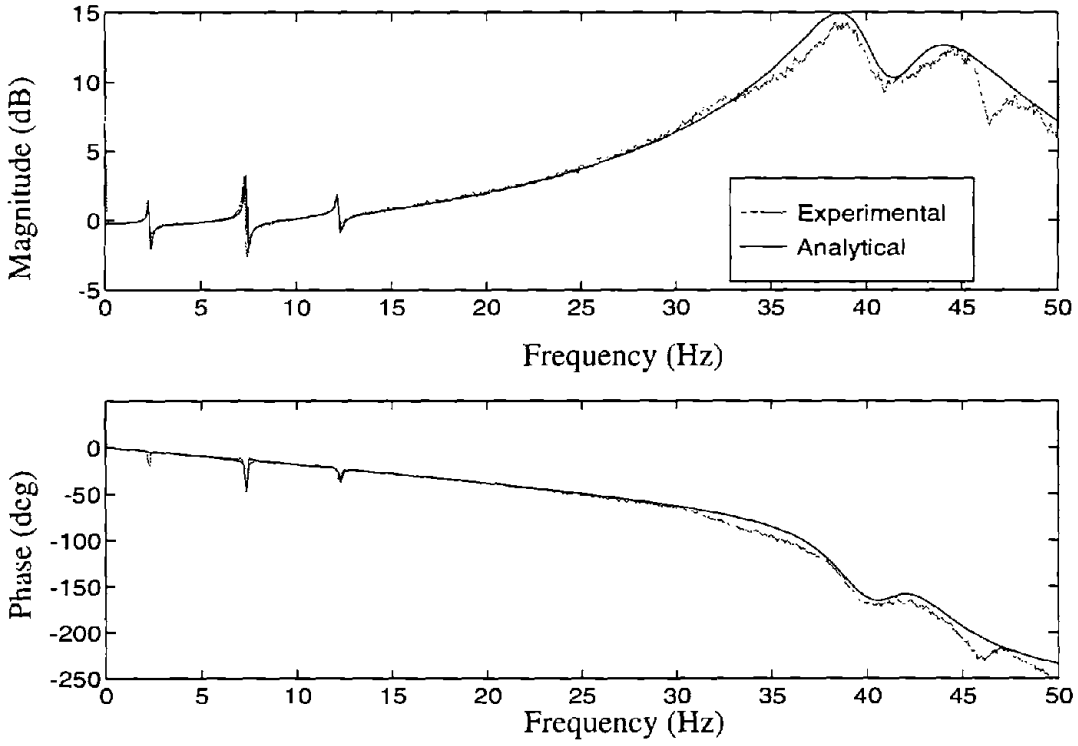

Figure 3.4 Transfer Function from Actuator Command to Actuator Displacement.

er, does not necessarily yield this result. Thus, the final locations of the poles and zeros were then adjusted as necessary to more accurately represent the physical system. A MATLAB (1993) computer code was written to automate this process.

Another important phenomenon that should be consistently incorporated into the identification process is control-structure interaction. Most of the current research in the field of structural control does not explicitly take into account the effects of control-structure interaction in the analysis and design of protective systems. Dyke, *et al.* (1993, 1994) have shown that the dynamics of the hydraulic actuators are integrally linked to the dynamics of the structure. By including the actuator in the structural system, the actuator dynamics and control-structure interaction effects are automatically taken into account in the experimental data. However, one must ensure that the effects of control-structure interaction are not neglected in obtaining a mathematical model of the experimental transfer functions.

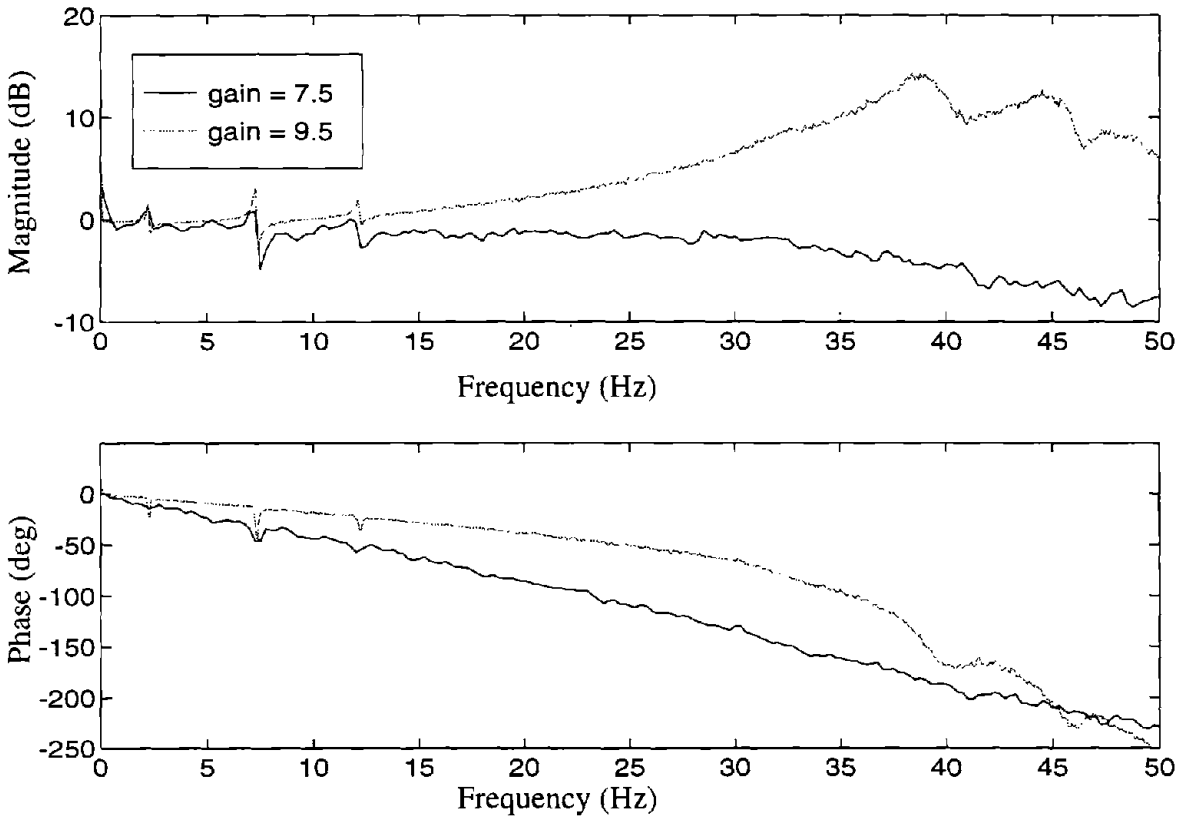

Figure 3.5 Comparison of Actuator Transfer Functions for Various Feedback Gains.

For the system under consideration, the results in Dyke, *et al.* (1993, 1994) show that the poles of the structure (including the active tendons) will appear as zeros of the transfer function from the command input to the actuator displacement. This phenomenon occurs regardless of how fast (or slow) the actuator responds. The predicted behavior is clearly seen in Fig. 3.4, where there is nearly a pole/zero cancellation at the first three modes of the structural system. These zeros correspond to the poles of the transfer function from the actuator displacement to the building responses. The near cancellation of these poles and zeros occurs because the tendons applying the control force to the structure are relatively flexible, as compared to the building stiffness. If one did not anticipate the effect of control-structure interaction, the transfer function for the actuator shown in Fig. 3.4 might have been assumed to be unity over the interval from 0–20 Hz. In addition, the mass of the frame connecting the tendons to the actuator is not negligible and has a significant effect on the dynamics of the system. The frame must be viewed as an additional degree-of-freedom in the system. This extra degree-of-freedom was implicitly incorporated into the system model.

Of course, the structural system is actually a continuous system and will have an infinite number of vibrational modes. One of the jobs of the control designer is to ascertain which of these modes are necessary to model for control purposes. Herein, it was decided that the control of the first three modes was desired; thus the model of the system needed to be accurate to approximately 20 Hz. However, a consequence of this decision is that significant control effort should not be applied at frequencies above 20 Hz. The techniques used to roll-off the control effort at higher frequencies are presented in Section 4.

The mathematical models of the transfer functions are overlaid in Figs. 3.2–3.4. The identified poles of the structural system are: $-0.005 \pm 2.33j$, $-0.030 \pm 7.37j$, $-0.050 \pm 12.24j$, $-2.01 \pm 39.22j$, $-3.03 \pm 43.26j$, and -140 (in Hz). The quality of the mathematical models for the remaining transfer functions was similar to that depicted in Figs. 3.2–3.4.

3.3 State Space Realization

The system was then assembled in a state space form using the analytical representation of the transfer functions (*i.e.*, the poles, zeros and gain) for each individual transfer function. Because the system under consideration is a multi-input/multi-output system (MIMO), such a construction was not straightforward.

First, two separate systems are formed, each with a single input corresponding to one of the two inputs to the system. The state equations modeling the input/output relationship between the disturbance, $\ddot{x}_g$, and the measured outputs can be realized as

$$\begin{aligned} \dot{\mathbf{x}}_1 &= \mathbf{A}_1\mathbf{x}_1 + \mathbf{B}_1\ddot{x}_g, \\ \mathbf{y} &= \mathbf{C}_1\mathbf{x}_1 + \mathbf{D}_1\ddot{x}_g, \end{aligned} \tag{3.10}$$

where $\mathbf{A}_1$, $\mathbf{B}_1$, $\mathbf{C}_1$, and $\mathbf{D}_1$ are in controller canonical form, $\mathbf{x}_1$ is the state vector, and the vector of measured structural responses is given by $\mathbf{y} = [x_a \;\; \ddot{x}_{a1} \;\; \ddot{x}_{a2} \;\; \ddot{x}_{a3}]'$. Because the transfer function characteristics from the ground to the building response were dominated by the dynamics of the building (see Fig. 3.2), the system in Eq. (3.10) required only six states, corresponding to the three modes of the building, to accurately model the experimental transfer function over the frequency range of interest.

The second state equations, modeling the input/output relationship between the actuator command u and the responses $\mathbf{y}$ are given by

$$\begin{aligned} \dot{\mathbf{x}}_2 &= \mathbf{A}_2\mathbf{x}_2 + \mathbf{B}_2u, \\ \mathbf{y} &= \mathbf{C}_2\mathbf{x}_2 + \mathbf{D}_2u. \end{aligned} \tag{3.11}$$

where $\mathbf{A}_2$, $\mathbf{B}_2$, $\mathbf{C}_2$, and $\mathbf{D}_2$ are in controller canonical form, and $\mathbf{x}_2$ is the state vector. This system contains eleven states corresponding to the eleven poles identified in the previous section.

Once both of the component system state equations have been identified, the MIMO system can be formed by stacking the states of the two individual systems. By defining a new state vector, $\mathbf{x} = [\mathbf{x}_1 \;\; \mathbf{x}_2]'$, the state equation for the two-input/four-output system is written

$$\dot{\mathbf{x}} = \begin{bmatrix} \mathbf{A}_1 & \mathbf{0} \\ \mathbf{0} & \mathbf{A}_2 \end{bmatrix} \mathbf{x} + \begin{bmatrix} \mathbf{0} \\ \mathbf{B}_2 \end{bmatrix} u + \begin{bmatrix} \mathbf{B}_1 \\ \mathbf{0} \end{bmatrix} \ddot{x}_g, \tag{3.12}$$

and the measurement equation becomes

$$\mathbf{y} = \begin{bmatrix} \mathbf{C}_1 & \mathbf{C}_2 \end{bmatrix} \mathbf{x} + \mathbf{D}_2 u + \mathbf{D}_1 \ddot{x}_g. \tag{3.13}$$

However, this is not a minimum realization of the system. The dynamics of the test structure itself are redundantly represented in this combined state space system, thus the 17 state system given in Eqs. 3.12 and 3.13 had repeated eigenvalues for which the eigenvectors were not linearly independent (*i.e.*, the associated modes are not linearly independent). Thus, a balanced realization of the system given in Eqs. (3.12) and (3.13) was found and a model reduction was performed (Moore, 1981; Laub, 1980). The system model was reduced to a tenth-order system. Six of the eliminated states corresponded to the six redundant states corresponding to the building dynamics. The additional state that was eliminated corresponded to the very fast pole at 140 Hz found in the original system identification. The state space representation of the reduced model is given by

$$\begin{aligned} \dot{\mathbf{x}}_r &= \mathbf{A}\mathbf{x}_r + \mathbf{B}u + \mathbf{E}\ddot{x}_g, \\ \mathbf{y} &= \mathbf{C}_y\mathbf{x}_r + \mathbf{D}_y u + \mathbf{v}, \end{aligned} \tag{3.14}$$

where $\mathbf{v}$ represents the measurement noise. The state space matrices $\mathbf{A}$, $\mathbf{B}$, $\mathbf{C}_y$, $\mathbf{D}_y$ and $\mathbf{E}$ which define the reduced-order model from Eq. 3.14 are provided in the Appendix. To simplify implementation of the controller, the model has been determined in units of Volts/Volt.

3.4 Verification of Mathematical Model

To ensure that information was not lost in the model reduction, the transfer functions of the reduced order system were compared to the transfer functions of the original model. All of the eight input/output relationships matched the original model well. A representative comparison of the reduced order model and the original model is shown in Figs. 3.6 (transfer function from actuator command to the first floor absolute acceleration) and 3.7 (transfer function from ground ac-

celeration to the first floor absolute acceleration). The two functions are almost indiscernible, indicating that little information was lost in the model reduction. The model given in Eq. (3.14) was used as a basis for the control designs discussed in the next section. All of the experimental transfer functions are compared to the reduced order model in Figs. 3.8 through 3.15.

Remark: Many researchers studying active control of civil engineering structures have partially accounted for the dynamics of the actuator by modeling them as a pure time delay. A phase-compensation approach has been successfully applied, with reasonable results being achieved for the state feedback situation. However, this approach does not account for control-structure interaction and does not appear to be tractable in output feedback situations. More importantly, examination of Fig. 3.4 clearly shows that the actuator dynamics do not result in a pure time delay in the system. In contrast, the system identification procedure outlined in this section systematically accounts for the dynamics of the actuator and the effect of control-structure interaction. As demonstrated herein, the ten-state model well represents the behavior of the actuator/structural system.

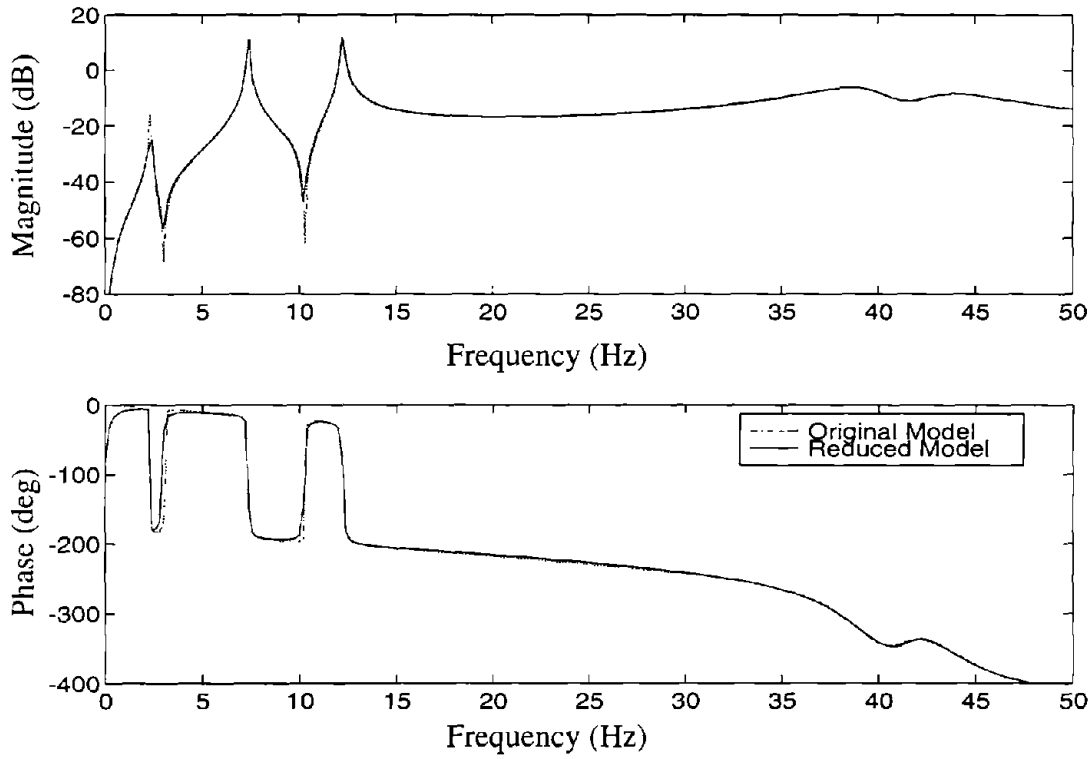

Figure 3.6 Comparison of the Reduced Order Model and Original Model Transfer Functions: Actuator Command to the First Floor Acceleration.

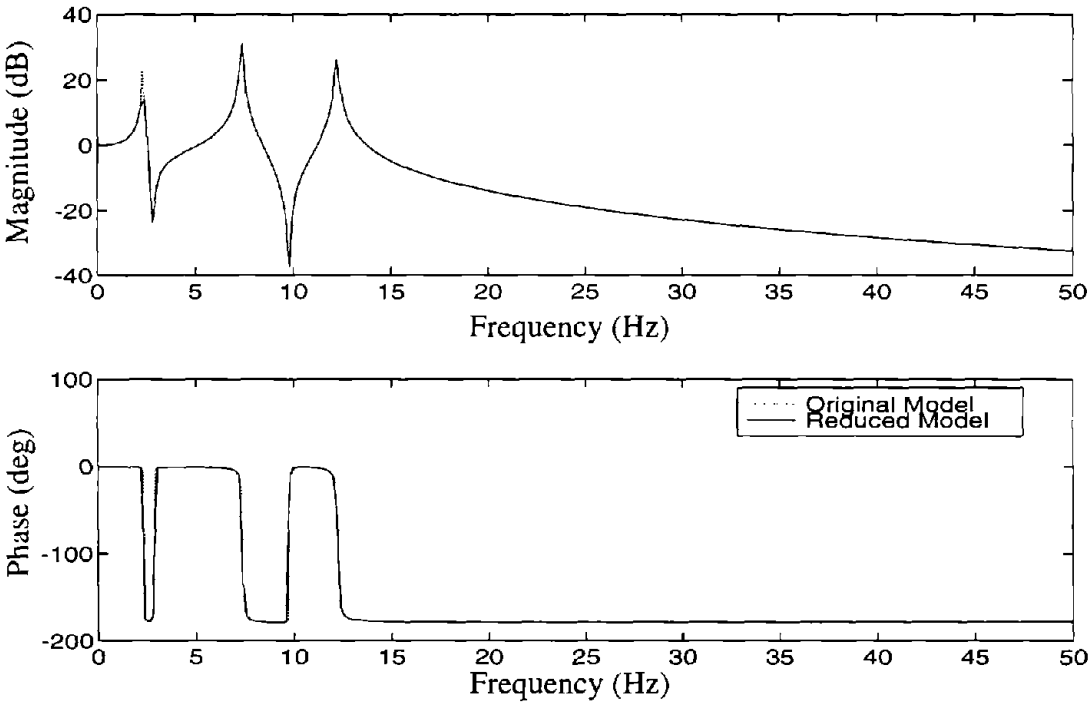

Figure 3.7 Comparison of the Reduced Order Model and Original Model Transfer Functions: Ground Acceleration to the First Floor Acceleration.

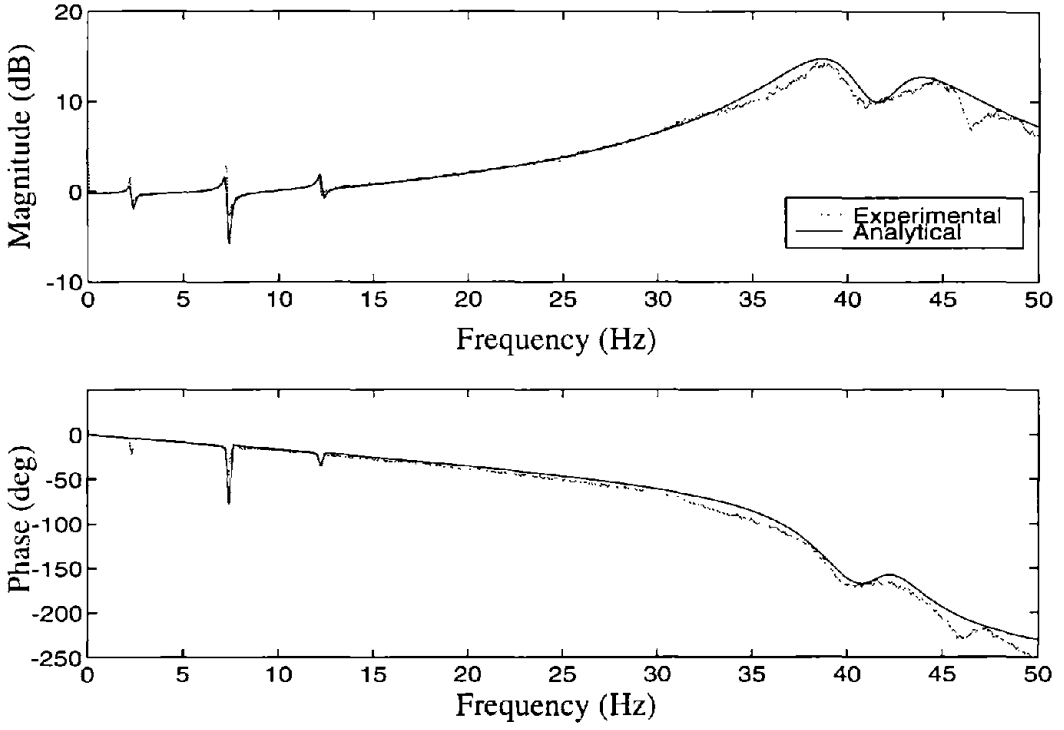

Figure 3.8 Comparison of Reduced-Order Model and Experimental Transfer Function from the Actuator Command to the Actuator Displacement.

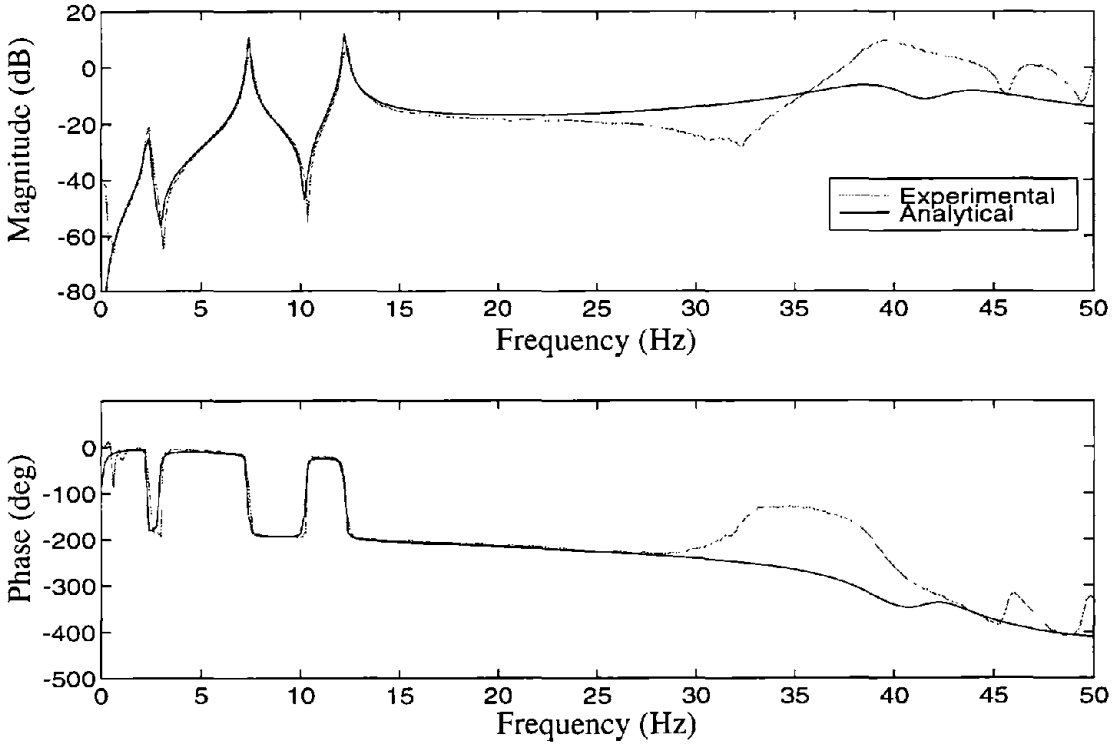

Figure 3.9 Comparison of Reduced-Order Model and Experimental Transfer Function from the Actuator Command to the First Floor Acceleration.

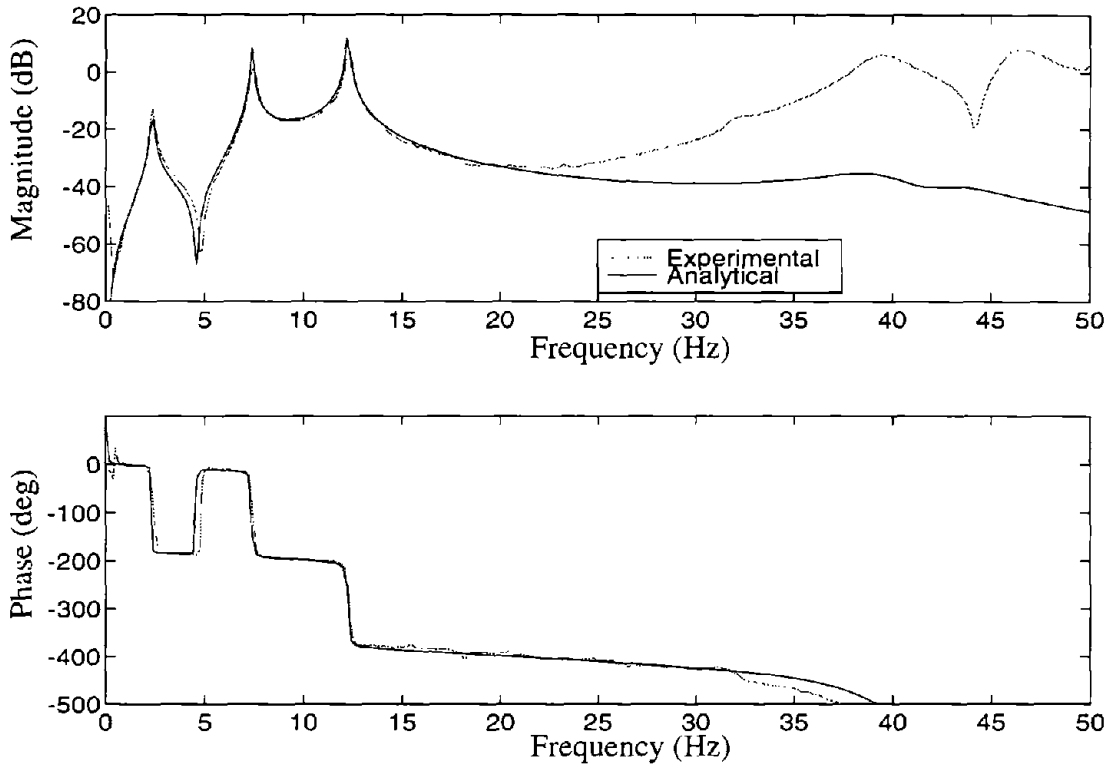

Figure 3.10 Comparison of Reduced-Order Model and Experimental Transfer Function from the Actuator Command to the Second Floor Acceleration.

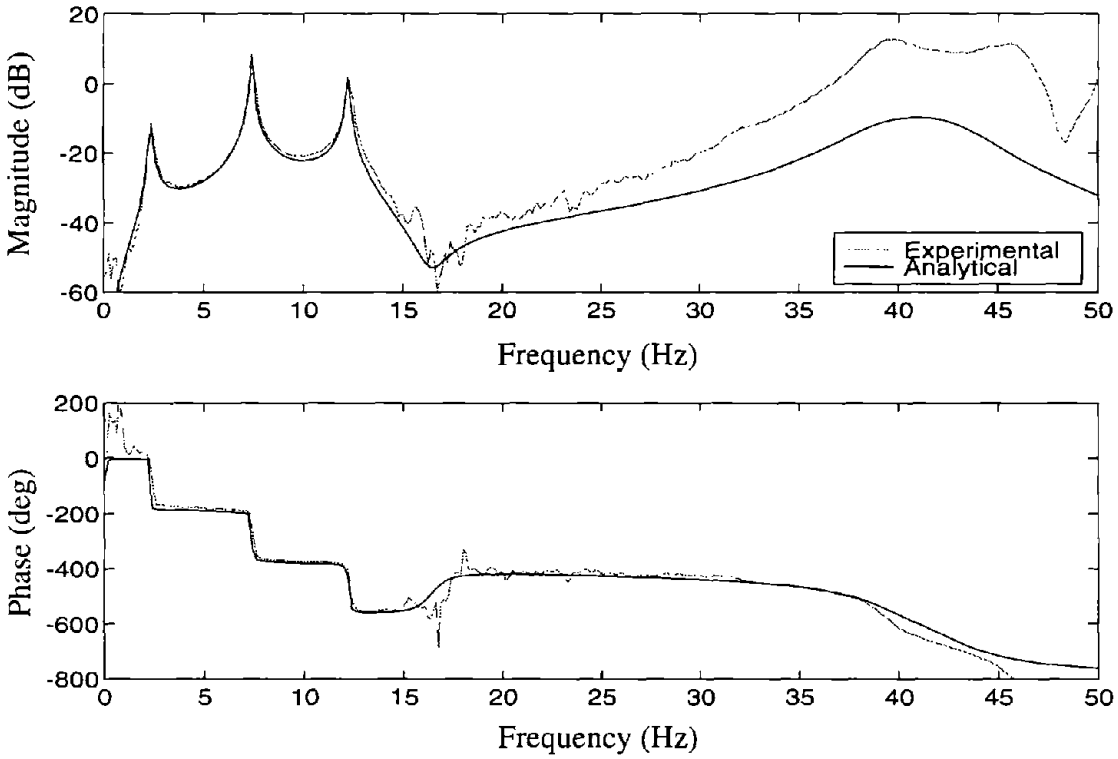

Figure 3.11 Comparison of Reduced-Order Model and Experimental Transfer Function from the Actuator Command to the Third Floor Acceleration.

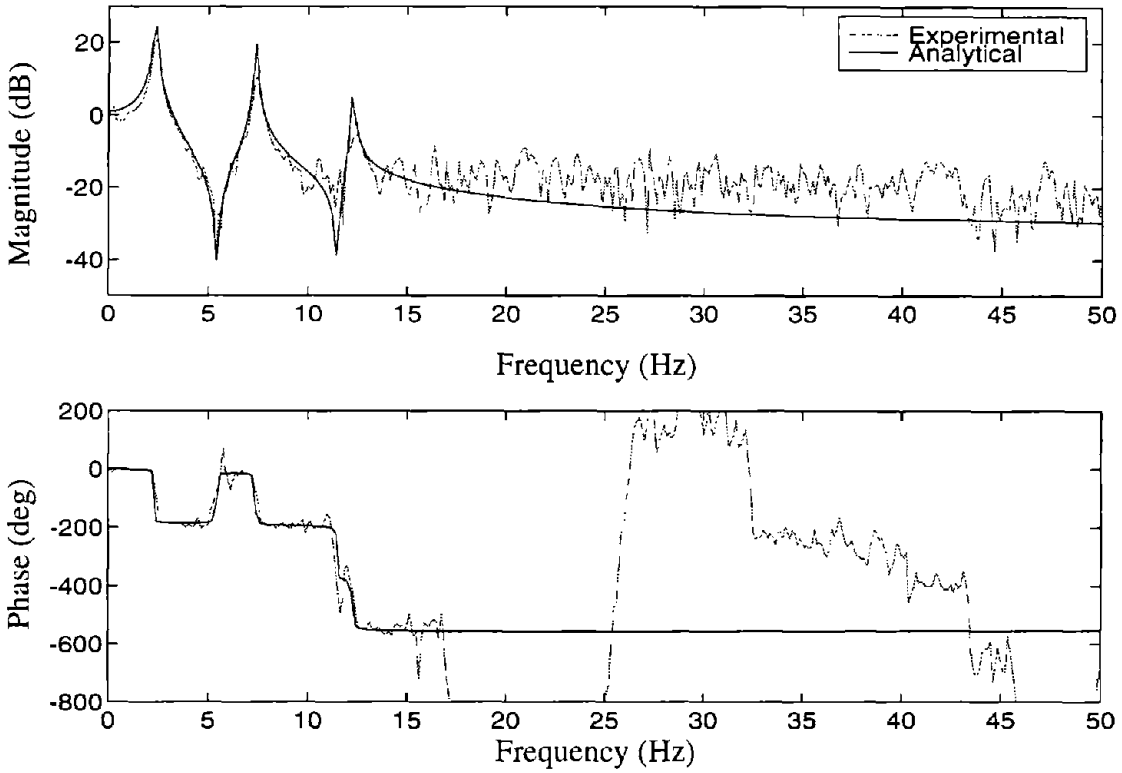

Figure 3.12 Comparison of Reduced-Order Model and Experimental Transfer Function from the Ground Acceleration to the Actuator Displacement.

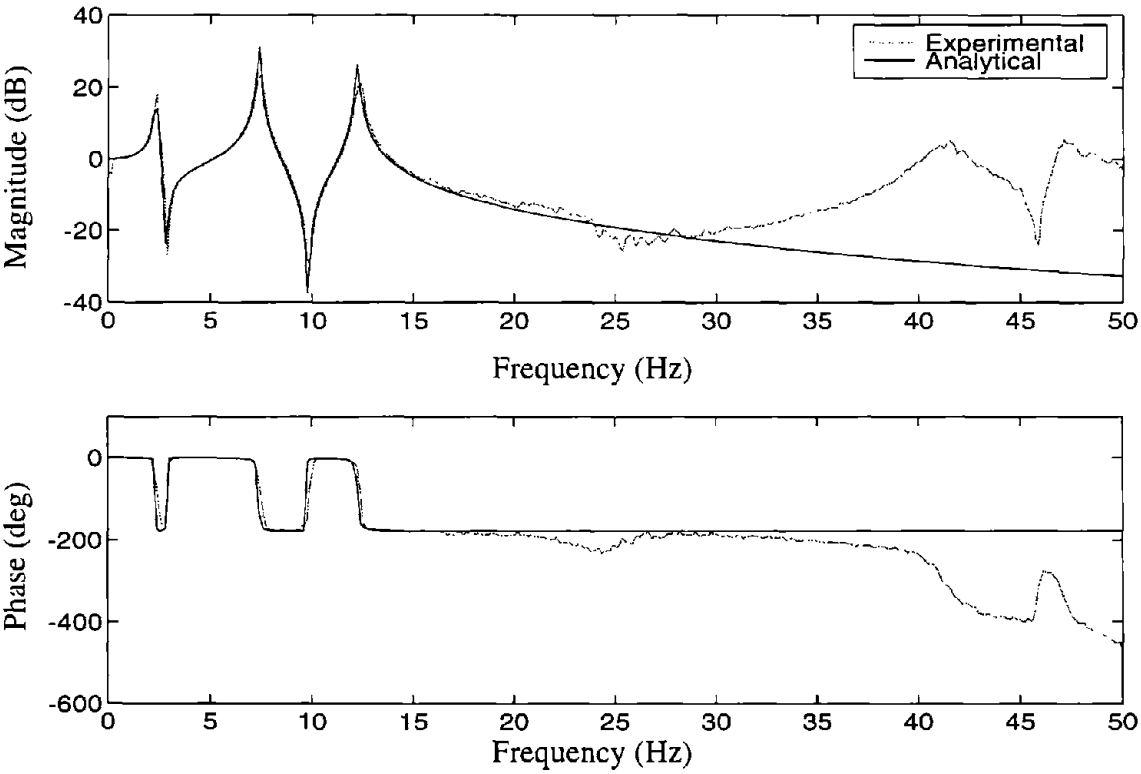

Figure 3.13 Comparison of Reduced-Order Model and Experimental Transfer Function from the Ground Acceleration to the First Floor Acceleration.

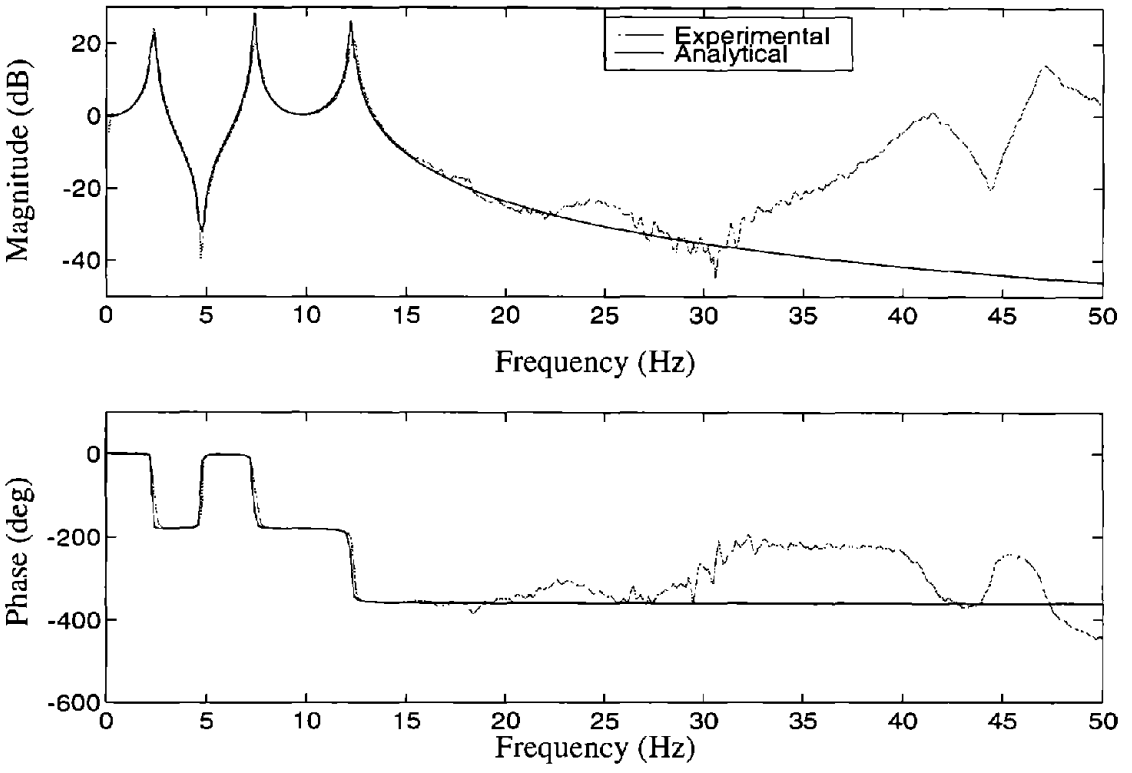

Figure 3.14 Comparison of Reduced-Order Model and Experimental Transfer Function from the Ground Acceleration to the Second Floor Acceleration.

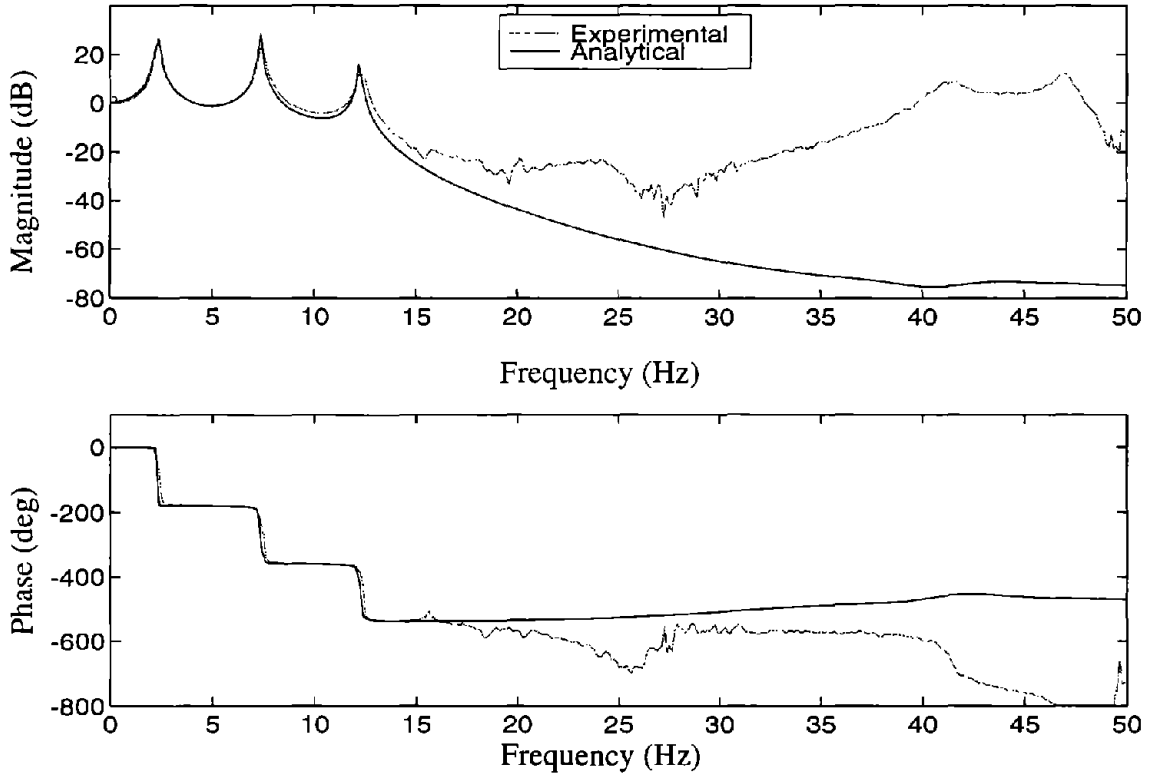

Figure 3.15 Comparison of Reduced-Order Model and Experimental Transfer Function from the Ground Acceleration to the Third Floor Acceleration.

SECTION 4
CONTROL DESIGN

In control design, a trade-off exists between good performance and robust stability. Better performance usually requires a more authoritative controller. However, uncertainties in the system model may result in severely degraded performance and perhaps even instabilities if the controller is too authoritative. Therefore, the uncertainties in the model are a limiting factor in the performance of the control system. Spencer, *et al.* (1994c) have shown that H_2/LQG design methods produce effective controllers for this class of problems. For the sake of completeness, a brief overview of H_2/LQG control design methods is given below.

4.1 Control Algorithm

Consider the general block diagram description of the control problem given in Fig. 4.1. Here **y** is the measured output vector of structural responses, **z** is the vector of structural responses which we desire to control, **u** is the control input vector, and **d** is the input excitation vector. For this experiment the measured output vector **y** includes the actuator displacement and the accelerations of the three floors of the test structure. The regulated output vector **z** may consist of any linear combination of the states of the system and components of the control input vector **u**, thus allowing a broad range of control design objectives to be formulated through appropriate choice

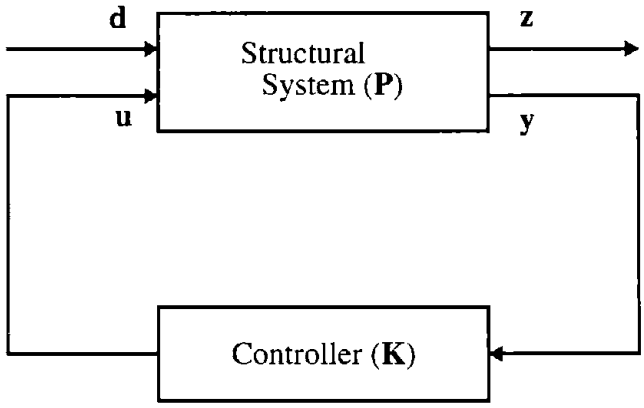

Figure 4.1 Basic Structural Control Block Diagram.

of elements of **z**. Weighting functions, or specifications, can be added to elements of **z** to specify the frequency range over which each element of **z** is minimized. The "structural system" in Fig. 4.1 then contains the test structure, actuator, tendons and connecting frame, plus filters and weighting functions in the frequency domain. The task here is to design the controller **K** such that it stabilizes the system and, within the class of all controllers which do so, minimizes the H_2 norm of the transfer function matrix $\mathbf{H}_{zd}$ from **d** to **z**. Alternatively, this norm may be specified to satisfy certain bounds.

More specifically, denote by $\mathcal{H}_s$ the set of controllers **K**, as in Fig. 4.1, which internally stabilizes the resulting closed-loop feedback system of the figure and whose transfer function matrices are proper. Then, for a suitably chosen matrix norm $\|\cdot\|$, the problem is

$$\min_{\mathbf{K} \in \mathcal{H}_s} \|\mathbf{H}_{zd}\|. \tag{4.1}$$

To obtain the transfer function $\mathbf{H}_{zd}$, we refer to Fig. 4.1 and partition the system transfer function matrix **P** into its components, *i.e.*,

$$\mathbf{P} = \begin{bmatrix} \mathbf{P}_{zd} & \mathbf{P}_{zu} \\ \mathbf{P}_{yd} & \mathbf{P}_{yu} \end{bmatrix}. \tag{4.2}$$

The overall transfer function from **d** to **z** can then be written as (Suhardjo, 1990),

$$\mathbf{H}_{zd} = \mathbf{P}_{zd} + \mathbf{P}_{zu}\mathbf{K}(\mathbf{I} - \mathbf{P}_{yu}\mathbf{K})^{-1}\mathbf{P}_{yd}. \tag{4.3}$$

As with **K**, it is assumed that **P** in Eq. (4.2) is proper. The reader should also note that the inverse in Eq. (4.3) must exist. For simplicity, this latter requirement may be included in the definition of $\mathcal{H}_s$. Because **P** may include appropriate filters and weighting functions in the frequency domain, as described above, it is clear that $\mathbf{H}_{zd}$ will embody them as well.

The controller resulting from Eqs. (4.1) and (4.3) will depend upon the norm employed in the minimization. As suggested by the name, the H_2 control design searches for a stabilizing control-

ler which minimizes the H_2 norm of $\mathbf{H}_{zd}$, $\|\mathbf{H}_{zd}\|_2$. The H_2 norm of a stable transfer function matrix $\mathbf{H}$ is defined as (Boyd and Barratt, 1991)

$$\|\mathbf{H}\|_2 \equiv \sqrt{\text{trace}\left\{\frac{1}{2\pi}\int_{-\infty}^{\infty}\mathbf{H}(j\omega)\,\mathbf{H}^*(j\omega)\,d\omega\right\}}\,. \tag{4.4}$$

More physical insight into the meaning of the H_2 norm can be obtained by noting that the H_2 norm of a transfer function measures the root mean square (rms) value of its output, in a vector sense, when the input is a unit white noise excitation vector. The *rms* output vector is defined by

$$\|\mathbf{d}\|_{rms} = \sqrt{\lim_{\tau\to\infty}\frac{1}{2\tau}\int_{-\tau}^{\tau}\mathbf{d}^T(t)\,\mathbf{d}(t)\,dt} \tag{4.5}$$

where for ease of notation, the symbol $\mathbf{d}$ is used for both the time function and its transform. When $\mathbf{d}(t)$ is an ergodic stochastic process, Eq. (4.5) can also be written as

$$\|\mathbf{d}\|_{rms} = \sqrt{\sum_i E[d_i^2(t)]}\,, \tag{4.6}$$

where $E[\cdot]$ is the expected value operator.

To illustrate these concepts, consider a structure under one-dimensional earthquake excitation $\ddot{x}_g$ and active control input $\mathbf{u}$. The structural system, which includes the structure, the actuator and any components required to apply the control force, can be represented in state space form as

$$\dot{\mathbf{x}} = \mathbf{A}\mathbf{x} + \mathbf{B}\mathbf{u} + \mathbf{E}\ddot{x}_g \tag{4.7}$$

$$\mathbf{y} = \mathbf{C}_y\mathbf{x} + \mathbf{D}_y\mathbf{u} + \mathbf{v} \tag{4.8}$$

where **x** is the state vector of the system, **y** is the vector of measured responses, and **v** represents the noise in the measurements. A detailed block diagram representation of the system given in Eqs. (4.7) and (4.8) is depicted in Fig. 4.2. In this figure, the transfer function **G** is given by

$$\mathbf{G} = (s\mathbf{I} - \mathbf{A})^{-1}\mathbf{B} = (s\mathbf{I} - \mathbf{A})^{-1}[\mathbf{B}\ \mathbf{E}] = [\mathbf{G}_1\ \mathbf{G}_2]. \tag{4.9}$$

The filter **F** shapes the spectral content of the disturbance modeling the excitation, $\mathbf{C}_y$ and $\mathbf{C}_z$ are constant matrices that dictate the components of structural response comprising the measured output vector **y** and the regulated response vector **z**, respectively. The matrix weighting functions $\alpha_1\mathbf{W}_1$ and $\alpha_2\mathbf{W}_2$ are generally frequency dependent, with $\alpha_1\mathbf{W}_1$ weighting the components of regulated response and $\alpha_2\mathbf{W}_2$ weighting the control force vector **u**. The input excitation vector **d** consists of a white noise excitation vector **w** and a measurement noise vector **v**. The scalar parameter k is used to express a preference in minimizing the norm of the transfer function from **w** to **z** versus minimizing the norm of the transfer function from **v** to **z**. For this block diagram representation, the partitioned elements of the system transfer function matrix **P** in Eq. (4.2) are given by

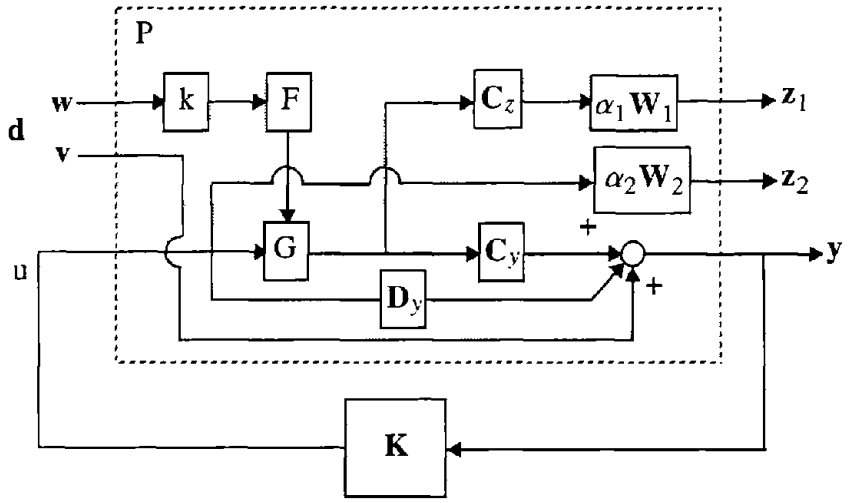

Figure 4.2 Typical structural control block for a seismically excited structure.

$$\mathbf{P}_{zd} = \begin{bmatrix} \mathbf{P}_{z_1 w} & \mathbf{P}_{z_1 v} \\ \mathbf{P}_{z_2 w} & \mathbf{P}_{z_2 v} \end{bmatrix} = \begin{bmatrix} k\alpha_1 \mathbf{W}_1 \mathbf{C}_z \mathbf{G}_2 \mathbf{F} & \mathbf{0} \\ \mathbf{0} & \mathbf{0} \end{bmatrix}, \tag{4.10}$$

$$\mathbf{P}_{zu} = \begin{bmatrix} \mathbf{P}_{z_1 u} \\ \mathbf{P}_{z_2 u} \end{bmatrix} = \begin{bmatrix} \alpha_1 \mathbf{W}_1 \mathbf{C}_z \mathbf{G}_1 \\ \alpha_2 \mathbf{W}_2 \end{bmatrix}, \tag{4.11}$$

$$\mathbf{P}_{yu} = \mathbf{C}_y \mathbf{G}_1 + \mathbf{D}_y, \tag{4.12}$$

and

$$\mathbf{P}_{yd} = \begin{bmatrix} \mathbf{P}_{yw} & \mathbf{P}_{yv} \end{bmatrix} = \begin{bmatrix} k\mathbf{C}_y \mathbf{G}_2 \mathbf{F} & \mathbf{I} \end{bmatrix}. \tag{4.13}$$

Equations (4.10)–(4.13) can then be substituted into Eq. (4.3) to yield an explicit expression for $\mathbf{H}_{zd}$. The solution of the H_2 control problem can now be solved via standard methods (*cf.*, Suhardjo, 1990; Spencer, *et al.*, 1994a).

4.2 Design Considerations and Procedure

To offer a basis for comparison, 21 candidate controllers were designed using H_2/LQG control design techniques, each employing a different performance objective. Designs which minimize either displacements relative to the foundation, interstory displacements or absolute accelerations of the structure were considered. Control designs were also considered which directly used the measured earthquake accelerations in control action determination. In this case, the matrix in Eq. (4.13) included an additional term due to the measurement of the disturbance. In all of the controller designs considered, the weighting function on the regulated output, $\alpha_1 \mathbf{W}_1$, and the weighting function on the control force, $\alpha_2 \mathbf{W}_2$, were constant matrices (*i.e.*, independent of frequency). The earthquake filter $\mathbf{F}$ was modeled based on the Kanai–Tajimi spectrum. The performance of all of the candidate controllers was evaluated analytically and experimentally.

In Section 3, we indicated that the model on which the control designs were based was acceptably accurate below 20 Hz, but that significant modeling errors occurred at higher frequen-

cies, particularly near the dominant actuator dynamics (~40 Hz). If one tries to affect high authority control at frequencies where the system model is poor, catastrophic results may occur. Thus, for the structural system under consideration, no significant control effort was allowed above 20 Hz.

The loop gain transfer function was examined in assessing the various control designs. Here, the loop gain transfer function is defined as the transfer function of the system formed by breaking the control loop at the input to the system, as shown in Fig. 4.3. Using the plant transfer function given in Eq. (4.12), the loop gain transfer function is given as

$$\mathbf{H}_{loop} = \mathbf{K}\mathbf{P}_{yu} = \mathbf{K}(\mathbf{C}_y\mathbf{G}_1 + \mathbf{D}_y) \tag{4.14}$$

By "connecting" the measured outputs of the analytical system model to the inputs of the mathematical representation of the controller, the loop gain transfer function from the actuator command input to the controller command output was calculated.

The loop gain transfer function was used to provide an indication of the closed-loop stability when the controller is implemented on the physical system. For stability purposes, the loop gain should be less than one at the higher frequencies where the model poorly represents the structural system (*i.e.*, above 20 Hz). Thus, the magnitude of the loop gain transfer function should roll off

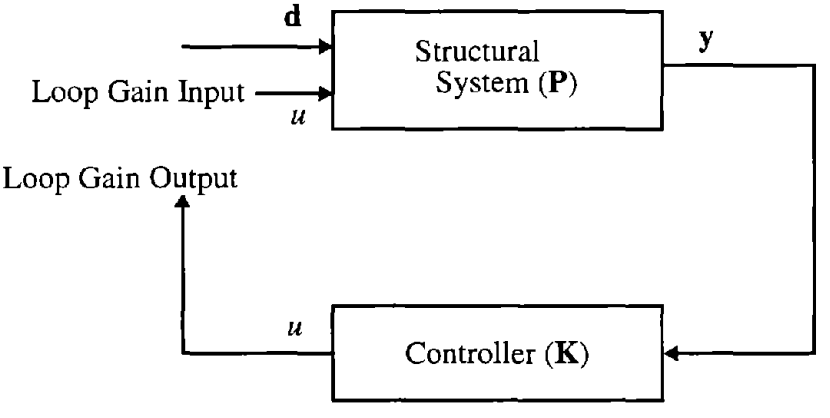

Figure 4.3 Diagram Describing the Loop Gain Transfer Function.

steadily and be well below unity at higher frequencies. Herein, a control design was considered to be acceptable for implementation if the magnitude of the loop gain at high frequencies was less than -5 dB at frequencies greater than 20 Hz.

SECTION 5
CONTROL IMPLEMENTATION

The controllers used in this experiment were implemented on digital computers. There are many issues that must be understood and addressed to successfully implement a control design on a computer. The resolution of these issues typically dictates that relatively high sampling rates need to be attained. Recently developed hardware based on dedicated DSP chips allows for very high sampling rates and offers new possibilities for control algorithm implementation.

A description of the digital control hardware used in this experiment is discussed below. Practical aspects of digital control implementation are also given. Further discussion of implementation concepts is provided in Spencer, *et al.* (1994b) and Quast, *et al.* (1994). Finally, experimental verification of successful digital implementation of the controllers used is presented.

5.1 Digital Controller Hardware

One typical way in which digital control schemes were implemented in the past was through the use of data acquisition boards in the expansion bus of a personal computer (PC). In this configuration, the data acquisition board would be programmed or commanded to take samples of system measured quantities at regular intervals. When available, the samples of the measured quantities would be passed to the PC's main CPU through the I/O space of the PC. The PC would then perform the arithmetic calculations required for implementation of the digital filter and forward the results through the I/O space to the D/A devices for output conversion. These continuous-time signals would then be used as the control inputs to the plant.

This configuration has many drawbacks. The time required to perform all of the A/D and D/A operations and pass these quantities over the I/O space of the PC, as well as perform the control algorithm computations on the PC, may require undesirably large sampling periods and induce unacceptable time delays. Also, with such an equipment configuration, it is difficult to create a scheme which allows the operator to monitor and interact with the controller while the PC is engaged in performing the control computations.

A more powerful arrangement for implementation of a digital control system is realizable through the use of one of many different DSP boards available that are placed in the expansion bus of a personal computer. State of the art DSP chips allow for very fast computational speeds as well as dedicated processing. The DSP boards have A/D and D/A converters locally on the board which reduces the delay involved in the transmission of signals between the processor and the I/O devices. Further, such configurations enable the control and monitoring of the DSP board by the PC in a supervisory control scheme.

The control system employed in this experiment utilized the Real-Time Digital Signal Processor System made by Spectrum Signal Processing, Inc. It is configured on a board that plugs into a 16-bit slot in a PC's expansion bus and features a Texas Instruments TMS320C30 Digital Signal Processor chip, RAM memory and on board A/D and D/A systems. The TMS320C30 DSP chip has single-cycle instructions, a 33.3 MHz clock, a 60 ns instruction cycle and can achieve a nominal performance of 16.7 MFLOPS. A special feature of the chip that allows a floating point multiplier and adder to be used in parallel yields a theoretical peak performance of 33.3 MFLOPS. Moreover, this board has a number of built-in functions that make it ideal for control applications. For example, there are notch filters to cancel mechanical resonances, adaptive Kalman filter algorithms to reduce sensor noise, vector control algorithms for real-time axis transformation and fuzzy set control algorithms.

In addition, the on-board A/D system has two channels, each with 16 bit precision and a maximum sampling rate of 200 kHz. The two D/A channels, also with 16 bit precision, allow for even greater output rates so as not to be limiting. An expansion I/O daughter board, which connects directly to the DSP board, provides an additional four channels of input and two channels of output capability, each with 12 bit precision. All four input channels share the same conversion device, which is the limiting factor for the board's sampling rate. The maximum sampling rate for the daughter board is 200 kHz for one channel and proportionally less for multiple channels, with a rate of 50 kHz per channel if all four channels are used. The maximum rate for each of the two daughter board output channels is 300k samples/second. Additional daughter cards may be added

to the system to further expand the system's I/O capabilities. Clearly, with the high computation rates of the DSP chip and the extremely fast sampling and output capability of the associated I/O system, high overall sampling rates for the digital control system are achievable.

As mentioned previously, the board plugs into a 16 bit expansion slot in a PC, which allows for communication between the DSP board and the PC through the I/O space of the PC. The PC is used to download the control code to the DSP board through this I/O interface. Further, while the DSP board runs the control algorithm, a supervisory program running on the PC can monitor the performance of the control system, monitor and display measured quantities, and allow the operator to send commands to the DSP board, starting and stopping the controller or changing control parameters. This configuration allows for a very powerful and flexible implementation of a digital control system for structural control.

5.2 Digital Control System Design

The method of "emulation" was used for the design of the discrete-time controller (Quast, *et. al.*, 1994). Using this technique, a continuous-time controller was first designed which produced satisfactory control performance. The continuous-time controller was then approximated or `emulated' with a discrete-time equivalent digital filter using the bilinear transformation. This configuration is illustrated in Figure 5.1. The controller samples the measured outputs of the plant and passes the samples through a digital filter implemented on the DSP board. The output of the digital filter was then passed through a hold device to create a continuous-time signal which became the control input to the plant. The series combination of sampler, digital filter and hold emulated the operation of a continuous-time controller. Typically, with the use of emulation, if the sampling rate of the digital controller is greater than about 10-25 times the closed-loop system bandwidth, the discrete equivalent system will adequately represent the behavior of the emulated continuous-time system over the frequency range of interest. This sampling rate was successfully achieved by the DSP system used in this experiment.

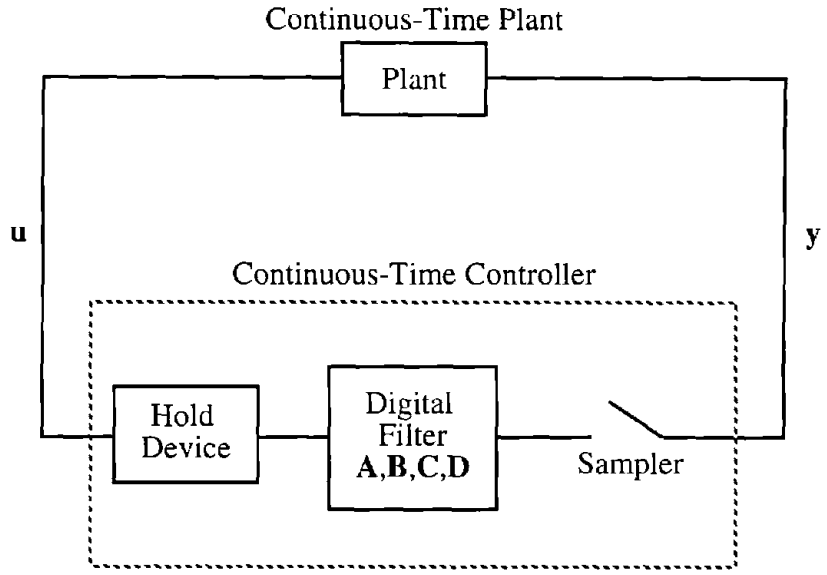

Figure 5.1 Digital Control System Design Using Emulation.

5.3 Digital Control Implementation Issues

Once a filter was designed for use in the digital control system, it was implemented on a DSP system using state space form:

$$\mathbf{x}(kT+T) = \mathbf{A}\mathbf{x}(kT) + \mathbf{B}\mathbf{y}(kT) \tag{5.1}$$

$$\mathbf{u}(kT) = \mathbf{C}\mathbf{x}(kT) + \mathbf{D}\mathbf{y}(kT) \tag{5.2}$$

where **y** represents the vector of measurement sampled inputs to the controller and **u** represents the vector of outputs of the digital filter. Performing the arithmetic to implement a state space realization of a digital filter is not elaborate. However, there are many practical considerations that needed to be addressed in order to successfully implement the filter, including such things as time delay and sampling rate.

Time Delay

For digital control systems, the only true time delays induced are due to latency (which results from A/D conversion time requirements and arithmetic associated with **D** matrix calcula-

tions) and the zero order hold. The delay due to latency will be reduced as the speed of the controller processor and I/O systems increases. Likewise, the delay due to the zero order hold will decrease in direct proportion to the sampling period. For the control system implemented in this experiment, the DSP processor and I/O systems were fast enough so that these time delays were on the order of 700 μsec and small enough so as to have no significant impact on system performance.

Sampling Rate

The sampling rate that is achievable by a digital control system is limited by such things as the rate at which A/D and D/A conversions can be performed, the speed of the processor and the number of calculations required to be performed by the processor during a sampling cycle. There are many factors that must be considered when evaluating the sampling rate that is required for satisfactory performance of a digital control system. These factors include such things as the prevention of aliasing, maintaining a sufficiently smooth control signal, and satisfactory controller performance of the controlled system with random disturbances. Accommodation of such factors usually requires a sampling rate of the controller that is 10-25 times greater than the significant frequencies in the measured responses, depending on the specific application. For this experiment, all I/O processes, control calculations, and supervisory functions were performed in less than 1 msec, allowing for sampling rates on the order of 1 kHz. Thus, the TMS320C30 DSP system readily accommodated this sampling rate guidance.

5.4 Software

Once the controller digital filter is designed, it is implemented using the Real-Time Digital Signal Processor System. The code for these programs can be written directly in the C programming language. The code is compiled, linked with library functions and made into executable files on the PC. The PC is then used to download the control code to the DSP board through the PC's I/O interface. The SPOX operating system provides standard I/O library support for the C language so that pre-existing C programs will execute with limited code modification. SPOX also

provides a library of standard DSP functions which free the operator from writing lower level code such as device drivers for managing incoming data. Applications written in C under SPOX are portable to other hardware environments supporting SPOX.

In addition to the implementation of the control algorithm difference equations (Eqs. (5.1) and (5.2)), several other tasks are performed on the DSP board during controller operation. In particular, standard deviations are calculated for all measured quantities. These values are read iteratively by the supervisory program running on the PC and are continuously displayed on the PC display so the operator can monitor performance of the system. Further, as is done extensively in control system implementation in general as well as in structural control, at each sample instant, the magnitudes of certain measured quantities such as the actuator force and displacement are compared to maximum allowable values specified by the user (Soong, *et al.*, 1991; Reinhorn, *et al.*, 1993). If at any instant the measured values exceed the maximum allowable values, the controller is immediately shut off and the command signal is set equal to zero. In addition, if the command output calculated by the control algorithm exceeds the range of the D/A devices, a controller shutdown also occurs. In this case, if the controller were allowed to continue to operate with a saturated command output, the control signal would effectively be corrupted by a noise signal equal in magnitude to the difference between the commanded output and the saturation level of the D/A device. Such a situation could have devastating effects on the performance and stability of the system.

If a shutdown occurs, the supervisory program on the PC, repeatedly checking the condition of the controller, detects the shutdown and displays an advisory on the monitor for the operator. This feature is designed to protect the system and structure from damage due to excessive or unstable response caused by modeling errors, high ground excitation or mistakes in the hardware or software implementation of the controller. The supervisory program running on the PC also allows the operator to turn the controller on and off as well as to change control parameters of the controller during its operation. Although changing parameters in the control algorithm while the

controller is running may be desirable in some cases, it is generally not advisable unless a careful assessment is made of the effects of such changes during control operation.

5.5 Verification of Digital Controller

After the data that was used for system identification was collected, a period of several weeks elapsed before the controllers were actually implemented. Before implementing the controllers, the transfer functions of the system were again determined to verify that the system model on which the controller designs were based was still valid. During the time between the system identification tests and implementation of the control designs the structural system *softened*, resulting in approximately a 1% decrease in the frequencies of the first three modes. However, the control designs were robust enough to account for the slight differences. All of the twenty-one control designs which were implemented produced a significant reduction in the responses. Ten of the controllers were thoroughly tested with various excitations, and the results of five representative controllers are provided in the following section.

Extensive testing was conducted for all components of the control hardware and software before the experiments on the controlled structure were performed. One of the final tests was to experimentally determine the loop gain transfer function by attaching the measured outputs from the building to the inputs of the controller (*i.e.*, the DSP board). The loop gain transfer function was then calculated by exciting the actuator command input with a broadband excitation and measuring the controller output. Figure 5.2 compares the experimental and analytical loop gain transfer functions for one of the test controllers (Controller E as defined in Table 6.1). The two transfer functions are nearly identical below 40 Hz, indicating that the controller was working as expected and the system model was accurate.

Note that except for built-in high frequency anti-aliasing filters on the input channels to the DSP board, no external filters were employed for either the feedback measurements or the control signal. All of the required frequency shaping was performed within the digital control algorithm.

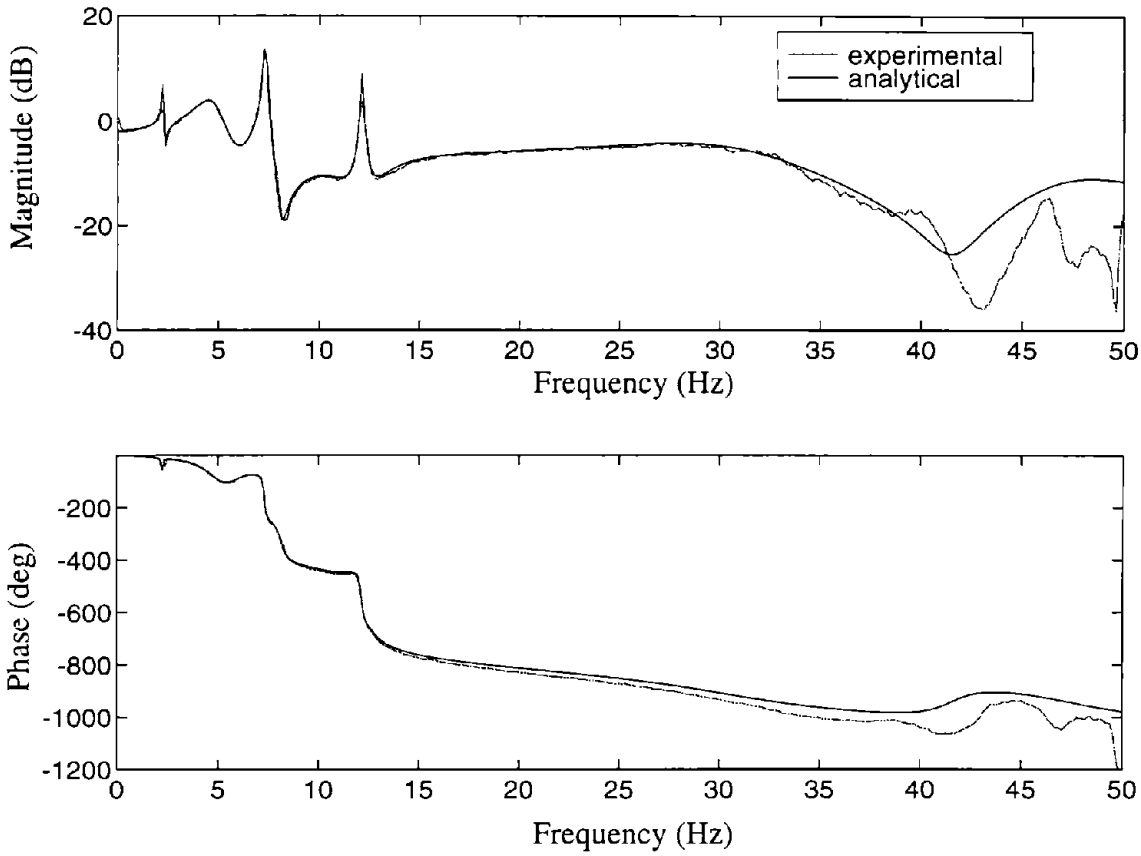

Figure 5.2 Experimental Loop Gain at the Input for Controller E.

SECTION 6
EXPERIMENTAL RESULTS

Two different types of tests were conducted on the earthquake simulator to verify the control designs. A bandlimited white noise ground excitation (0-10 Hz) was first used to excite the structure to observe the ability of the controllers to reduce the *rms* values of the structural responses. In the second type of test, the earthquake simulator reproduced a recorded accelerogram to determine the ability of the controllers to reduce the peak structural responses. For this test, two earthquakes were chosen for controller verification: 1) an El Centro earthquake excitation (N-S component) and 2) a Taft earthquake excitation (North 21 East component). The magnitude of the earthquakes were reduced to one-quarter (El Centro) and one-half (Taft) of the recorded intensity to reduce the possibility of damaging the structure. Also, because the test structure was a scaled model of a prototype structure, similitude relations dictated that both earthquakes be reproduced at double the speed of the recorded earthquakes.

6.1 Development and Validation of Simulation Model

As discussed previously, the characteristics of the system changed slightly between the time that the original data (used for control design) was taken and the controllers were implemented. After completion of the experiments, a revised simulation model was developed based on the data taken when the control experiments were conducted. This was the model used in all comparisons between the analytical and experimental results. Using the eigenvectors of the system matrix for the original model, and modified values for the eigenvalues from the new data, a revised system matrix was formed.

By exciting the model with the measured base accelerations, a simulation of the uncontrolled system was performed to verify the new model of the structural system. *Uncontrolled*, in this context, refers to the structural system with the tendons in place and the actuator command set to zero. In Figs. 6.1a-c and 6.2a-c, the experimental and simulated time responses of the first, second and third floor relative displacements and absolute accelerations for a quarter scale El Centro excitation are compared for verification of the simulation model. In all cases, the experimental and

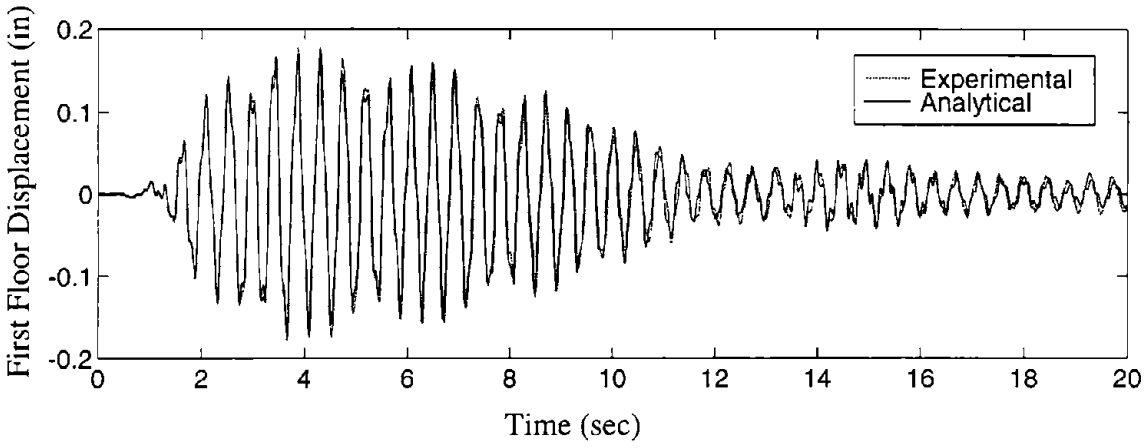

a) First Floor Relative Displacement

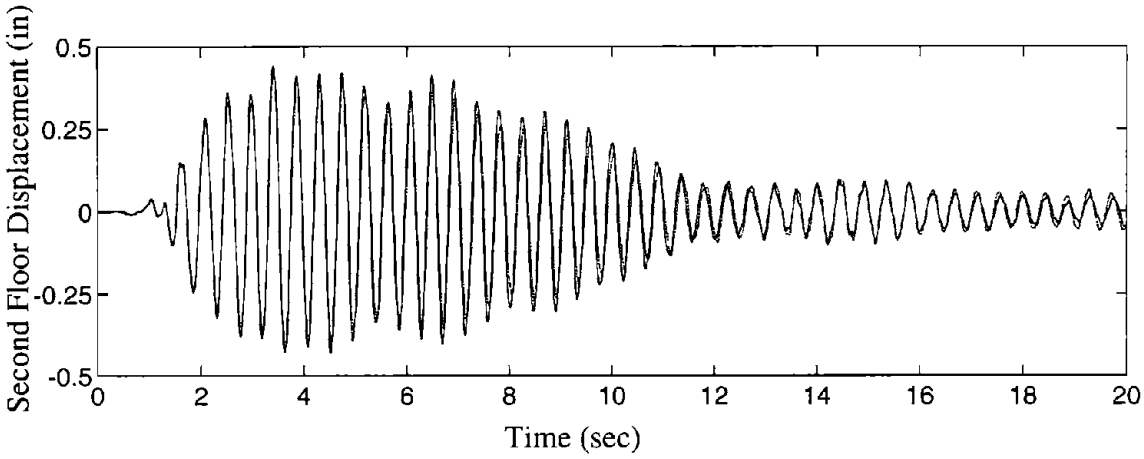

b) Second Floor Relative Displacement

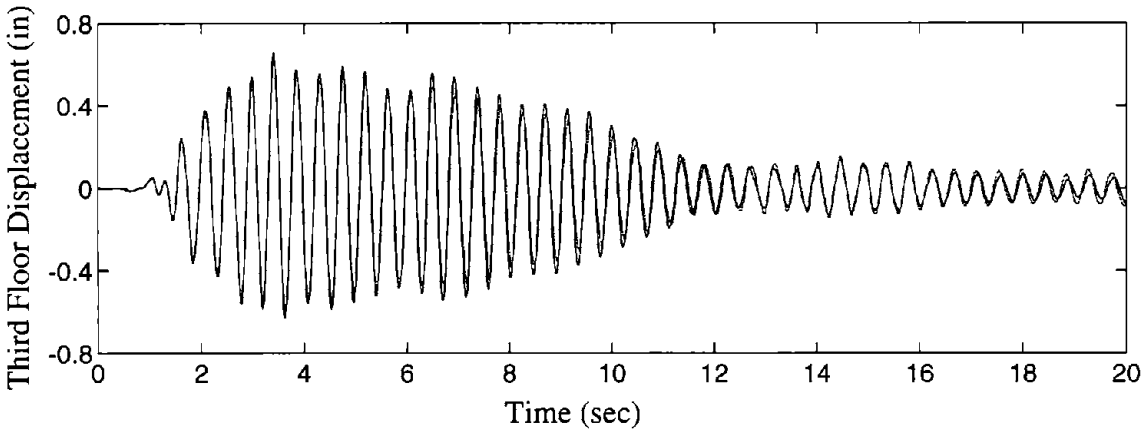

c) Third Floor Relative Displacement

Figure 6.1 Uncontrolled Experimental and Simulated Relative Displacements with Scaled El Centro Excitation.

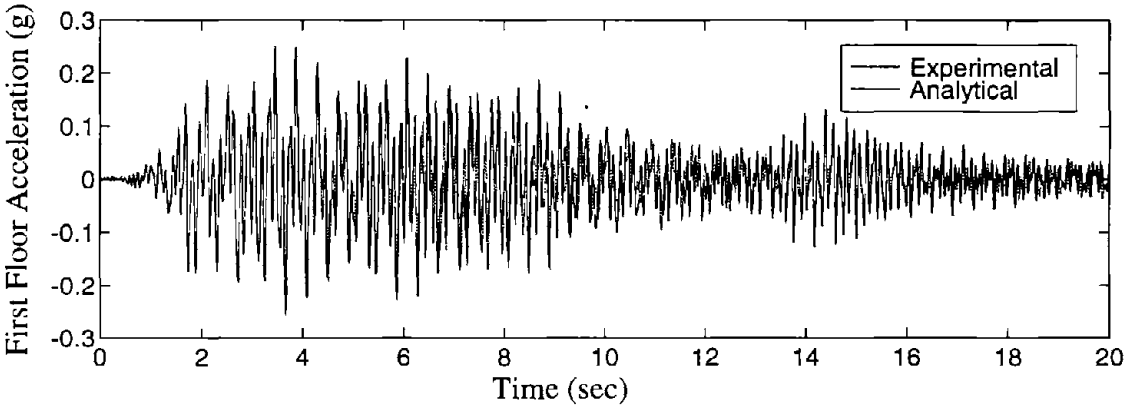

a) First Floor Absolute Acceleration

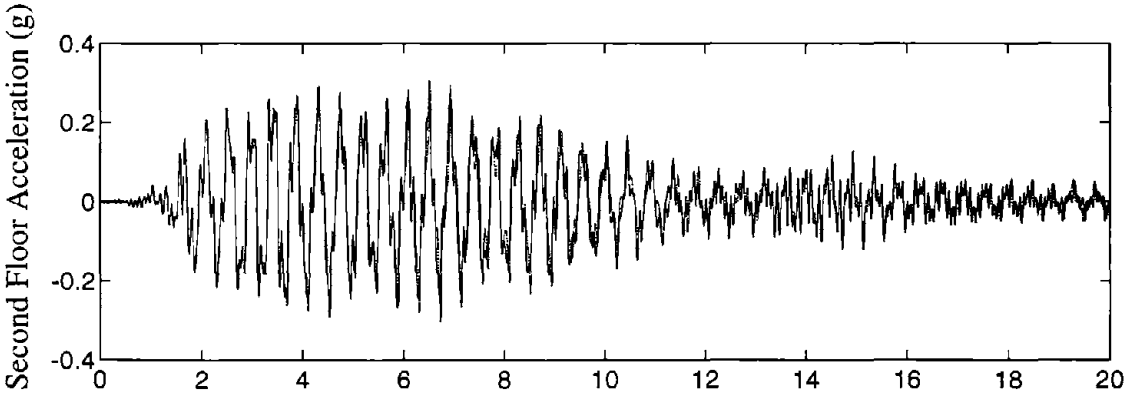

b) Second Floor Absolute Acceleration

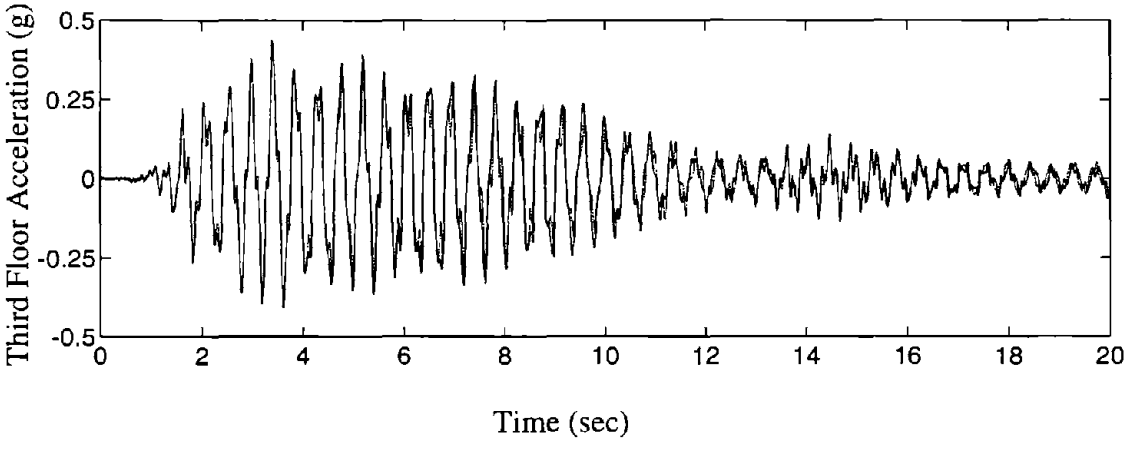

c) Third Floor Absolute Acceleration

Figure 6.2 Uncontrolled Experimental and Simulated Absolute Accelerations with Scaled El Centro Excitation.

analytical responses matched well, indicating that the simulation model is quite accurate. In addition, the analytical loop gain shown in Fig. 5.2 corresponds to this model. The analytical and experimental loop gains match well, indicating that the controller was operating as expected. Again, notice that the experimental and analytical loop gains match well in the frequency range of interest, indicating that the model is accurate and the control system is behaving as expected.

6.2 Discussion of Results and Comparison to Simulation

Twenty-one control designs were implemented, all of which were designed based on the original model. Each controller performed well and none resulted in unstable systems. Ten of the control designs were chosen for further study. The results of five representative control designs, designated A–E, are presented herein. Table 6.1 lists the five controllers with a description of the corresponding control strategy employed for each design. The performance objective in the design of Controller A was to minimize the relative displacements of the structure. This was achieved by weighting the three displacements equally and applying a smaller weighting to the actuator displacement. Controller B was designed to minimize the interstory displacements. In this case a weighting matrix was chosen which corresponded to weighting the three interstory displacements and a smaller weighting was applied to the actuator displacement. The performance

Table 6.1: Description of Control Strategies for Each Design.

Controller	*Control Strategy*
A	*Equal weighting on all three relative displacements and small weighting on the actuator displacement*
B	*Weighting on the interstory displacements and small weighting on the actuator displacement*
C	*Equal weighting on all three absolute accelerations*
D	*Weighting on third floor absolute acceleration*
E	*Weighting on third floor absolute acceleration and measurement of ground excitation*

objective in the design of Controller C was to minimize the absolute accelerations of the structure. This was achieved by placing equal weighting on all three absolute accelerations. Controller D was designed by weighting only the absolute acceleration of the third floor. Since the largest response in the fundamental mode is at the third floor, this approach serves to minimize all the structural responses in the fundamental mode. In Controller E an additional measurement, the base acceleration, was included in the measurement vector, and the absolute acceleration of the third floor was weighted.

The experimental and simulated responses for Controllers A–E are provided in Tables 6.2, 6.3 and 6.4. Table 6.2 provides *rms* responses of each controlled system to a broadband excitation (0-10 Hz) and Tables 6.3 and 6.4 report peak responses to the scaled El Centro and Taft excitations, respectively. Values for the absolute accelerations, $\ddot{x}_{ai}$, relative displacements, x_i, interstory displacements, actuator displacement, x_a, and control signal, u_c, are provided. The results include *rms* responses in the case of the bandlimited white noise excitation and peak responses for the scaled El Centro and Taft excitations. The percent reduction of each controlled response relative to the corresponding uncontrolled response is given in parentheses. Note the excellent agreement between the results predicted by the simulation and those obtained in the experiment. The force in the tendons (above the pretensioned value), f, was also measured during the experiment and is included in each table. Notice that the measured force in the tendons during the controlled tests was less than the force during the uncontrolled test for all control designs.

Comparing Controllers A and B, it is evident that no particular advantage was gained by weighting interstory displacements in this experiment. In all response categories except the first floor displacement, Controller A consistently performed better than Controller B. In the first floor relative displacement response, Controller B produced slightly better results than Controller A. However, Controller A reduced the remaining interstory displacements (*i.e.*, $x_2 - x_1$ and $x_3 - x_2$) 5-10% more than Controller B. Also, Controller A reduced the *rms* relative displacements of each floor by almost 62% and reduced the peak relative displacement responses by approximately 45-50%, whereas Controller B could only produce a 56% reduction in the *rms* relative displacements.

Table 6.2: *RMS* Responses of Controlled System to Broadband Excitation.

Controller	$\ddot{x}_{a1}, \frac{in}{s^2}$	$\ddot{x}_{a2}, \frac{in}{s^2}$	$\ddot{x}_{a3}, \frac{in}{s^2}$	x_1, in	x_2, in	x_3, in	$x_2 - x_1$ in	$x_3 - x_2$ in	f, lbf	x_a, in	u_c *Volts*
Experimental RMS Response for Bandlimited White Noise Ground Excitation (10 Hz)											
uncontrolled	36.1	39.7	53.0	0.065	0.161	0.228	0.097	0.071	444.0	0.002	—
A	20.5 (43.2)	18.2 (54.0)	23.8 (55.1)	0.026 (60.8)	0.061 (61.9)	0.087 (61.9)	0.037 (61.5)	0.029 (59.1)	183.6 (58.6)	0.008	0.162
B	17.7 (51.0)	18.2 (54.1)	24.4 (53.9)	0.028 (57.0)	0.070 (56.4)	0.100 (56.2)	0.043 (55.7)	0.032 (55.1)	205.6 (53.7)	0.006	0.125
C	14.1 (61.0)	15.1 (62.0)	20.3 (61.6)	0.025 (61.2)	0.062 (61.7)	0.087 (61.8)	0.037 (61.7)	0.027 (62.0)	170.1 (61.7)	0.008	0.168
D	13.7 (62.0)	13.8 (65.3)	18.2 (65.6)	0.024 (64.0)	0.055 (65.9)	0.077 (66.4)	0.033 (66.5)	0.024 (66.6)	147.2 (66.8)	0.010	0.210
E	13.5 (62.7)	13.3 (66.4)	17.5 (67.0)	0.023 (65.0)	0.053 (67.2)	0.074 (67.7)	0.031 (67.9)	0.023 (68.1)	141.3 (68.2)	0.011	0.220
Simulation RMS Response for Bandlimited White Noise Ground Excitation (10 Hz)											
uncontrolled	34.7	39.5	52.5	0.059	0.160	0.225	0.104	0.071	413.6	0.002	—
A	19.7 (43.2)	18.6 (52.9)	22.7 (56.9)	0.025 (57.8)	0.062 (61.3)	0.087 (61.4)	0.040 (61.4)	0.029 (58.7)	175.4 (57.6)	0.009	0.187
B	17.0 (50.8)	18.7 (52.7)	24.3 (53.8)	0.027 (54.1)	0.072 (54.9)	0.102 (54.7)	0.047 (54.7)	0.033 (54.3)	195.3 (52.8)	0.007	0.141
C	13.5 (61.0)	15.3 (61.2)	20.2 (61.6)	0.025 (57.3)	0.064 (60.2)	0.089 (60.6)	0.040 (61.1)	0.027 (61.9)	157.9 (61.8)	0.010	0.195
D	13.1 (62.1)	13.9 (64.9)	17.7 (66.4)	0.024 (59.5)	0.056 (64.9)	0.077 (65.7)	0.035 (66.6)	0.023 (67.3)	134.0 (67.6)	0.013	0.250
E	12.9 (62.9)	13.4 (66.1)	16.9 (67.9)	0.023 (60.1)	0.054 (66.1)	0.074 (67.2)	0.033 (68.2)	0.022 (68.9)	132.8 (67.9)	0.013	0.266

Table 6.3: Peak Responses of Controlled System to Scaled El Centro Excitation.

Controller	$\ddot{x}_{a1}, \frac{in}{s^2}$	$\ddot{x}_{a2}, \frac{in}{s^2}$	$\ddot{x}_{a3}, \frac{in}{s^2}$	x_1, *in*	x_2, *in*	x_3, *in*	$x_2 - x_1$ *in*	$x_3 - x_2$ *in*	*f, lbf*	x_a, *in*	u_c, *Volts*
Experimental Peak Response for Quarter Scale El Centro Earthquake Excitation.											
uncontrolled	93.0	118.7	158.6	0.178	0.421	0.627	0.273	0.209	1156	0.005	—
A	68.3 (26.6)	64.6 (45.5)	97.7 (38.4)	0.100 (44.1)	0.221 (47.6)	0.318 (49.4)	0.140 (48.9)	0.115 (44.8)	629.6 (45.5)	0.031	0.625
B	67.2 (27.7)	68.2 (42.6)	94.6 (40.3)	0.102 (42.6)	0.263 (37.5)	0.388 (38.1)	0.167 (38.9)	0.127 (39.2)	698.9 (39.5)	0.024	0.500
C	55.9 (39.9)	57.8 (51.3)	84.1 (47.0)	0.095 (46.6)	0.230 (45.5)	0.333 (46.9)	0.142 (47.9)	0.104 (50.5)	584.0 (49.5)	0.034	0.688
D	57.3 (38.5)	56.5 (52.3)	82.2 (48.2)	0.094 (47.2)	0.211 (50.0)	0.293 (53.3)	0.129 (52.9)	0.095 (54.5)	495.2 (57.2)	0.041	0.824
E	51.7 (44.4)	53.3 (55.0)	78.4 (50.6)	0.093 (47.8)	0.206 (51.1)	0.284 (54.7)	0.125 (54.3)	0.091 (56.3)	927.5 (19.8)	0.044	0.284
Simulation Peak Response for Quarter Scale El Centro Earthquake Excitation.											
uncontrolled	99.1	103.9	168.5	0.169	0.438	0.660	0.309	0.221	1194	0.006	—
A	64.1 (35.3)	66.1 (36.4)	93.7 (44.4)	0.098 (41.7)	0.225 (48.8)	0.327 (50.4)	0.153 (50.5)	0.116 (47.6	622.2 (47.9)	0.035	0.700
B	64.1 (35.3)	70.9 (31.8)	95.6 (43.3)	0.097 (42.4)	0.265 (39.5)	0.390 (40.8)	0.183 (40.8)	0.126 (42.9)	692.1 (42.0)	0.027	0.538
C	52.7 (46.8)	59.4 (42.8)	81.3 (51.7)	0.093 (44.6)	0.236 (46.1)	0.341 (48.3)	0.158 (48.9)	0.106 (52.1)	553.2 (53.7)	0.039	0.770
D	52.9 (46.6)	56.8 (45.4)	76.2 (54.8)	0.095 (43.5)	0.214 (51.1)	0.299 (54.6)	0.140 (54.7)	0.097 (56.3)	474.9 (60.2)	0.048	0.953
E	48.7 (50.9)	51.8 (50.2)	72.9 (56.8)	0.094 (44.2)	0.207 (52.9)	0.287 (56.4)	0.133 (56.9)	0.093 (58.0)	459.8 (61.5)	0.051	1.026

Table 6.4: Peak Response of Controlled System to Scaled Taft Earthquake Excitation.

Controller	$\ddot{x}_{a1}, \frac{in}{s^2}$	$\ddot{x}_{a2}, \frac{in}{s^2}$	$\ddot{x}_{a3}, \frac{in}{s^2}$	x_1, *in*	x_2, *in*	x_3, *in*	$x_2 - x_1$ *in*	$x_3 - x_2$ *in*	*f, lbf*	x_a, *in*	u_c, *Volts*
Experimental Peak Response for One-Half Scale Taft Earthquake Excitation.											
uncontrolled	102.7	104.5	146.4	0.165	0.408	0.585	0.248	0.187	1079	0.005	—
A	55.9 (45.5)	55.6 (46.8)	98.9 (32.4)	0.086 (48.0)	0.222 (45.6)	0.341 (41.8)	0.146 (41.1)	0.122 (34.9)	576.2 (46.6)	0.029	0.617
B	57.3 (44.2)	60.9 (41.7)	102.9 (29.7)	0.099 (39.9)	0.260 (36.2)	0.390 (33.4)	0.169 (32.1)	0.134 (28.4)	657.4 (39.0)	0.023	0.492
C	49.4 (51.8)	52.1 (50.1)	84.8 (42.1)	0.083 (49.4)	0.224 (45.1)	0.333 (43.2)	0.144 (42.0)	0.112 (40.2)	562.9 (47.8)	0.031	0.629
D	44.5 (56.7)	48.2 (53.8)	75.3 (48.6)	0.072 (56.0)	0.190 (53.5)	0.282 (51.8)	0.123 (50.3)	0.097 (48.3)	473.3 (56.1)	0.036	0.741
E	43.5 (57.7)	46.4 (55.6)	71.8 (50.9)	0.070 (57.2)	0.184 (54.8)	0.273 (53.4)	0.121 (51.2)	0.094 (49.7)	460.4 (57.3)	0.038	0.786
Simulation Peak Response for One-Half Scale Taft Earthquake Excitation.											
uncontrolled	89.6	109.9	144.3	0.149	0.417	0.601	0.272	0.191	1054	0.005	—
A	57.1 (36.3)	59.0 (46.3)	94.0 (34.8)	0.079 (46.8)	0.216 (48.2)	0.310 (43.2)	0.161 (40.8)	0.125 (34.5)	602.0 (42.8)	0.032	0.668
B	57.9 (35.4)	61.6 (44.0)	102.9 (28.7)	0.090 (39.9)	0.262 (37.1)	0.363 (33.5)	0.188 (31.1)	0.137 (28.2)	604.1 (42.7)	0.025	0.528
C	46.0 (48.7)	54.8 (50.1)	84.9 (41.2)	0.077 (48.7)	0.222 (46.9)	0.336 (44.1)	0.158 (41.9)	0.114 (40.4)	516.0 (51.0)	0.033	0.685
D	42.7 (52.3)	49.9 (54.6)	71.9 (50.2)	0.066 (55.6)	0.180 (56.8)	0.276 (54.1)	0.130 (52.4)	0.096 (49.9)	479.8 (54.5)	0.040	0.805
E	40.7 (54.6)	47.7 (56.6)	69.0 (52.2)	0.068 (54.3)	0.175 (58.0)	0.242 (55.7)	0.125 (54.1)	0.091 (52.3)	478.5 (54.6)	0.042	0.863

Comparing Controllers C and D, which both weight various accelerations of the structure, Controller D performs significantly better. In the design of Controller D, the absolute acceleration of the third floor was weighted heavily, which forced the controller to concentrate most of its efforts on the fundamental mode of the structure. In the design of Controller C, the absolute acceleration of each floor was weighted equally, and the controller had less of an effect in the fundamental mode. Choosing to weight only the absolute acceleration of the third floor also made it possible to design a higher authority controller. Therefore, application of Controller D resulted in a moderate increase in the ability of the controller to reduce the acceleration responses and a significant increase in the ability of the controller to reduce all of the displacement responses as compared to Controller C.

In all response categories, Controller E performed best, achieving a 62-68% reduction in all *rms* responses to a broadband disturbance. Controller E performed best because it had the advantage of measuring the ground acceleration, in addition to the structural accelerations and actuator displacement. Including the disturbance as a measurement produced moderately better results than Controller D, which had the same performance objective, but did not measure the ground acceleration. With Controller E the peak relative displacement of the third floor due to the scaled El Centro and Taft earthquakes was reduced by 55% and 53%, respectively, indicating that a significant reduction in the response in the fundamental mode was achieved.

Damping ratios for the first three modes were also determined for each controlled system. These values are provided in Table 6.5 for each of the controllers mentioned above. The results exhibit the same trends as the *rms* and peak responses discussed above. Again, Controller E performed best, increasing the damping in the fundamental mode from 1.0% to 11.1%. Comparing Controllers C and D, one observes that Controller D has a significant effect on the damping ratio of the fundamental mode of the system. Therefore, weighting only the third floor absolute acceleration had the intended effect on the responses of the system in the fundamental mode. Generally, the control strategies which weighted the absolute accelerations of the structure (Controllers C,

Table 6.5: Estimated Damping Ratios of Structural Modes.

Controller	*Mode 1* (%)	*Mode 2* (%)	*Mode 3* (%)
uncontrolled	1.0	0.7	0.4
A	6.7	5.0	1.1
B	4.9	3.5	1.5
C	7.6	6.6	2.0
D	10.6	6.4	1.7
E	11.1	6.8	1.9

D, and E) resulted in higher damping ratios than those weighting relative displacements (Controllers A and B).

The experimental relative displacement and absolute acceleration responses of the closed-loop system formed with the best control design, Controller E, are compared to the experimental uncontrolled responses for the scaled El Centro excitation in Figs. 6.3a-c and 6.4a-c, respectively. Clearly, the controller has a significant effect on the magnitude of the system responses and on the damping characteristics. The experimental transfer functions of the uncontrolled system are compared to the experimental transfer functions of the controlled system (using Controller E) in Figs. 6.5-6.10. The experimental and simulated closed-loop responses are compared in Figs. 6.11a-c and 6.12a-c. Notice the excellent agreement between the simulated and experimental responses, indicating that the model is very accurate and there were no unforeseen problems in the implementation of the controller.

6.3 Comments

Notice from the results that by weighting the absolute accelerations, both the absolute accelerations and relative displacements are significantly reduced. However, weighting the relative displacements does not effectively minimize the absolute accelerations. This observation can be explained by considering the relationship between the relative displacements and absolute accel-

erations. In the relative displacement responses, the fundamental mode accounts for the largest component of the responses. Therefore, a controller which concentrates on the response in this mode will cause a significant reduction in the relative displacements. However, because the higher modes contribute significantly to the acceleration responses, and these modes are not significantly affected by the controller, the accelerations will not be reduced as greatly as the displacements. By placing weighting on the absolute accelerations, the response in all modes is affected, thus reducing the displacements as well as the accelerations.

Finally, as empirical evidence of robustness of the controllers, it should be mentioned that during one of the controlled experiments a sensor was left disconnected. Nevertheless, the resulting structural responses were reduced, although not as greatly as when all sensors were connected.

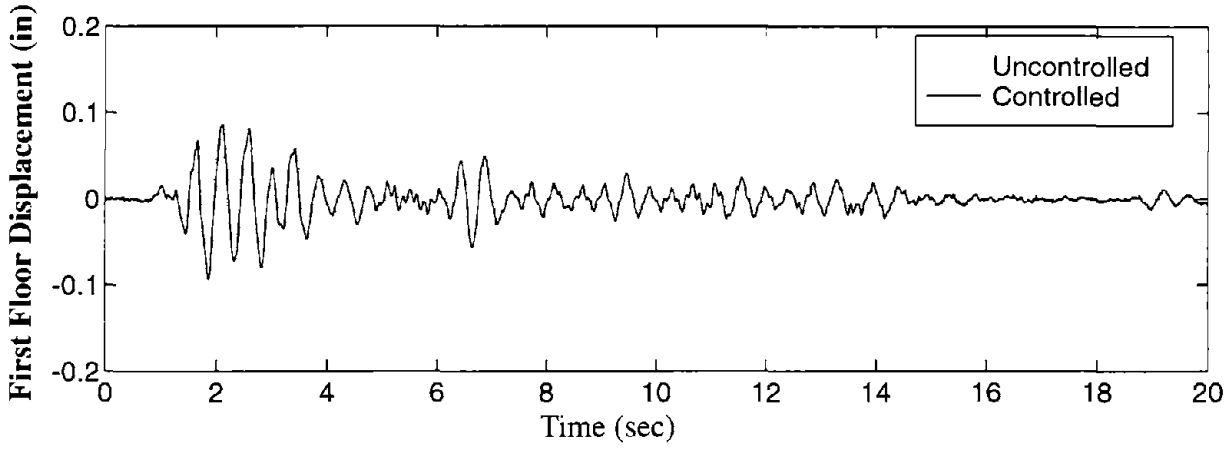

a) First Floor Relative Displacement

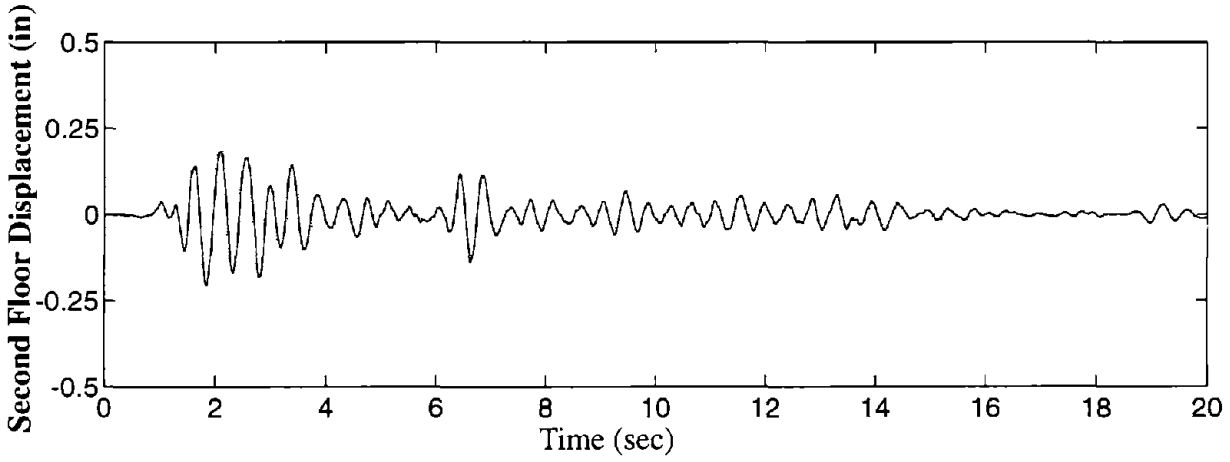

b) Second Floor Relative Displacement

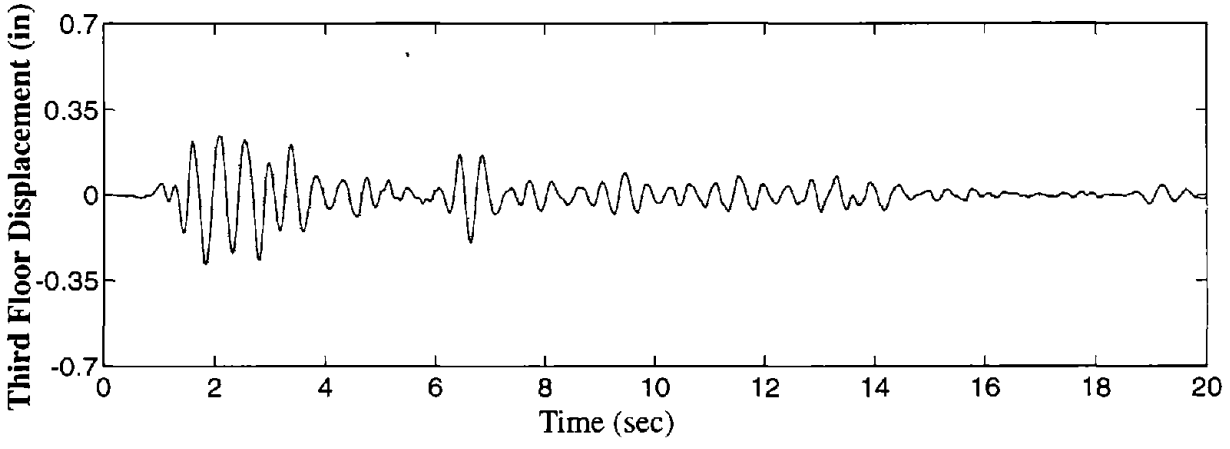

c) Third Floor Relative Displacement

Figure 6.3 Uncontrolled and Controlled Experimental Relative Displacements (Controller E).

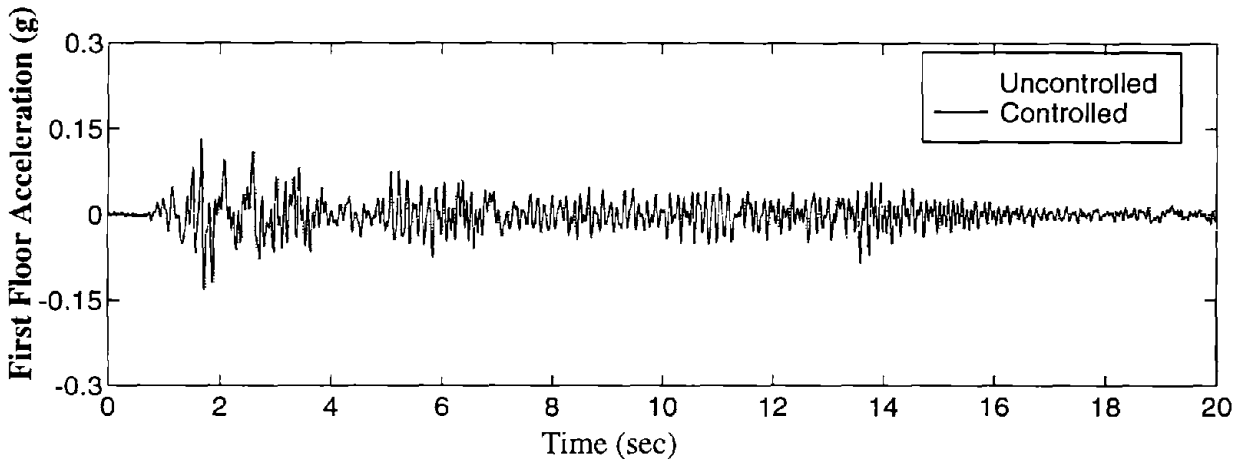

a) First Floor Absolute Acceleration

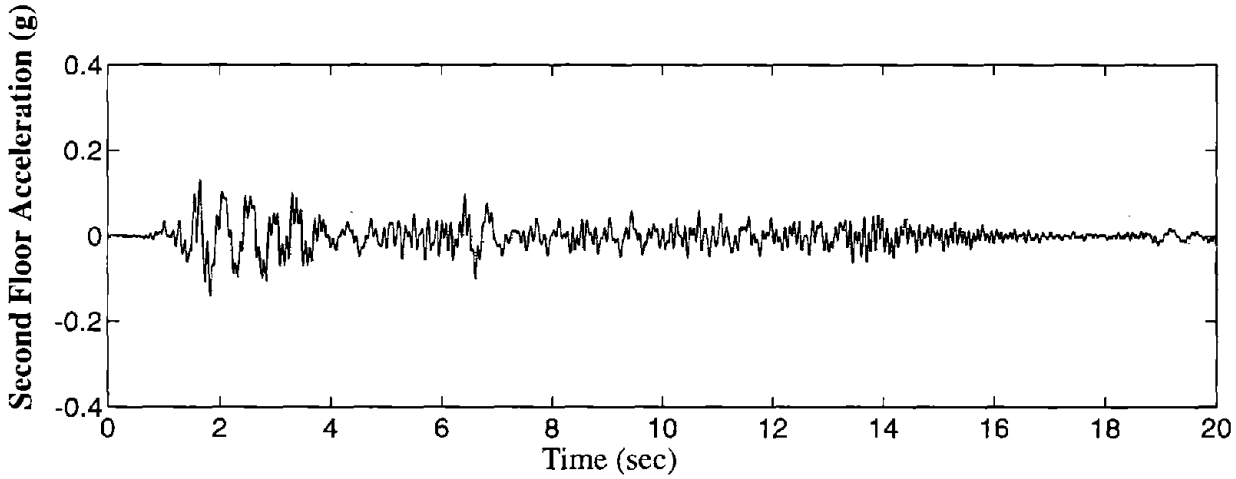

b) Second Floor Absolute Acceleration

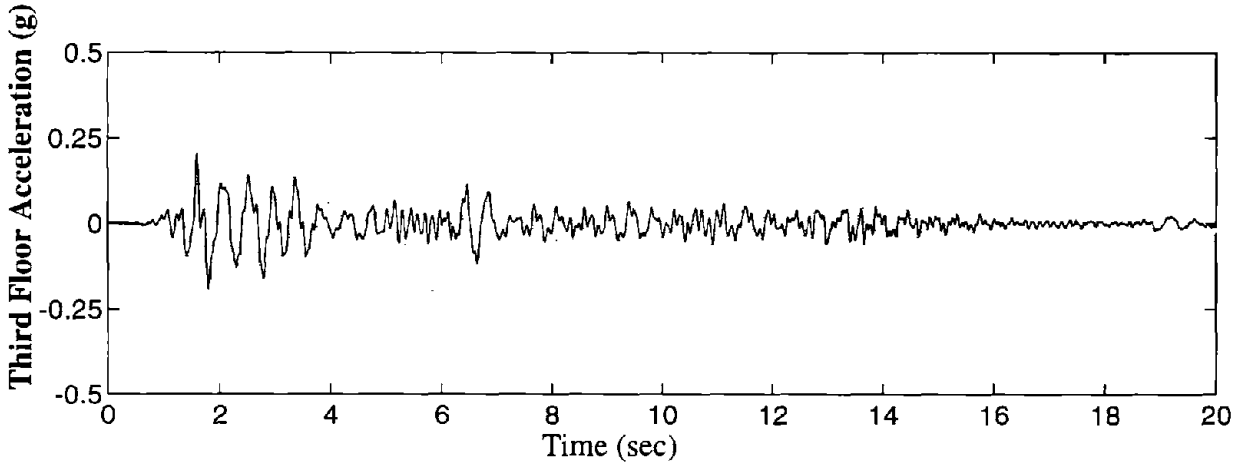

c) Third Floor Absolute Acceleration

Figure 6.4 Uncontrolled and Controlled Experimental Absolute Accelerations (Controller E).

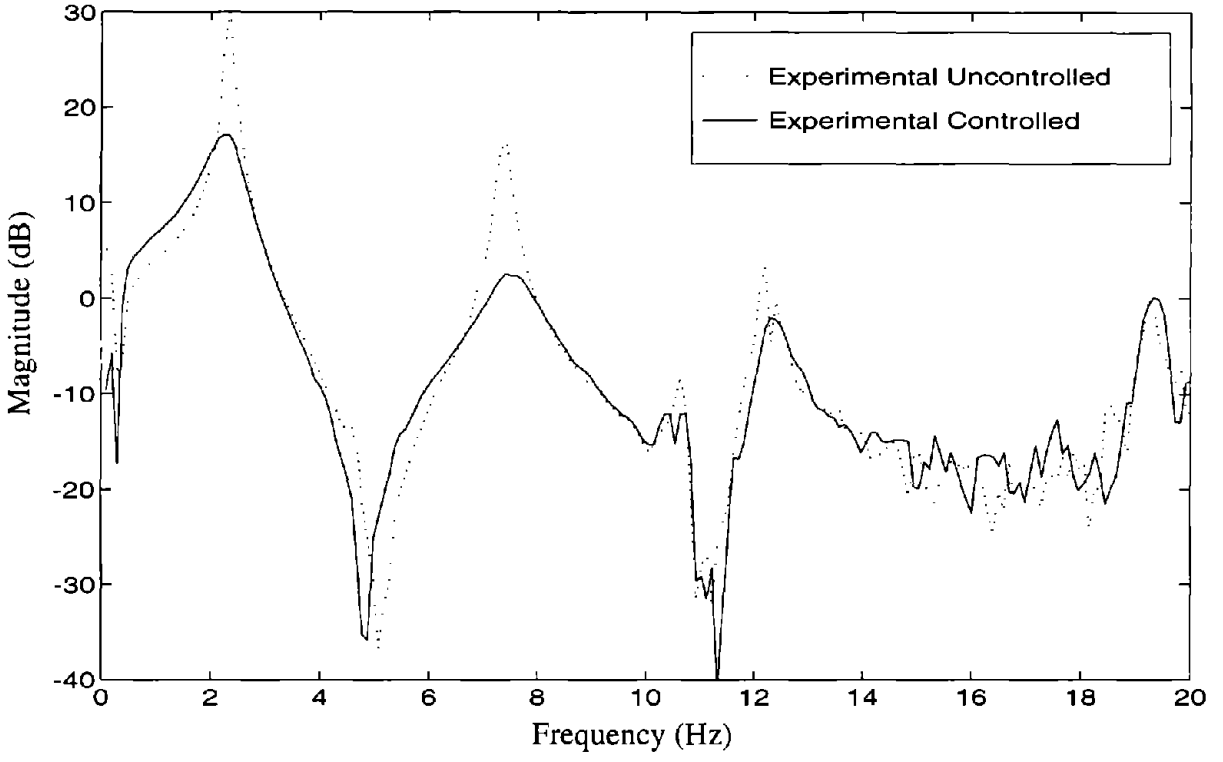

Figure 6.5 Comparison of Uncontrolled and Controlled Transfer Functions from the Ground Acceleration to the First Floor Relative Displacement.

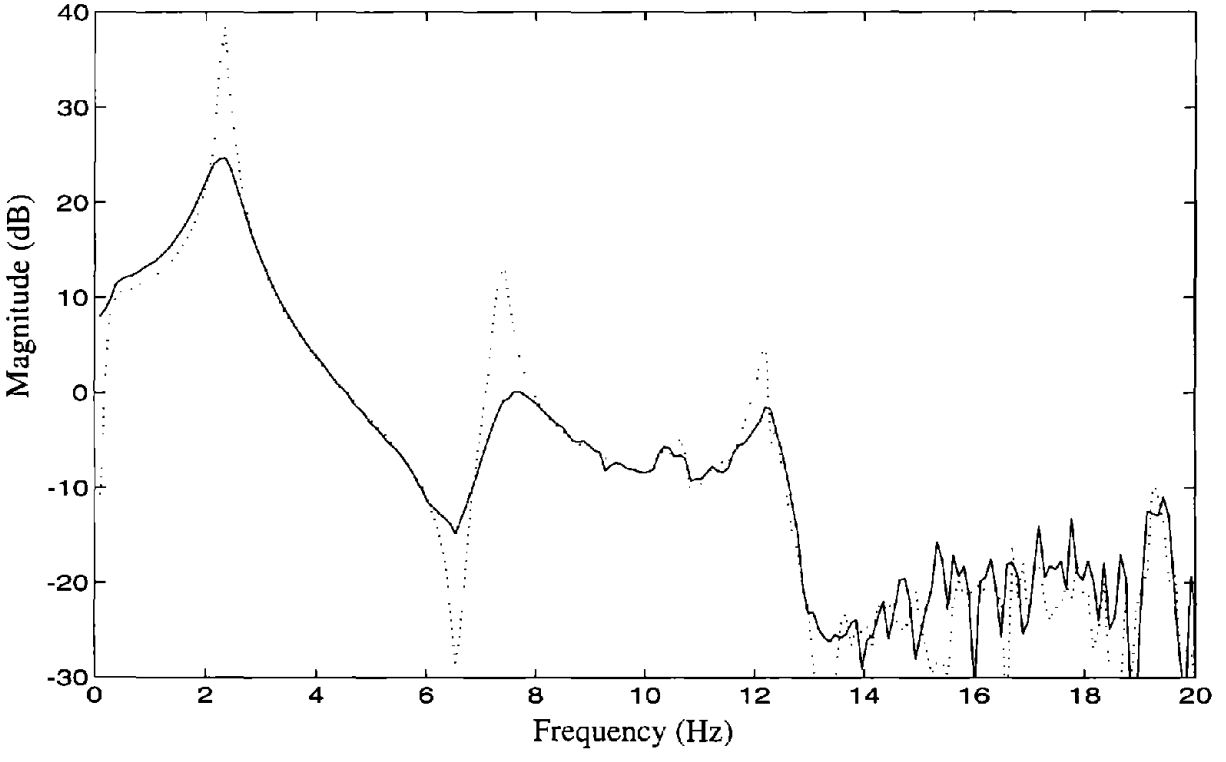

Figure 6.6 Comparison of Uncontrolled and Controlled Transfer Functions from the Ground Acceleration to the Second Floor Relative Displacement.

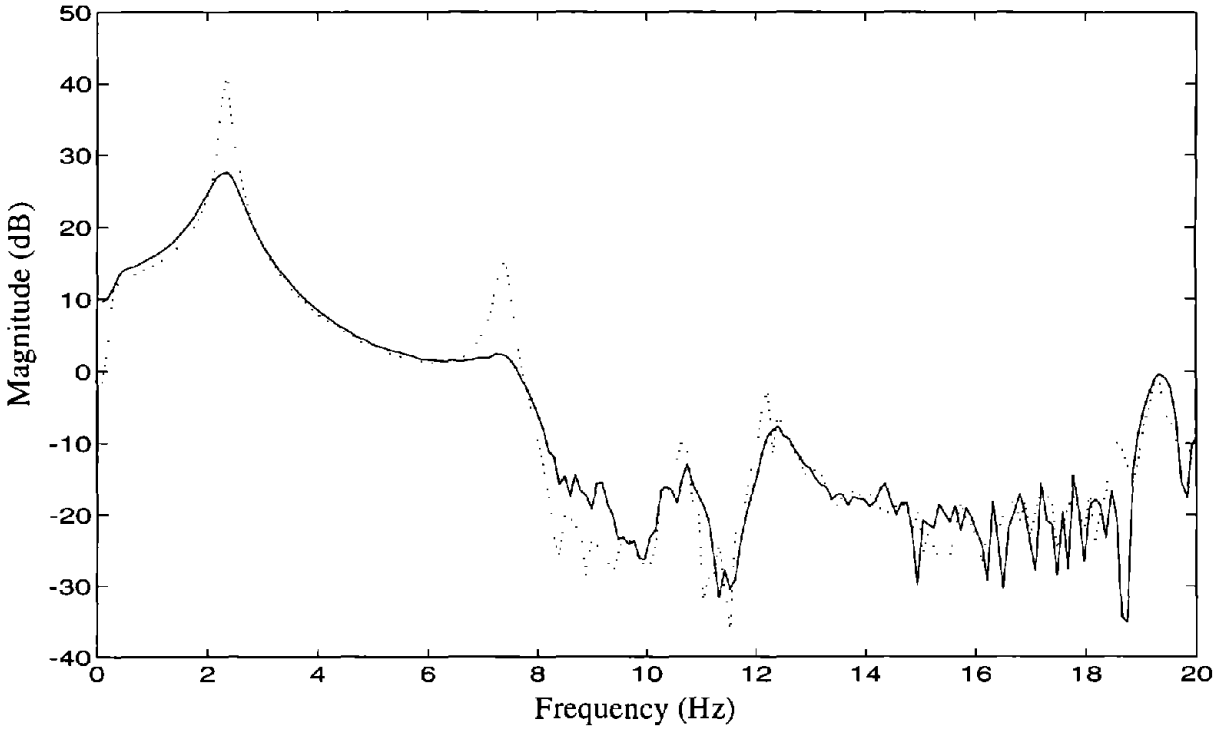

Figure 6.7 Comparison of Uncontrolled and Controlled Transfer Functions from the Ground Acceleration to the Third Floor Relative Displacement.

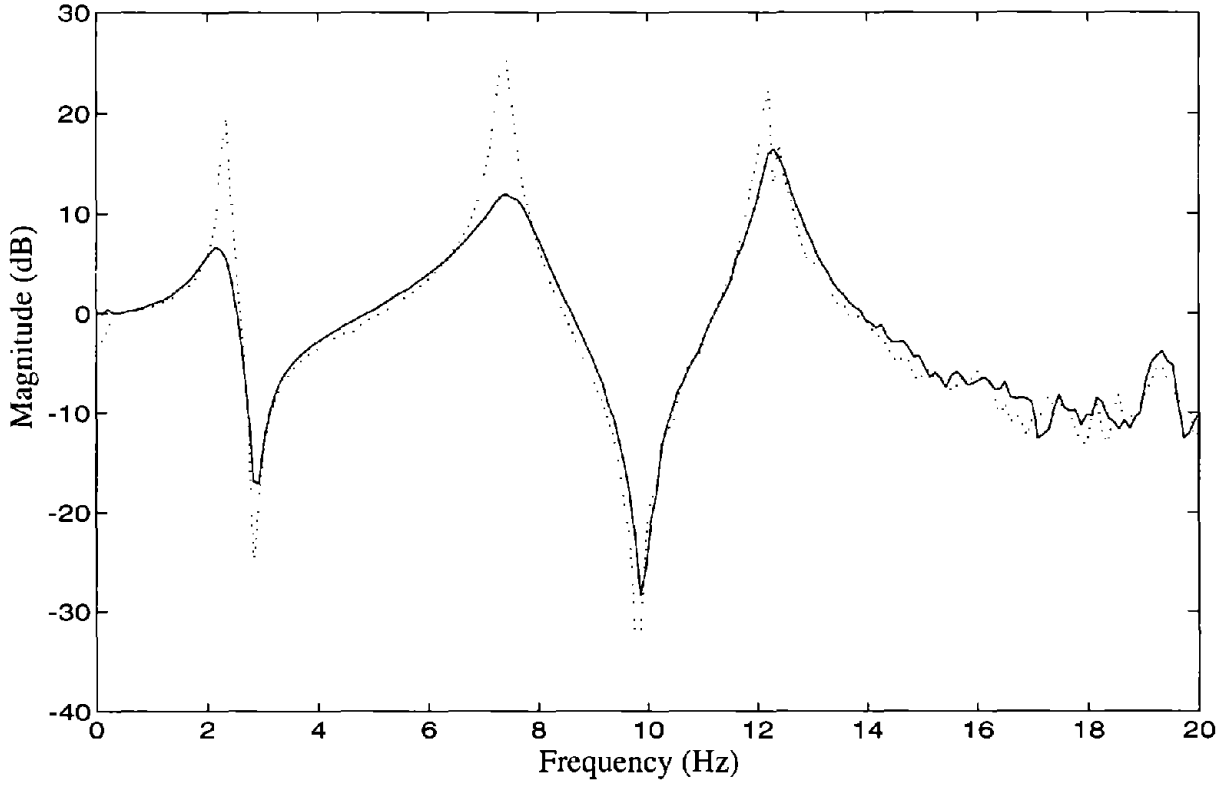

Figure 6.8 Comparison of Uncontrolled and Controlled Transfer Functions from the Ground Acceleration to the First Floor Absolute Acceleration.

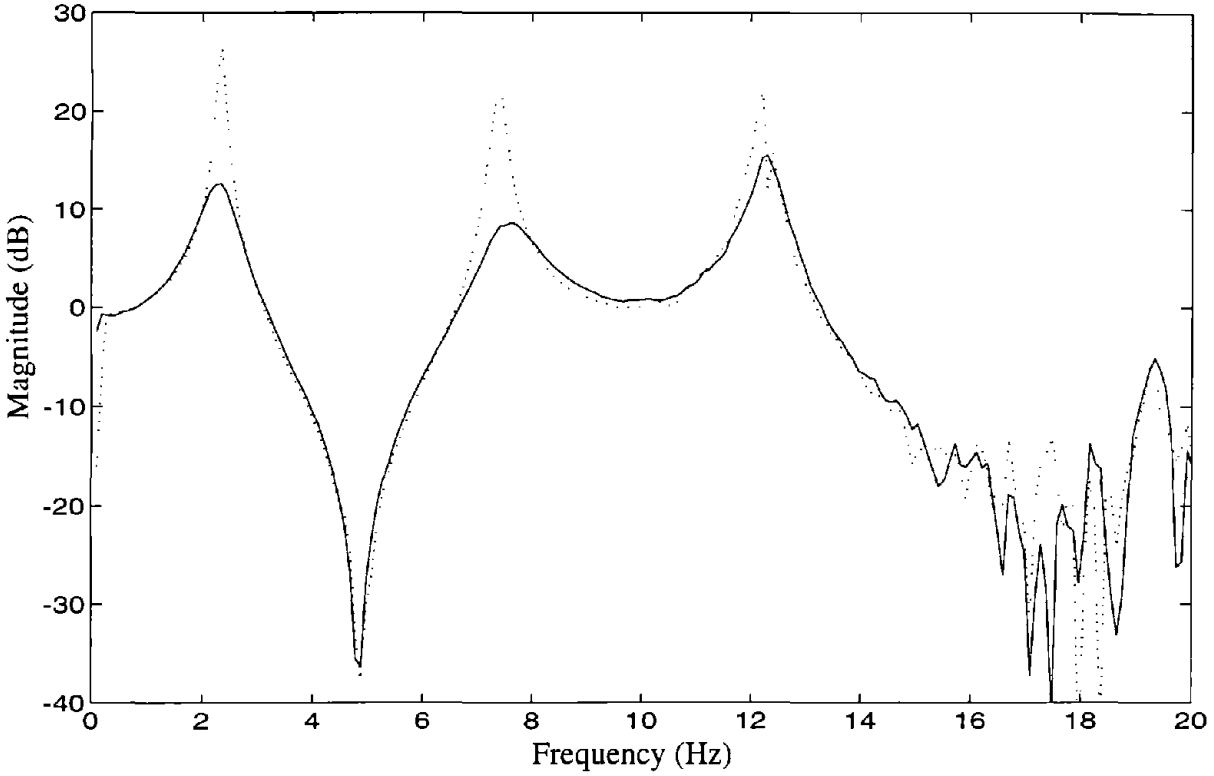

Figure 6.9 Comparison of Uncontrolled and Controlled Transfer Functions from the Ground Acceleration to the Second Floor Absolute Acceleration.

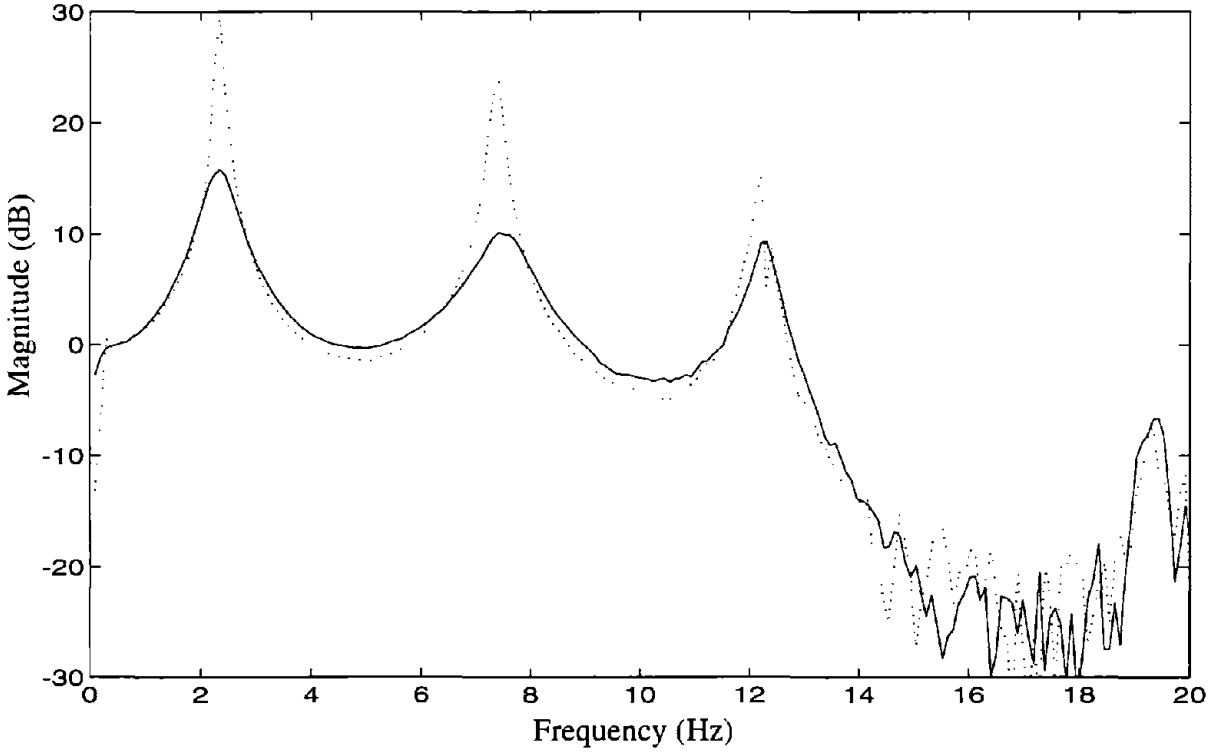

Figure 6.10 Comparison of Uncontrolled and Controlled Transfer Functions from the Ground Acceleration to the Third Floor Absolute Acceleration.

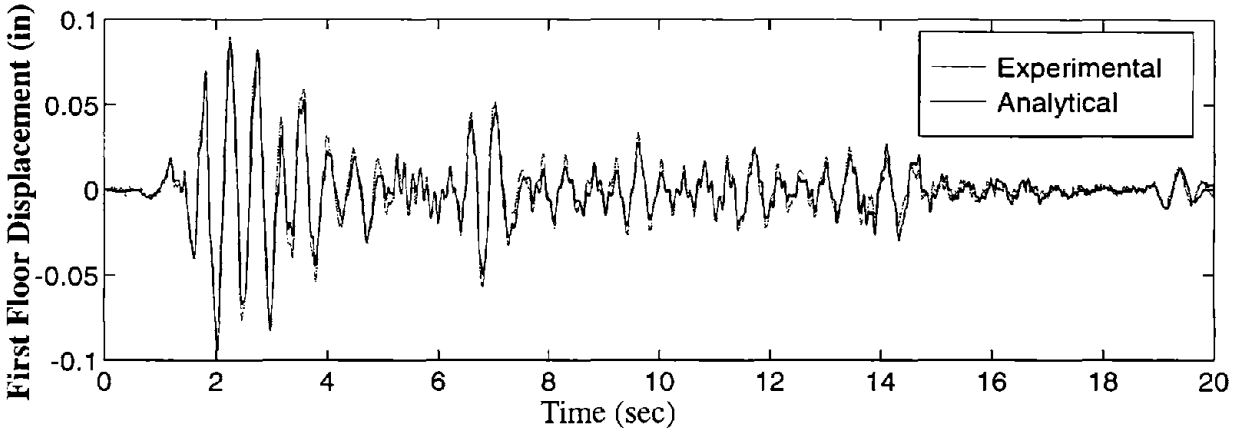

a) First Floor Relative Displacement

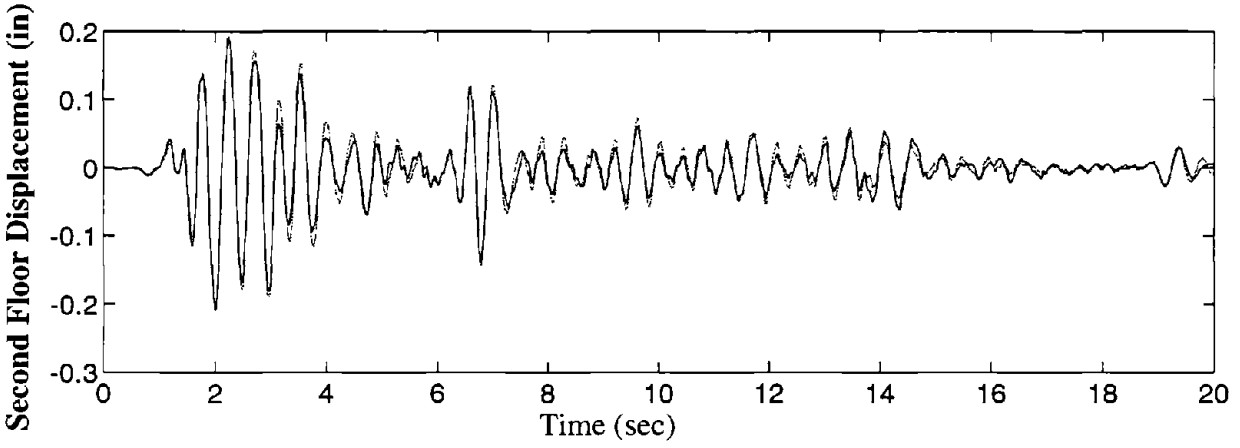

b) Second Floor Relative Displacement

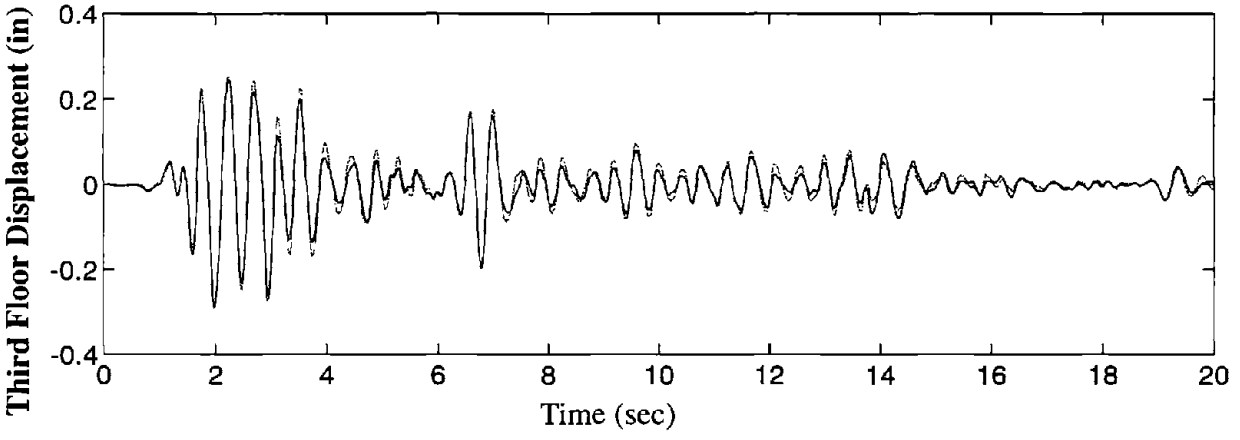

c) Third Floor Relative Displacement

Figure 6.11 Comparison of Experimental and Simulated Controlled Relative Displacement Responses (Controller E).

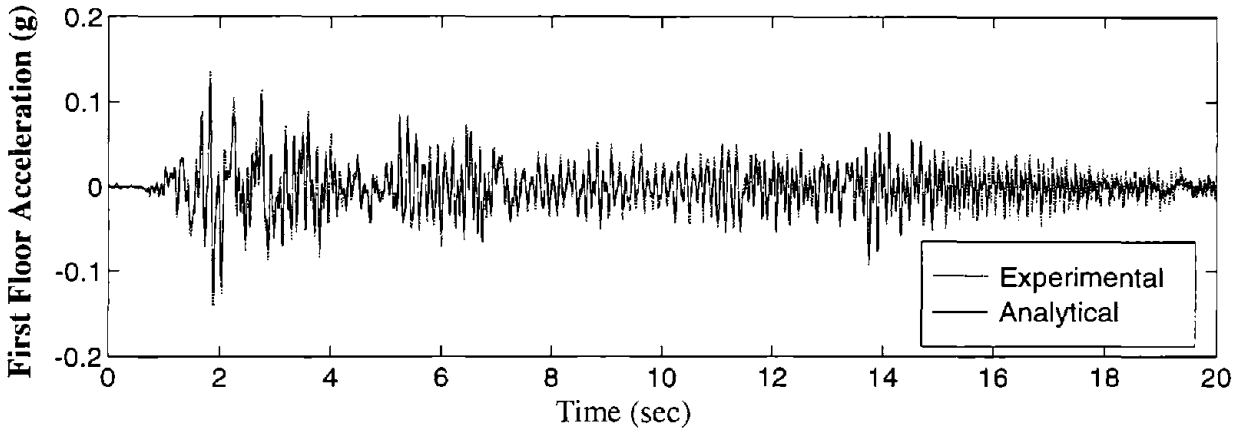

a) First Floor Absolute Acceleration

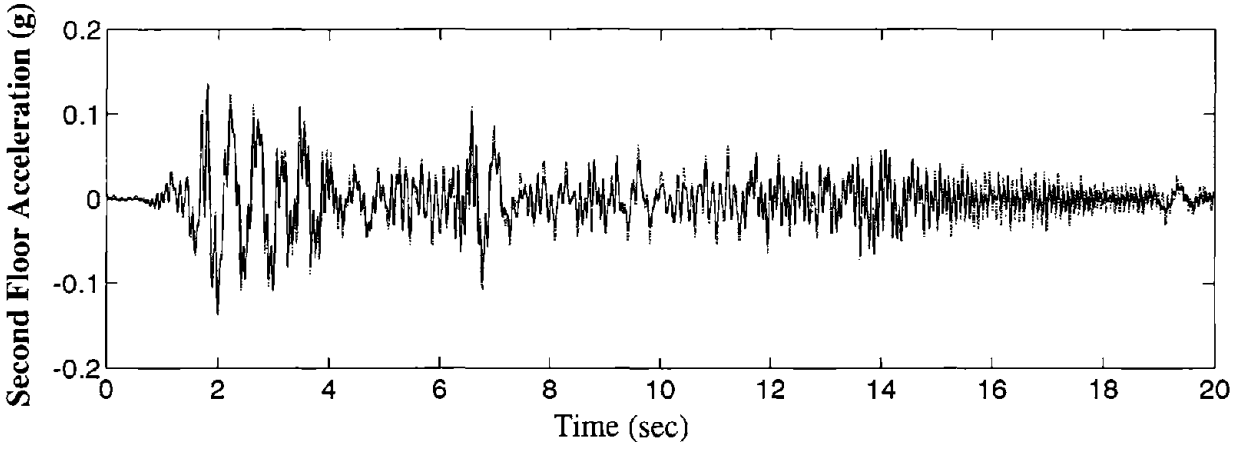

b) Second Floor Absolute Acceleration

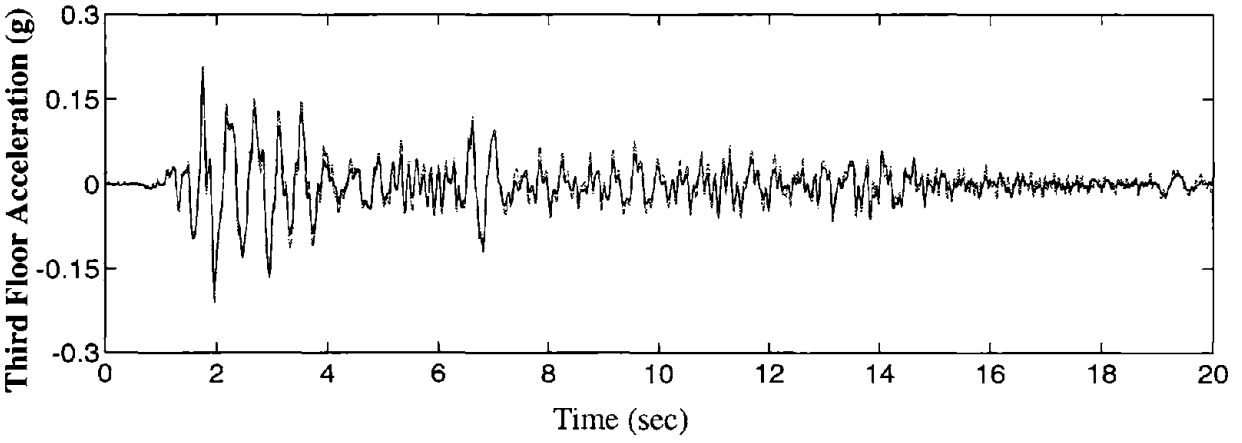

c) Third Floor Absolute Acceleration

Figure 6.12 Comparison of Experimental and Simulated Controlled Absolute Acceleration Responses (Controller E).

SECTION 7
CONCLUSION

Active control designs based on acceleration feedback have been successfully implemented and verified on a tendon-controlled, MDOF test structure at the National Center for Earthquake Engineering Research at SUNY, Buffalo. The effects of actuator dynamics and control-structure-interaction were incorporated into the system identification procedure. The identified ten-state model reproduced the experimental results well in both the frequency domain and the time domain. Experimental results indicate that effective and robust controllers can be designed using an acceleration feedback control strategy, and full state feedback performance can be recovered.

Using H_2/LQG control design techniques, many different controllers were designed, each with a different performance objective. Some controllers were designed to minimize the three relative displacements of the structure while others minimized the absolute acceleration of the third floor. The best control design, which was designed to minimize the third floor acceleration and included the ground acceleration as an additional measurement (Controller E), achieved a 60-68% reduction in all *rms* displacement and acceleration measurements. Similarly, a 55% and 53% reduction in the peak response of the third floor displacement under the scaled El Centro earthquake and Taft excitations, respectively, was achieved. Comparable reductions were obtained for the other peak responses. In all cases, including the ground acceleration as an additional measurement resulted in a better control system. Additionally, excellent agreement was obtained between the simulations based on the identified analytical model and the experimental results.

By comparing the various control designs it was observed that weighting the displacements of the structure did not effectively reduce the acceleration responses. However, by weighting the accelerations in the control design, both the displacements and accelerations were efficiently reduced.

SECTION 8
REFERENCES

Antoniou, Andreas. 1993. *Digital Filters: Analysis, Design, and Applications*, McGraw-Hill, Inc., New York, pp. 444–446.

Bergland, G.D. 1969. A Guided Tour of the Fast Fourier Transform. *IEEE Spectrum*, vol. 6, pp. 41–52, July.

Bendat, J.S. and Piersol, A.G. 1980. *Engineering Applications of Correlation and Spectral Analysis*, John Wiley & Sons, Inc., New York, pp. 57-–76.

Chung, L.L., R.C. Lin, T.T. Soong & A.M. Reinhorn. 1989. Experiments on Active Control for MDOF Seismic Structures," *J. of Engrg. Mech.*, ASCE, Vol. 115, No. 8, pp. 1609–1627.

Dyke, S.J., B.F. Spencer Jr., P. Quast & M.K. Sain. 1993. Protective System Design: The Role of Control-Structure Interaction. *Proc. of the Int. Workshop on Structural Control*, Univ. of Southern California, pp. 100–114.

Dyke, S.J., B.F. Spencer Jr., P. Quast & M.K. Sain. 1994. The Role of Control-Structure Interaction in Protective System Design. *J. of Engrg. Mech*, ASCE (in press).

Friedlander, B. 1982. Lattice Filters for Adaptive Processing. *Proc. of the IEEE*, 70(3).

Harris, F.J. 1978. On the Use of Windows for Harmonic Analysis with Discrete Fourier Transforms. *Proc. of the IEEE*, 66(1), pp. 51–83.

Housner, G.W. & S.F. Masri, Eds. 1990. *Proc. of the U.S. National Workshop on Structural Control Research*, USC Publications No. M9013, University of Southern California.

Housner, G.W. & S.F. Masri, Eds. 1993. *Proc. of the Int. Workshop on Structural Control*, Univ. of Southern California.

Laub, A.J. 1980. Computation of Balancing Transformations. *Proc. JACC*, Vol. 2, paper FA8-E.

MATLAB. 1993. The Math Works, Inc. Natick, Massachusetts.

Moore, B.C. 1981. Principal Component Analysis in Linear Systems: Controllability, Observability, and Model Reduction. *IEEE Trans. on Automatic Control*, pp. 26–31.

Quast, P., B.F. Spencer Jr., M.K. Sain & S.J. Dyke 1994. Microcomputer Implementation of Digital Control Strategies for Structural Response Reduction. *Microcomputers in Civil Engrg.*, (in press).

Reinhorn, A.M., T.T. Soong, M.A. Riley, R.C. Lin, S. Aizawa, & M. Higashino, Full Scale Implementation of Active Control. II: Installation and Performance., *Journal of Structural Engineering*, ASCE, Vol. 119, No. 6, June 1993, pp. 1935–1960.

Schoukens, J. and R. Pintelon. 1991. *Identification of Linear Systems, A Pratical Guide to Accurate Modeling*. Pergamon Press. New York, pp. 39–49.

Soong, T.T. 1990. *Active Structural Control: Theory and Practice*, Longman Scientific and Technical, Essex, England.

Soong, T.T., A.M. Reinhorn, Y.P. Wang, & R.C. Lin. Full Scale Implementation of Active Control. I: Design and Simulation., *Journal of Structural Engineering*, ASCE, Vol. 117, Noveember 1991, pp. 3516–3536.

Spencer Jr., B.F., J. Suhardjo & M.K. Sain. 1991. Frequency Domain Control Algorithms for Civil Engineering Applications. *Proc. of the Int. Workshop on Tech. for Hong Kong's Infrastructure Development*, Hong Kong, December 19–20, 169–178.

Spencer Jr., B.F., J. Suhardjo & M.K. Sain. 1994a. Frequency Domain Optimal Control Strategies for Aseismic Protection. *J. of Engrg. Mech*, ASCE, Vol. 120, No. 1, pp. 135–159.

Spencer Jr., B.F., P. Quast., S.J. Dyke & M.K. Sain. 1994b. Digital Signal Processing Techniques for Active Structural Control. *Proc. of the 1994 ASCE Structures Congress*, Atlanta, Georgia.

Spencer Jr., B.F., M.K. Sain, C.-H. Won, D. Kaspari, Jr., & P.M. Sain 1994c. Reliability-Based Measures of Structural Control Robustness. *Structural Safety*, (in press).

Suhardjo, J. 1990. *Frequency Domain Techniques for Control of Civil Engineering Structures with Some Robustness Considerations*, Ph.D. Dissertation, Univ. of Notre Dame, Dept. of Civil Engineering.

SECTION 9

APPENDIX: STATE SPACE MODEL

The structural system model is provided in this section in the form:

$$\dot{\mathbf{x}} = \mathbf{A}\mathbf{x} + \mathbf{B}u + \mathbf{E}\ddot{x}_g \tag{9.1}$$

$$\mathbf{y} = \mathbf{C}_y\mathbf{x} + \mathbf{D}_y u + \mathbf{D}_g\ddot{x}_g \tag{9.2}$$

where the output vector $\mathbf{y}$ is defined as $\mathbf{y} = \begin{bmatrix} x_a & \ddot{x}_{a1} & \ddot{x}_{a2} & \ddot{x}_{a3} & x_1 & x_2 & x_3 & f \end{bmatrix}'$, u is the control command, and $\ddot{x}_g$ is the ground excitation. The units of all of the inputs and outputs are Volts. The following conversions can be employed:

Actuator Displacement (x_a):	0 .05 in/Volt
Accelerometers ($\ddot{x}_g$, $\ddot{x}_{a1}$, $\ddot{x}_{a2}$, $\ddot{x}_{a3}$):	2 g/Volt
Building Displacements (x_1, x_2, x_3):	1Volt/in
Tendon Force (f):	1000 lb/Volt.

$$\mathbf{A} = \begin{bmatrix}
-1.3880e-01 & -1.4200e+01 & -1.3129e-03 & 7.1615e-03 & -2.5477e-03 & -1.2008e-03 & 5.4326e-03 & -2.3166e-02 & -8.6131e-04 & 3.8061e-03 \\
1.4200e+01 & -1.3767e-01 & 3.2811e-03 & 1.2775e-03 & -6.8615e-05 & 6.8102e-04 & 6.2938e-03 & -2.7073e-02 & -1.3567e-03 & 4.4396e-03 \\
3.9238e-02 & -3.8138e-02 & -3.0817e-01 & -4.5931e+01 & 1.6880e-01 & 2.1023e-01 & -2.4148e-02 & 7.5488e-02 & 6.0191e-02 & -9.3421e-03 \\
-3.9955e-02 & 3.9371e-02 & 4.5933e+01 & -3.2019e-01 & -2.1388e-01 & -1.9449e+01 & -5.1253e-02 & 1.4326e-01 & 7.3696e-02 & -2.4496e-02 \\
3.4544e-02 & -3.3616e-02 & -3.9956e-01 & 4.3305e-01 & -3.0775e-01 & 7.6150e-01 & 2.5877e-02 & 5.5751e-03 & -4.1105e-02 & 9.1244e-03 \\
3.4065e-02 & -3.3763e-02 & -4.2231e-01 & 4.2713e-01 & -7.6148e+01 & -3.2043e-01 & 2.1709e-02 & 1.3397e-01 & 4.9504e-02 & 1.8115e-03 \\
1.9683e-04 & -3.1649e-04 & -2.5557e-02 & 4.7792e-02 & -8.1919e-02 & 1.8696e-01 & -2.8627e+00 & 2.5254+02 & 5.2916e+00 & -2.8282e+00 \\
1.9471e-03 & -1.9914e-03 & -1.2349e-01 & 1.7808e-01 & -3.2140e-01 & -7.8272e-01 & -2.5255e+02 & -5.1390e+01 & -1.1399e+01 & 2.4131e+01 \\
2.6339e-04 & -3.0405e-04 & -2.0763e-02 & 2.9223e-02 & -5.1273e-02 & -1.2889e-01 & -5.4727e+00 & -1.3380e+01 & -4.3019e+00 & 2.6486e+02 \\
3.3035e-04 & -3.8469e-04 & -1.8965e-02 & 3.0792e-02 & -5.1828e-02 & -1.2211e-01 & -2.8357e+00 & -2.4132e+01 & -2.6520e+02 & -3.9908e+00
\end{bmatrix} \tag{9.3}$$

$$\mathbf{B} = \begin{bmatrix} -6.6251e-02 \\ 7.5839e-02 \\ 2.8684e-01 \\ -4.5186e-01 \\ 3.6584e-01 \\ 8.6395e-01 \\ 4.1844e+00 \\ 1.6899e+01 \\ 2.8260e+00 \\ 2.6813e+00 \end{bmatrix} \tag{9.1}$$

$$\mathbf{E} = \begin{bmatrix} -6.3355e+00 \\ 6.2056e+00 \\ 3.8638e+00 \\ -3.9590e+00 \\ 3.4298e+00 \\ 3.3980e+00 \\ -2.2131e-02 \\ 5.9883e-03 \\ -3.6845e-03 \\ 5.2707e-03 \end{bmatrix} \tag{9.2}$$

$$\mathbf{C}_y = \begin{bmatrix} -8.8482e-01 & -1.0256e+00 & 4.1046e-01 & 6.1565e-01 & 1.6489e-01 & -1.8675e-01 & 4.1676e+00 & -1.6830e+01 & -2.6109e+00 & 2.6702e+00 \\ -4.1212e-01 & -4.0830e-01 & 2.5694e+00 & 2.4921e+00 & 2.3908e+00 & -2.3803e+00 & -3.5009e-01 & 1.5032e+00 & 2.2974e-01 & -2.3613e-01 \\ -1.0067e+00 & -1.0149e+00 & 1.8111e+00 & 1.8571e+00 & -2.3079e+00 & 2.4223e+00 & 1.6660e-03 & -3.6938e-02 & 6.4788e-03 & 2.0946e-02 \\ -1.4785e+00 & -1.5234e+00 & -1.8573e+00 & -1.8816e+00 & 6.9617e-01 & -7.4251e-01 & -1.3385e-01 & -1.8872e-01 & 1.0562e+00 & 5.6696e-02 \\ -1.3629e+00 & -1.3797e+00 & 1.0662e+00 & 1.0641e+00 & 3.9198e-01 & -3.9045e-01 & -8.0577e-04 & 1.6463e-02 & -5.5993e-03 & -8.9581e-03 \\ -4.1331e+00 & -3.6623e+00 & 5.1383e-01 & 1.0986e+00 & -4.9777e-01 & 1.9869e-01 & 6.6440e-03 & -1.1032e-02 & -2.8659e-03 & -7.0213e-03 \\ -5.4567e+00 & -5.5829e+00 & -7.1950e-01 & -7.3234e-01 & 1.2978e-01 & -1.4361e-01 & 3.9679e-03 & 2.1299e-02 & 3.4121e-02 & 1.3934e-02 \\ -9.6568e+00 & -9.6970e+00 & 7.7246e+00 & 7.5849e+00 & 2.8316e+00 & -2.8069e+00 & -2.5274e+00 & 1.0306e+01 & 1.5377e+00 & -1.6825e+00 \end{bmatrix} \tag{9.3}$$

$$\mathbf{D}_y = \begin{bmatrix} 4.5194e-01 \\ -3.9346e-02 \\ -2.4050e-03 \\ -8.1783e-04 \\ 4.3686e-04 \\ 8.9232e-04 \\ -3.9145e-03 \\ -2.7016e-01 \end{bmatrix} \tag{9.4}$$

$$\mathbf{D}_g = \begin{bmatrix} -2.1421e-02 \\ 4.4146e-04 \\ 3.8614e-04 \\ -2.0967e-04 \\ 3.4337e-04 \\ 1.4126e-04 \\ 2.5871-04 \\ 1.5528e-02 \end{bmatrix} \tag{9.5}$$

A MATLAB file containing this model can be requested by contacting Prof. B.F. Spencer through e-mail at spencer.1@nd.edu.

NATIONAL CENTER FOR EARTHQUAKE ENGINEERING RESEARCH
LIST OF TECHNICAL REPORTS

The National Center for Earthquake Engineering Research (NCEER) publishes technical reports on a variety of subjects related to earthquake engineering written by authors funded through NCEER. These reports are available from both NCEER's Publications Department and the National Technical Information Service (NTIS). Requests for reports should be directed to the Publications Department, National Center for Earthquake Engineering Research, State University of New York at Buffalo, Red Jacket Quadrangle, Buffalo, New York 14261. Reports can also be requested through NTIS, 5285 Port Royal Road, Springfield, Virginia 22161. NTIS accession numbers are shown in parenthesis, if available.

NCEER-87-0001 "First-Year Program in Research, Education and Technology Transfer," 3/5/87, (PB88-134275).

NCEER-87-0002 "Experimental Evaluation of Instantaneous Optimal Algorithms for Structural Control," by R.C. Lin, T.T. Soong and A.M. Reinhorn, 4/20/87, (PB88-134341).

NCEER-87-0003 "Experimentation Using the Earthquake Simulation Facilities at University at Buffalo," by A.M. Reinhorn and R.L. Ketter, to be published.

NCEER-87-0004 "The System Characteristics and Performance of a Shaking Table," by J.S. Hwang, K.C. Chang and G.C. Lee, 6/1/87, (PB88-134259). This report is available only through NTIS (see address given above).

NCEER-87-0005 "A Finite Element Formulation for Nonlinear Viscoplastic Material Using a Q Model," by O. Gyebi and G. Dasgupta, 11/2/87, (PB88-213764).

NCEER-87-0006 "Symbolic Manipulation Program (SMP) - Algebraic Codes for Two and Three Dimensional Finite Element Formulations," by X. Lee and G. Dasgupta, 11/9/87, (PB88-218522).

NCEER-87-0007 "Instantaneous Optimal Control Laws for Tall Buildings Under Seismic Excitations," by J.N. Yang, A. Akbarpour and P. Ghaemmaghami, 6/10/87, (PB88-134333). This report is only available through NTIS (see address given above).

NCEER-87-0008 "IDARC: Inelastic Damage Analysis of Reinforced Concrete Frame - Shear-Wall Structures," by Y.J. Park, A.M. Reinhorn and S.K. Kunnath, 7/20/87, (PB88-134325).

NCEER-87-0009 "Liquefaction Potential for New York State: A Preliminary Report on Sites in Manhattan and Buffalo," by M. Budhu, V. Vijayakumar, R.F. Giese and L. Baumgras, 8/31/87, (PB88-163704). This report is available only through NTIS (see address given above).

NCEER-87-0010 "Vertical and Torsional Vibration of Foundations in Inhomogeneous Media," by A.S. Veletsos and K.W. Dotson, 6/1/87, (PB88-134291).

NCEER-87-0011 "Seismic Probabilistic Risk Assessment and Seismic Margins Studies for Nuclear Power Plants," by Howard H.M. Hwang, 6/15/87, (PB88-134267).

NCEER-87-0012 "Parametric Studies of Frequency Response of Secondary Systems Under Ground-Acceleration Excitations," by Y. Yong and Y.K. Lin, 6/10/87, (PB88-134309).

NCEER-87-0013 "Frequency Response of Secondary Systems Under Seismic Excitation," by J.A. HoLung, J. Cai and Y.K. Lin, 7/31/87, (PB88-134317).

NCEER-87-0014 "Modelling Earthquake Ground Motions in Seismically Active Regions Using Parametric Time Series Methods," by G.W. Ellis and A.S. Cakmak, 8/25/87, (PB88-134283).

NCEER-87-0015 "Detection and Assessment of Seismic Structural Damage," by E. DiPasquale and A.S. Cakmak, 8/25/87, (PB88-163712).

NCEER-87-0016 "Pipeline Experiment at Parkfield, California," by J. Isenberg and E. Richardson, 9/15/87, (PB88-163720). This report is available only through NTIS (see address given above).

NCEER-87-0017 "Digital Simulation of Seismic Ground Motion," by M. Shinozuka, G. Deodatis and T. Harada, 8/31/87, (PB88-155197). This report is available only through NTIS (see address given above).

NCEER-87-0018 "Practical Considerations for Structural Control: System Uncertainty, System Time Delay and Truncation of Small Control Forces," J.N. Yang and A. Akbarpour, 8/10/87, (PB88-163738).

NCEER-87-0019 "Modal Analysis of Nonclassically Damped Structural Systems Using Canonical Transformation," by J.N. Yang, S. Sarkani and F.X. Long, 9/27/87, (PB88-187851).

NCEER-87-0020 "A Nonstationary Solution in Random Vibration Theory," by J.R. Red-Horse and P.D. Spanos, 11/3/87, (PB88-163746).

NCEER-87-0021 "Horizontal Impedances for Radially Inhomogeneous Viscoelastic Soil Layers," by A.S. Veletsos and K.W. Dotson, 10/15/87, (PB88-150859).

NCEER-87-0022 "Seismic Damage Assessment of Reinforced Concrete Members," by Y.S. Chung, C. Meyer and M. Shinozuka, 10/9/87, (PB88-150867). This report is available only through NTIS (see address given above).

NCEER-87-0023 "Active Structural Control in Civil Engineering," by T.T. Soong, 11/11/87, (PB88-187778).

NCEER-87-0024 "Vertical and Torsional Impedances for Radially Inhomogeneous Viscoelastic Soil Layers," by K.W. Dotson and A.S. Veletsos, 12/87, (PB88-187786).

NCEER-87-0025 "Proceedings from the Symposium on Seismic Hazards, Ground Motions, Soil-Liquefaction and Engineering Practice in Eastern North America," October 20-22, 1987, edited by K.H. Jacob, 12/87, (PB88-188115).

NCEER-87-0026 "Report on the Whittier-Narrows, California, Earthquake of October 1, 1987," by J. Pantelic and A. Reinhorn, 11/87, (PB88-187752). This report is available only through NTIS (see address given above).

NCEER-87-0027 "Design of a Modular Program for Transient Nonlinear Analysis of Large 3-D Building Structures," by S. Srivastav and J.F. Abel, 12/30/87, (PB88-187950).

NCEER-87-0028 "Second-Year Program in Research, Education and Technology Transfer," 3/8/88, (PB88-219480).

NCEER-88-0001 "Workshop on Seismic Computer Analysis and Design of Buildings With Interactive Graphics," by W. McGuire, J.F. Abel and C.H. Conley, 1/18/88, (PB88-187760).

NCEER-88-0002 "Optimal Control of Nonlinear Flexible Structures," by J.N. Yang, F.X. Long and D. Wong, 1/22/88, (PB88-213772).

NCEER-88-0003 "Substructuring Techniques in the Time Domain for Primary-Secondary Structural Systems," by G.D. Manolis and G. Juhn, 2/10/88, (PB88-213780).

NCEER-88-0004 "Iterative Seismic Analysis of Primary-Secondary Systems," by A. Singhal, L.D. Lutes and P.D. Spanos, 2/23/88, (PB88-213798).

NCEER-88-0005 "Stochastic Finite Element Expansion for Random Media," by P.D. Spanos and R. Ghanem, 3/14/88, (PB88-213806).

NCEER-88-0006 "Combining Structural Optimization and Structural Control," by F.Y. Cheng and C.P. Pantelides, 1/10/88, (PB88-213814).

NCEER-88-0007 "Seismic Performance Assessment of Code-Designed Structures," by H.H-M. Hwang, J-W. Jaw and H-J. Shau, 3/20/88, (PB88-219423).

NCEER-88-0008 "Reliability Analysis of Code-Designed Structures Under Natural Hazards," by H.H-M. Hwang, H. Ushiba and M. Shinozuka, 2/29/88, (PB88-229471).

NCEER-88-0009 "Seismic Fragility Analysis of Shear Wall Structures," by J-W Jaw and H.H-M. Hwang, 4/30/88, (PB89-102867).

NCEER-88-0010 "Base Isolation of a Multi-Story Building Under a Harmonic Ground Motion - A Comparison of Performances of Various Systems," by F-G Fan, G. Ahmadi and I.G. Tadjbakhsh, 5/18/88, (PB89-122238).

NCEER-88-0011 "Seismic Floor Response Spectra for a Combined System by Green's Functions," by F.M. Lavelle, L.A. Bergman and P.D. Spanos, 5/1/88, (PB89-102875).

NCEER-88-0012 "A New Solution Technique for Randomly Excited Hysteretic Structures," by G.Q. Cai and Y.K. Lin, 5/16/88, (PB89-102883).

NCEER-88-0013 "A Study of Radiation Damping and Soil-Structure Interaction Effects in the Centrifuge," by K. Weissman, supervised by J.H. Prevost, 5/24/88, (PB89-144703).

NCEER-88-0014 "Parameter Identification and Implementation of a Kinematic Plasticity Model for Frictional Soils," by J.H. Prevost and D.V. Griffiths, to be published.

NCEER-88-0015 "Two- and Three- Dimensional Dynamic Finite Element Analyses of the Long Valley Dam," by D.V. Griffiths and J.H. Prevost, 6/17/88, (PB89-144711).

NCEER-88-0016 "Damage Assessment of Reinforced Concrete Structures in Eastern United States," by A.M. Reinhorn, M.J. Seidel, S.K. Kunnath and Y.J. Park, 6/15/88, (PB89-122220).

NCEER-88-0017 "Dynamic Compliance of Vertically Loaded Strip Foundations in Multilayered Viscoelastic Soils," by S. Ahmad and A.S.M. Israil, 6/17/88, (PB89-102891).

NCEER-88-0018 "An Experimental Study of Seismic Structural Response With Added Viscoelastic Dampers," by R.C. Lin, Z. Liang, T.T. Soong and R.H. Zhang, 6/30/88, (PB89-122212). This report is available only through NTIS (see address given above).

NCEER-88-0019 "Experimental Investigation of Primary - Secondary System Interaction," by G.D. Manolis, G. Juhn and A.M. Reinhorn, 5/27/88, (PB89-122204).

NCEER-88-0020 "A Response Spectrum Approach For Analysis of Nonclassically Damped Structures," by J.N. Yang, S. Sarkani and F.X. Long, 4/22/88, (PB89-102909).

NCEER-88-0021 "Seismic Interaction of Structures and Soils: Stochastic Approach," by A.S. Veletsos and A.M. Prasad, 7/21/88, (PB89-122196).

NCEER-88-0022 "Identification of the Serviceability Limit State and Detection of Seismic Structural Damage," by E. DiPasquale and A.S. Cakmak, 6/15/88. (PB89-122188). This report is available only through NTIS (see address given above).

NCEER-88-0023 "Multi-Hazard Risk Analysis: Case of a Simple Offshore Structure," by B.K. Bhartia and E.H. Vanmarcke, 7/21/88, (PB89-145213).

NCEER-88-0024 "Automated Seismic Design of Reinforced Concrete Buildings," by Y.S. Chung, C. Meyer and M. Shinozuka, 7/5/88, (PB89-122170). This report is available only through NTIS (see address given above).

NCEER-88-0025 "Experimental Study of Active Control of MDOF Structures Under Seismic Excitations," by L.L. Chung, R.C. Lin, T.T. Soong and A.M. Reinhorn, 7/10/88, (PB89-122600).

NCEER-88-0026 "Earthquake Simulation Tests of a Low-Rise Metal Structure," by J.S. Hwang, K.C. Chang, G.C. Lee and R.L. Ketter, 8/1/88, (PB89-102917).

NCEER-88-0027 "Systems Study of Urban Response and Reconstruction Due to Catastrophic Earthquakes," by F. Kozin and H.K. Zhou, 9/22/88, (PB90-162348).

NCEER-88-0028 "Seismic Fragility Analysis of Plane Frame Structures," by H.H-M. Hwang and Y.K. Low, 7/31/88, (PB89-131445).

NCEER-88-0029 "Response Analysis of Stochastic Structures," by A. Kardara, C. Bucher and M. Shinozuka, 9/22/88, (PB89-174429).

NCEER-88-0030 "Nonnormal Accelerations Due to Yielding in a Primary Structure," by D.C.K. Chen and L.D. Lutes, 9/19/88, (PB89-131437).

NCEER-88-0031 "Design Approaches for Soil-Structure Interaction," by A.S. Veletsos, A.M. Prasad and Y. Tang, 12/30/88, (PB89-174437). This report is available only through NTIS (see address given above).

NCEER-88-0032 "A Re-evaluation of Design Spectra for Seismic Damage Control," by C.J. Turkstra and A.G. Tallin, 11/7/88, (PB89-145221).

NCEER-88-0033 "The Behavior and Design of Noncontact Lap Splices Subjected to Repeated Inelastic Tensile Loading," by V.E. Sagan, P. Gergely and R.N. White, 12/8/88, (PB89-163737).

NCEER-88-0034 "Seismic Response of Pile Foundations," by S.M. Mamoon, P.K. Banerjee and S. Ahmad, 11/1/88, (PB89-145239).

NCEER-88-0035 "Modeling of R/C Building Structures With Flexible Floor Diaphragms (IDARC2)," by A.M. Reinhorn, S.K. Kunnath and N. Panahshahi, 9/7/88, (PB89-207153).

NCEER-88-0036 "Solution of the Dam-Reservoir Interaction Problem Using a Combination of FEM, BEM with Particular Integrals, Modal Analysis, and Substructuring," by C-S. Tsai, G.C. Lee and R.L. Ketter, 12/31/88, (PB89-207146).

NCEER-88-0037 "Optimal Placement of Actuators for Structural Control," by F.Y. Cheng and C.P. Pantelides, 8/15/88, (PB89-162846).

NCEER-88-0038 "Teflon Bearings in Aseismic Base Isolation: Experimental Studies and Mathematical Modeling," by A. Mokha, M.C. Constantinou and A.M. Reinhorn, 12/5/88, (PB89-218457). This report is available only through NTIS (see address given above).

NCEER-88-0039 "Seismic Behavior of Flat Slab High-Rise Buildings in the New York City Area," by P. Weidlinger and M. Ettouney, 10/15/88, (PB90-145681).

NCEER-88-0040 "Evaluation of the Earthquake Resistance of Existing Buildings in New York City," by P. Weidlinger and M. Ettouney, 10/15/88, to be published.

NCEER-88-0041 "Small-Scale Modeling Techniques for Reinforced Concrete Structures Subjected to Seismic Loads," by W. Kim, A. El-Attar and R.N. White, 11/22/88, (PB89-189625).

NCEER-88-0042 "Modeling Strong Ground Motion from Multiple Event Earthquakes," by G.W. Ellis and A.S. Cakmak, 10/15/88, (PB89-174445).

NCEER-88-0043 "Nonstationary Models of Seismic Ground Acceleration," by M. Grigoriu, S.E. Ruiz and E. Rosenblueth, 7/15/88, (PB89-189617).

NCEER-88-0044 "SARCF User's Guide: Seismic Analysis of Reinforced Concrete Frames," by Y.S. Chung, C. Meyer and M. Shinozuka, 11/9/88, (PB89-174452).

NCEER-88-0045 "First Expert Panel Meeting on Disaster Research and Planning," edited by J. Pantelic and J. Stoyle, 9/15/88, (PB89-174460).

NCEER-88-0046 "Preliminary Studies of the Effect of Degrading Infill Walls on the Nonlinear Seismic Response of Steel Frames," by C.Z. Chrysostomou, P. Gergely and J.F. Abel, 12/19/88, (PB89-208383).

NCEER-88-0047 "Reinforced Concrete Frame Component Testing Facility - Design, Construction, Instrumentation and Operation," by S.P. Pessiki, C. Conley, T. Bond, P. Gergely and R.N. White, 12/16/88, (PB89-174478).

NCEER-89-0001 "Effects of Protective Cushion and Soil Compliancy on the Response of Equipment Within a Seismically Excited Building," by J.A. HoLung, 2/16/89, (PB89-207179).

NCEER-89-0002 "Statistical Evaluation of Response Modification Factors for Reinforced Concrete Structures," by H.H-M. Hwang and J-W. Jaw, 2/17/89, (PB89-207187).

NCEER-89-0003 "Hysteretic Columns Under Random Excitation," by G-Q. Cai and Y.K. Lin, 1/9/89, (PB89-196513).

NCEER-89-0004 "Experimental Study of 'Elephant Foot Bulge' Instability of Thin-Walled Metal Tanks," by Z-H. Jia and R.L. Ketter, 2/22/89, (PB89-207195).

NCEER-89-0005 "Experiment on Performance of Buried Pipelines Across San Andreas Fault," by J. Isenberg, E. Richardson and T.D. O'Rourke, 3/10/89, (PB89-218440). This report is available only through NTIS (see address given above).

NCEER-89-0006 "A Knowledge-Based Approach to Structural Design of Earthquake-Resistant Buildings," by M. Subramani, P. Gergely, C.H. Conley, J.F. Abel and A.H. Zaghw, 1/15/89, (PB89-218465).

NCEER-89-0007 "Liquefaction Hazards and Their Effects on Buried Pipelines," by T.D. O'Rourke and P.A. Lane, 2/1/89, (PB89-218481).

NCEER-89-0008 "Fundamentals of System Identification in Structural Dynamics," by H. Imai, C-B. Yun, O. Maruyama and M. Shinozuka, 1/26/89, (PB89-207211).

NCEER-89-0009 "Effects of the 1985 Michoacan Earthquake on Water Systems and Other Buried Lifelines in Mexico," by A.G. Ayala and M.J. O'Rourke, 3/8/89, (PB89-207229).

NCEER-89-R010 "NCEER Bibliography of Earthquake Education Materials," by K.E.K. Ross, Second Revision, 9/1/89, (PB90-125352).

NCEER-89-0011 "Inelastic Three-Dimensional Response Analysis of Reinforced Concrete Building Structures (IDARC-3D), Part I - Modeling," by S.K. Kunnath and A.M. Reinhorn, 4/17/89, (PB90-114612).

NCEER-89-0012 "Recommended Modifications to ATC-14," by C.D. Poland and J.O. Malley, 4/12/89, (PB90-108648).

NCEER-89-0013 "Repair and Strengthening of Beam-to-Column Connections Subjected to Earthquake Loading," by M. Corazao and A.J. Durrani, 2/28/89, (PB90-109885).

NCEER-89-0014 "Program EXKAL2 for Identification of Structural Dynamic Systems," by O. Maruyama, C-B. Yun, M. Hoshiya and M. Shinozuka, 5/19/89, (PB90-109877).

NCEER-89-0015 "Response of Frames With Bolted Semi-Rigid Connections, Part I - Experimental Study and Analytical Predictions," by P.J. DiCorso, A.M. Reinhorn, J.R. Dickerson, J.B. Radziminski and W.L. Harper, 6/1/89, to be published.

NCEER-89-0016 "ARMA Monte Carlo Simulation in Probabilistic Structural Analysis," by P.D. Spanos and M.P. Mignolet, 7/10/89, (PB90-109893).

NCEER-89-P017 "Preliminary Proceedings from the Conference on Disaster Preparedness - The Place of Earthquake Education in Our Schools," Edited by K.E.K. Ross, 6/23/89, (PB90-108606).

NCEER-89-0017 "Proceedings from the Conference on Disaster Preparedness - The Place of Earthquake Education in Our Schools," Edited by K.E.K. Ross, 12/31/89, (PB90-207895). This report is available only through NTIS (see address given above).

NCEER-89-0018 "Multidimensional Models of Hysteretic Material Behavior for Vibration Analysis of Shape Memory Energy Absorbing Devices, by E.J. Graesser and F.A. Cozzarelli, 6/7/89, (PB90-164146).

NCEER-89-0019 "Nonlinear Dynamic Analysis of Three-Dimensional Base Isolated Structures (3D-BASIS)," by S. Nagarajaiah, A.M. Reinhorn and M.C. Constantinou, 8/3/89, (PB90-161936). This report is available only through NTIS (see address given above).

NCEER-89-0020 "Structural Control Considering Time-Rate of Control Forces and Control Rate Constraints," by F.Y. Cheng and C.P. Pantelides, 8/3/89, (PB90-120445).

NCEER-89-0021 "Subsurface Conditions of Memphis and Shelby County," by K.W. Ng, T-S. Chang and H-H.M. Hwang, 7/26/89, (PB90-120437).

NCEER-89-0022 "Seismic Wave Propagation Effects on Straight Jointed Buried Pipelines," by K. Elhmadi and M.J. O'Rourke, 8/24/89, (PB90-162322).

NCEER-89-0023 "Workshop on Serviceability Analysis of Water Delivery Systems," edited by M. Grigoriu, 3/6/89, (PB90-127424).

NCEER-89-0024 "Shaking Table Study of a 1/5 Scale Steel Frame Composed of Tapered Members," by K.C. Chang, J.S. Hwang and G.C. Lee, 9/18/89, (PB90-160169).

NCEER-89-0025 "DYNA1D: A Computer Program for Nonlinear Seismic Site Response Analysis - Technical Documentation," by Jean H. Prevost, 9/14/89, (PB90-161944). This report is available only through NTIS (see address given above).

NCEER-89-0026 "1:4 Scale Model Studies of Active Tendon Systems and Active Mass Dampers for Aseismic Protection," by A.M. Reinhorn, T.T. Soong, R.C. Lin, Y.P. Yang, Y. Fukao, H. Abe and M. Nakai, 9/15/89, (PB90-173246).

NCEER-89-0027 "Scattering of Waves by Inclusions in a Nonhomogeneous Elastic Half Space Solved by Boundary Element Methods," by P.K. Hadley, A. Askar and A.S. Cakmak, 6/15/89, (PB90-145699).

NCEER-89-0028 "Statistical Evaluation of Deflection Amplification Factors for Reinforced Concrete Structures," by H.H.M. Hwang, J-W. Jaw and A.L. Ch'ng, 8/31/89, (PB90-164633).

NCEER-89-0029 "Bedrock Accelerations in Memphis Area Due to Large New Madrid Earthquakes," by H.H.M. Hwang, C.H.S. Chen and G. Yu, 11/7/89, (PB90-162330).

NCEER-89-0030 "Seismic Behavior and Response Sensitivity of Secondary Structural Systems," by Y.Q. Chen and T.T. Soong, 10/23/89, (PB90-164658).

NCEER-89-0031 "Random Vibration and Reliability Analysis of Primary-Secondary Structural Systems," by Y. Ibrahim, M. Grigoriu and T.T. Soong, 11/10/89, (PB90-161951).

NCEER-89-0032 "Proceedings from the Second U.S. - Japan Workshop on Liquefaction, Large Ground Deformation and Their Effects on Lifelines, September 26-29, 1989," Edited by T.D. O'Rourke and M. Hamada, 12/1/89, (PB90-209388).

NCEER-89-0033 "Deterministic Model for Seismic Damage Evaluation of Reinforced Concrete Structures," by J.M. Bracci, A.M. Reinhorn, J.B. Mander and S.K. Kunnath, 9/27/89.

NCEER-89-0034 "On the Relation Between Local and Global Damage Indices," by E. DiPasquale and A.S. Cakmak, 8/15/89, (PB90-173865).

NCEER-89-0035 "Cyclic Undrained Behavior of Nonplastic and Low Plasticity Silts," by A.J. Walker and H.E. Stewart, 7/26/89, (PB90-183518).

NCEER-89-0036 "Liquefaction Potential of Surficial Deposits in the City of Buffalo, New York," by M. Budhu, R. Giese and L. Baumgrass, 1/17/89, (PB90-208455).

NCEER-89-0037 "A Deterministic Assessment of Effects of Ground Motion Incoherence," by A.S. Veletsos and Y. Tang, 7/15/89, (PB90-164294).

NCEER-89-0038 "Workshop on Ground Motion Parameters for Seismic Hazard Mapping," July 17-18, 1989, edited by R.V. Whitman, 12/1/89, (PB90-173923).

NCEER-89-0039 "Seismic Effects on Elevated Transit Lines of the New York City Transit Authority," by C.J. Costantino, C.A. Miller and E. Heymsfield, 12/26/89, (PB90-207887).

NCEER-89-0040 "Centrifugal Modeling of Dynamic Soil-Structure Interaction," by K. Weissman, Supervised by J.H. Prevost, 5/10/89, (PB90-207879).

NCEER-89-0041 "Linearized Identification of Buildings With Cores for Seismic Vulnerability Assessment," by I-K. Ho and A.E. Aktan, 11/1/89, (PB90-251943).

NCEER-90-0001 "Geotechnical and Lifeline Aspects of the October 17, 1989 Loma Prieta Earthquake in San Francisco," by T.D. O'Rourke, H.E. Stewart, F.T. Blackburn and T.S. Dickerman, 1/90, (PB90-208596).

NCEER-90-0002 "Nonnormal Secondary Response Due to Yielding in a Primary Structure," by D.C.K. Chen and L.D. Lutes, 2/28/90, (PB90-251976).

NCEER-90-0003 "Earthquake Education Materials for Grades K-12," by K.E.K. Ross, 4/16/90, (PB91-251984).

NCEER-90-0004 "Catalog of Strong Motion Stations in Eastern North America," by R.W. Busby, 4/3/90, (PB90-251984).

NCEER-90-0005 "NCEER Strong-Motion Data Base: A User Manual for the GeoBase Release (Version 1.0 for the Sun3)," by P. Friberg and K. Jacob, 3/31/90 (PB90-258062).

NCEER-90-0006 "Seismic Hazard Along a Crude Oil Pipeline in the Event of an 1811-1812 Type New Madrid Earthquake," by H.H.M. Hwang and C-H.S. Chen, 4/16/90(PB90-258054).

NCEER-90-0007 "Site-Specific Response Spectra for Memphis Sheahan Pumping Station," by H.H.M. Hwang and C.S. Lee, 5/15/90, (PB91-108811).

NCEER-90-0008 "Pilot Study on Seismic Vulnerability of Crude Oil Transmission Systems," by T. Ariman, R. Dobry, M. Grigoriu, F. Kozin, M. O'Rourke, T. O'Rourke and M. Shinozuka, 5/25/90, (PB91-108837).

NCEER-90-0009 "A Program to Generate Site Dependent Time Histories: EQGEN," by G.W. Ellis, M. Srinivasan and A.S. Cakmak, 1/30/90, (PB91-108829).

NCEER-90-0010 "Active Isolation for Seismic Protection of Operating Rooms," by M.E. Talbott, Supervised by M. Shinozuka, 6/8/9, (PB91-110205).

NCEER-90-0011 "Program LINEARID for Identification of Linear Structural Dynamic Systems," by C-B. Yun and M. Shinozuka, 6/25/90, (PB91-110312).

NCEER-90-0012 "Two-Dimensional Two-Phase Elasto-Plastic Seismic Response of Earth Dams," by A.N. Yiagos, Supervised by J.H. Prevost, 6/20/90, (PB91-110197).

NCEER-90-0013 "Secondary Systems in Base-Isolated Structures: Experimental Investigation, Stochastic Response and Stochastic Sensitivity," by G.D. Manolis, G. Juhn, M.C. Constantinou and A.M. Reinhorn, 7/1/90, (PB91-110320).

NCEER-90-0014 "Seismic Behavior of Lightly-Reinforced Concrete Column and Beam-Column Joint Details," by S.P. Pessiki, C.H. Conley, P. Gergely and R.N. White, 8/22/90, (PB91-108795).

NCEER-90-0015 "Two Hybrid Control Systems for Building Structures Under Strong Earthquakes," by J.N. Yang and A. Danielians, 6/29/90, (PB91-125393).

NCEER-90-0016 "Instantaneous Optimal Control with Acceleration and Velocity Feedback," by J.N. Yang and Z. Li, 6/29/90, (PB91-125401).

NCEER-90-0017 "Reconnaissance Report on the Northern Iran Earthquake of June 21, 1990," by M. Mehrain, 10/4/90, (PB91-125377).

NCEER-90-0018 "Evaluation of Liquefaction Potential in Memphis and Shelby County," by T.S. Chang, P.S. Tang, C.S. Lee and H. Hwang, 8/10/90, (PB91-125427).

NCEER-90-0019 "Experimental and Analytical Study of a Combined Sliding Disc Bearing and Helical Steel Spring Isolation System," by M.C. Constantinou, A.S. Mokha and A.M. Reinhorn, 10/4/90, (PB91-125385).

NCEER-90-0020 "Experimental Study and Analytical Prediction of Earthquake Response of a Sliding Isolation System with a Spherical Surface," by A.S. Mokha, M.C. Constantinou and A.M. Reinhorn, 10/11/90, (PB91-125419).

NCEER-90-0021 "Dynamic Interaction Factors for Floating Pile Groups," by G. Gazetas, K. Fan, A. Kaynia and E. Kausel, 9/10/90, (PB91-170381).

NCEER-90-0022 "Evaluation of Seismic Damage Indices for Reinforced Concrete Structures," by S. Rodriguez-Gomez and A.S. Cakmak, 9/30/90, PB91-171322).

NCEER-90-0023 "Study of Site Response at a Selected Memphis Site," by H. Desai, S. Ahmad, E.S. Gazetas and M.R. Oh, 10/11/90, (PB91-196857).

NCEER-90-0024 "A User's Guide to Strongmo: Version 1.0 of NCEER's Strong-Motion Data Access Tool for PCs and Terminals," by P.A. Friberg and C.A.T. Susch, 11/15/90, (PB91-171272).

NCEER-90-0025 "A Three-Dimensional Analytical Study of Spatial Variability of Seismic Ground Motions," by L-L. Hong and A.H.-S. Ang, 10/30/90, (PB91-170399).

NCEER-90-0026 "MUMOID User's Guide - A Program for the Identification of Modal Parameters," by S. Rodriguez-Gomez and E. DiPasquale, 9/30/90, (PB91-171298).

NCEER-90-0027 "SARCF-II User's Guide - Seismic Analysis of Reinforced Concrete Frames," by S. Rodriguez-Gomez, Y.S. Chung and C. Meyer, 9/30/90, (PB91-171280).

NCEER-90-0028 "Viscous Dampers: Testing, Modeling and Application in Vibration and Seismic Isolation," by N. Makris and M.C. Constantinou, 12/20/90 (PB91-190561).

NCEER-90-0029 "Soil Effects on Earthquake Ground Motions in the Memphis Area," by H. Hwang, C.S. Lee, K.W. Ng and T.S. Chang, 8/2/90, (PB91-190751).

NCEER-91-0001 "Proceedings from the Third Japan-U.S. Workshop on Earthquake Resistant Design of Lifeline Facilities and Countermeasures for Soil Liquefaction, December 17-19, 1990," edited by T.D. O'Rourke and M. Hamada, 2/1/91, (PB91-179259).

NCEER-91-0002 "Physical Space Solutions of Non-Proportionally Damped Systems," by M. Tong, Z. Liang and G.C. Lee, 1/15/91, (PB91-179242).

NCEER-91-0003 "Seismic Response of Single Piles and Pile Groups," by K. Fan and G. Gazetas, 1/10/91, (PB92-174994).

NCEER-91-0004 "Damping of Structures: Part 1 - Theory of Complex Damping," by Z. Liang and G. Lee, 10/10/91, (PB92-197235).

NCEER-91-0005 "3D-BASIS - Nonlinear Dynamic Analysis of Three Dimensional Base Isolated Structures: Part II," by S. Nagarajaiah, A.M. Reinhorn and M.C. Constantinou, 2/28/91, (PB91-190553).

NCEER-91-0006 "A Multidimensional Hysteretic Model for Plasticity Deforming Metals in Energy Absorbing Devices," by E.J. Graesser and F.A. Cozzarelli, 4/9/91, (PB92-108364).

NCEER-91-0007 "A Framework for Customizable Knowledge-Based Expert Systems with an Application to a KBES for Evaluating the Seismic Resistance of Existing Buildings," by E.G. Ibarra-Anaya and S.J. Fenves, 4/9/91, (PB91-210930).

NCEER-91-0008 "Nonlinear Analysis of Steel Frames with Semi-Rigid Connections Using the Capacity Spectrum Method," by G.G. Deierlein, S-H. Hsieh, Y-J. Shen and J.F. Abel, 7/2/91, (PB92-113828).

NCEER-91-0009 "Earthquake Education Materials for Grades K-12," by K.E.K. Ross, 4/30/91, (PB91-212142).

NCEER-91-0010 "Phase Wave Velocities and Displacement Phase Differences in a Harmonically Oscillating Pile," by N. Makris and G. Gazetas, 7/8/91, (PB92-108356).

NCEER-91-0011 "Dynamic Characteristics of a Full-Size Five-Story Steel Structure and a 2/5 Scale Model," by K.C. Chang, G.C. Yao, G.C. Lee, D.S. Hao and Y.C. Yeh," 7/2/91, (PB93-116648).

NCEER-91-0012 "Seismic Response of a 2/5 Scale Steel Structure with Added Viscoelastic Dampers," by K.C. Chang, T.T. Soong, S-T. Oh and M.L. Lai, 5/17/91, (PB92-110816).

NCEER-91-0013 "Earthquake Response of Retaining Walls; Full-Scale Testing and Computational Modeling," by S. Alampalli and A-W.M. Elgamal, 6/20/91, to be published.

NCEER-91-0014 "3D-BASIS-M: Nonlinear Dynamic Analysis of Multiple Building Base Isolated Structures," by P.C. Tsopelas, S. Nagarajaiah, M.C. Constantinou and A.M. Reinhorn, 5/28/91, (PB92-113885).

NCEER-91-0015 "Evaluation of SEAOC Design Requirements for Sliding Isolated Structures," by D. Theodossiou and M.C. Constantinou, 6/10/91, (PB92-114602).

NCEER-91-0016 "Closed-Loop Modal Testing of a 27-Story Reinforced Concrete Flat Plate-Core Building," by H.R. Somaprasad, T. Toksoy, H. Yoshiyuki and A.E. Aktan, 7/15/91, (PB92-129980).

NCEER-91-0017 "Shake Table Test of a 1/6 Scale Two-Story Lightly Reinforced Concrete Building," by A.G. El-Attar, R.N. White and P. Gergely, 2/28/91, (PB92-222447).

NCEER-91-0018 "Shake Table Test of a 1/8 Scale Three-Story Lightly Reinforced Concrete Building," by A.G. El-Attar, R.N. White and P. Gergely, 2/28/91, (PB93-116630).

NCEER-91-0019 "Transfer Functions for Rigid Rectangular Foundations," by A.S. Veletsos, A.M. Prasad and W.H. Wu, 7/31/91.

NCEER-91-0020 "Hybrid Control of Seismic-Excited Nonlinear and Inelastic Structural Systems," by J.N. Yang, Z. Li and A. Danielians, 8/1/91, (PB92-143171).

NCEER-91-0021 "The NCEER-91 Earthquake Catalog: Improved Intensity-Based Magnitudes and Recurrence Relations for U.S. Earthquakes East of New Madrid," by L. Seeber and J.G. Armbruster, 8/28/91, (PB92-176742).

NCEER-91-0022 "Proceedings from the Implementation of Earthquake Planning and Education in Schools: The Need for Change - The Roles of the Changemakers," by K.E.K. Ross and F. Winslow, 7/23/91, (PB92-129998).

NCEER-91-0023 "A Study of Reliability-Based Criteria for Seismic Design of Reinforced Concrete Frame Buildings," by H.H.M. Hwang and H-M. Hsu, 8/10/91, (PB92-140235).

NCEER-91-0024 "Experimental Verification of a Number of Structural System Identification Algorithms," by R.G. Ghanem, H. Gavin and M. Shinozuka, 9/18/91, (PB92-176577).

NCEER-91-0025 "Probabilistic Evaluation of Liquefaction Potential," by H.H.M. Hwang and C.S. Lee," 11/25/91, (PB92-143429).

NCEER-91-0026 "Instantaneous Optimal Control for Linear, Nonlinear and Hysteretic Structures - Stable Controllers," by J.N. Yang and Z. Li, 11/15/91, (PB92-163807).

NCEER-91-0027 "Experimental and Theoretical Study of a Sliding Isolation System for Bridges," by M.C. Constantinou, A. Kartoum, A.M. Reinhorn and P. Bradford, 11/15/91, (PB92-176973).

NCEER-92-0001 "Case Studies of Liquefaction and Lifeline Performance During Past Earthquakes, Volume 1: Japanese Case Studies," Edited by M. Hamada and T. O'Rourke, 2/17/92, (PB92-197243).

NCEER-92-0002 "Case Studies of Liquefaction and Lifeline Performance During Past Earthquakes, Volume 2: United States Case Studies," Edited by T. O'Rourke and M. Hamada, 2/17/92, (PB92-197250).

NCEER-92-0003 "Issues in Earthquake Education," Edited by K. Ross, 2/3/92, (PB92-222389).

NCEER-92-0004 "Proceedings from the First U.S. - Japan Workshop on Earthquake Protective Systems for Bridges," Edited by I.G. Buckle, 2/4/92, (PB94-142239, A99, MF-A06).

NCEER-92-0005 "Seismic Ground Motion from a Haskell-Type Source in a Multiple-Layered Half-Space," A.P. Theoharis, G. Deodatis and M. Shinozuka, 1/2/92, to be published.

NCEER-92-0006 "Proceedings from the Site Effects Workshop," Edited by R. Whitman, 2/29/92, (PB92-197201).

NCEER-92-0007 "Engineering Evaluation of Permanent Ground Deformations Due to Seismically-Induced Liquefaction," by M.H. Baziar, R. Dobry and A-W.M. Elgamal, 3/24/92, (PB92-222421).

NCEER-92-0008 "A Procedure for the Seismic Evaluation of Buildings in the Central and Eastern United States," by C.D. Poland and J.O. Malley, 4/2/92, (PB92-222439).

NCEER-92-0009 "Experimental and Analytical Study of a Hybrid Isolation System Using Friction Controllable Sliding Bearings," by M.Q. Feng, S. Fujii and M. Shinozuka, 5/15/92, (PB93-150282).

NCEER-92-0010 "Seismic Resistance of Slab-Column Connections in Existing Non-Ductile Flat-Plate Buildings," by A.J. Durrani and Y. Du, 5/18/92.

NCEER-92-0011 "The Hysteretic and Dynamic Behavior of Brick Masonry Walls Upgraded by Ferrocement Coatings Under Cyclic Loading and Strong Simulated Ground Motion," by H. Lee and S.P. Prawel, 5/11/92, to be published.

NCEER-92-0012 "Study of Wire Rope Systems for Seismic Protection of Equipment in Buildings," by G.F. Demetriades, M.C. Constantinou and A.M. Reinhorn, 5/20/92.

NCEER-92-0013 "Shape Memory Structural Dampers: Material Properties, Design and Seismic Testing," by P.R. Witting and F.A. Cozzarelli, 5/26/92.

NCEER-92-0014 "Longitudinal Permanent Ground Deformation Effects on Buried Continuous Pipelines," by M.J. O'Rourke, and C. Nordberg, 6/15/92.

NCEER-92-0015 "A Simulation Method for Stationary Gaussian Random Functions Based on the Sampling Theorem," by M. Grigoriu and S. Balopoulou, 6/11/92, (PB93-127496).

NCEER-92-0016 "Gravity-Load-Designed Reinforced Concrete Buildings: Seismic Evaluation of Existing Construction and Detailing Strategies for Improved Seismic Resistance," by G.W. Hoffmann, S.K. Kunnath, A.M. Reinhorn and J.B. Mander, 7/15/92, (PB94-142007, A08, MF-A02).

NCEER-92-0017 "Observations on Water System and Pipeline Performance in the Limón Area of Costa Rica Due to the April 22, 1991 Earthquake," by M. O'Rourke and D. Ballantyne, 6/30/92, (PB93-126811).

NCEER-92-0018 "Fourth Edition of Earthquake Education Materials for Grades K-12," Edited by K.E.K. Ross, 8/10/92.

NCEER-92-0019 "Proceedings from the Fourth Japan-U.S. Workshop on Earthquake Resistant Design of Lifeline Facilities and Countermeasures for Soil Liquefaction," Edited by M. Hamada and T.D. O'Rourke, 8/12/92, (PB93-163939).

NCEER-92-0020 "Active Bracing System: A Full Scale Implementation of Active Control," by A.M. Reinhorn, T.T. Soong, R.C. Lin, M.A. Riley, Y.P. Wang, S. Aizawa and M. Higashino, 8/14/92, (PB93-127512).

NCEER-92-0021 "Empirical Analysis of Horizontal Ground Displacement Generated by Liquefaction-Induced Lateral Spreads," by S.F. Bartlett and T.L. Youd, 8/17/92, (PB93-188241).

NCEER-92-0022 "IDARC Version 3.0: Inelastic Damage Analysis of Reinforced Concrete Structures," by S.K. Kunnath, A.M. Reinhorn and R.F. Lobo, 8/31/92, (PB93-227502, A07, MF-A02).

NCEER-92-0023 "A Semi-Empirical Analysis of Strong-Motion Peaks in Terms of Seismic Source, Propagation Path and Local Site Conditions, by M. Kamiyama, M.J. O'Rourke and R. Flores-Berrones, 9/9/92, (PB93-150266).

NCEER-92-0024 "Seismic Behavior of Reinforced Concrete Frame Structures with Nonductile Details, Part I: Summary of Experimental Findings of Full Scale Beam-Column Joint Tests," by A. Beres, R.N. White and P. Gergely, 9/30/92, (PB93-227783, A05, MF-A01).

NCEER-92-0025 "Experimental Results of Repaired and Retrofitted Beam-Column Joint Tests in Lightly Reinforced Concrete Frame Buildings," by A. Beres, S. El-Borgi, R.N. White and P. Gergely, 10/29/92, (PB93-227791, A05, MF-A01).

NCEER-92-0026 "A Generalization of Optimal Control Theory: Linear and Nonlinear Structures," by J.N. Yang, Z. Li and S. Vongchavalitkul, 11/2/92, (PB93-188621).

NCEER-92-0027 "Seismic Resistance of Reinforced Concrete Frame Structures Designed Only for Gravity Loads: Part I - Design and Properties of a One-Third Scale Model Structure," by J.M. Bracci, A.M. Reinhorn and J.B. Mander, 12/1/92, (PB94-104502, A08, MF-A02).

NCEER-92-0028 "Seismic Resistance of Reinforced Concrete Frame Structures Designed Only for Gravity Loads: Part II - Experimental Performance of Subassemblages," by L.E. Aycardi, J.B. Mander and A.M. Reinhorn, 12/1/92, (PB94-104510, A08, MF-A02).

NCEER-92-0029 "Seismic Resistance of Reinforced Concrete Frame Structures Designed Only for Gravity Loads: Part III - Experimental Performance and Analytical Study of a Structural Model," by J.M. Bracci, A.M. Reinhorn and J.B. Mander, 12/1/92, (PB93-227528, A09, MF-A01).

NCEER-92-0030 "Evaluation of Seismic Retrofit of Reinforced Concrete Frame Structures: Part I - Experimental Performance of Retrofitted Subassemblages," by D. Choudhuri, J.B. Mander and A.M. Reinhorn, 12/8/92, (PB93-198307, A07, MF-A02).

NCEER-92-0031 "Evaluation of Seismic Retrofit of Reinforced Concrete Frame Structures: Part II - Experimental Performance and Analytical Study of a Retrofitted Structural Model," by J.M. Bracci, A.M. Reinhorn and J.B. Mander, 12/8/92, (PB93-198315, A09, MF-A03).

NCEER-92-0032 "Experimental and Analytical Investigation of Seismic Response of Structures with Supplemental Fluid Viscous Dampers," by M.C. Constantinou and M.D. Symans, 12/21/92, (PB93-191435).

NCEER-92-0033 "Reconnaissance Report on the Cairo, Egypt Earthquake of October 12, 1992," by M. Khater, 12/23/92, (PB93-188621).

NCEER-92-0034 "Low-Level Dynamic Characteristics of Four Tall Flat-Plate Buildings in New York City," by H. Gavin, S. Yuan, J. Grossman, E. Pekelis and K. Jacob, 12/28/92, (PB93-188217).

NCEER-93-0001 "An Experimental Study on the Seismic Performance of Brick-Infilled Steel Frames With and Without Retrofit," by J.B. Mander, B. Nair, K. Wojtkowski and J. Ma, 1/29/93, (PB93-227510, A07, MF-A02).

NCEER-93-0002 "Social Accounting for Disaster Preparedness and Recovery Planning," by S. Cole, E. Pantoja and V. Razak, 2/22/93, (PB94-142114, A12, MF-A03).

NCEER-93-0003 "Assessment of 1991 NEHRP Provisions for Nonstructural Components and Recommended Revisions," by T.T. Soong, G. Chen, Z. Wu, R-H. Zhang and M. Grigoriu, 3/1/93, (PB93-188639).

NCEER-93-0004 "Evaluation of Static and Response Spectrum Analysis Procedures of SEAOC/UBC for Seismic Isolated Structures," by C.W. Winters and M.C. Constantinou, 3/23/93, (PB93-198299).

NCEER-93-0005 "Earthquakes in the Northeast - Are We Ignoring the Hazard? A Workshop on Earthquake Science and Safety for Educators," edited by K.E.K. Ross, 4/2/93, (PB94-103066, A09, MF-A02).

NCEER-93-0006 "Inelastic Response of Reinforced Concrete Structures with Viscoelastic Braces," by R.F. Lobo, J.M. Bracci, K.L. Shen, A.M. Reinhorn and T.T. Soong, 4/5/93, (PB93-227486, A05, MF-A02).

NCEER-93-0007 "Seismic Testing of Installation Methods for Computers and Data Processing Equipment," by K. Kosar, T.T. Soong, K.L. Shen, J.A. HoLung and Y.K. Lin, 4/12/93, (PB93-198299).

NCEER-93-0008 "Retrofit of Reinforced Concrete Frames Using Added Dampers," by A. Reinhorn, M. Constantinou and C. Li, to be published.

NCEER-93-0009 "Seismic Behavior and Design Guidelines for Steel Frame Structures with Added Viscoelastic Dampers," by K.C. Chang, M.L. Lai, T.T. Soong, D.S. Hao and Y.C. Yeh, 5/1/93, (PB94-141959, A07, MF-A02).

NCEER-93-0010 "Seismic Performance of Shear-Critical Reinforced Concrete Bridge Piers," by J.B. Mander, S.M. Waheed, M.T.A. Chaudhary and S.S. Chen, 5/12/93, (PB93-227494, A08, MF-A02).

NCEER-93-0011 "3D-BASIS-TABS: Computer Program for Nonlinear Dynamic Analysis of Three Dimensional Base Isolated Structures," by S. Nagarajaiah, C. Li, A.M. Reinhorn and M.C. Constantinou, 8/2/93, (PB94-141819, A09, MF-A02).

NCEER-93-0012 "Effects of Hydrocarbon Spills from an Oil Pipeline Break on Ground Water," by O.J. Helweg and H.H.M. Hwang, 8/3/93, (PB94-141942, A06, MF-A02).

NCEER-93-0013 "Simplified Procedures for Seismic Design of Nonstructural Components and Assessment of Current Code Provisions," by M.P. Singh, L.E. Suarez, E.E. Matheu and G.O. Maldonado, 8/4/93, (PB94-141827, A09, MF-A02).

NCEER-93-0014 "An Energy Approach to Seismic Analysis and Design of Secondary Systems," by G. Chen and T.T. Soong, 8/6/93, (PB94-142767, A11, MF-A03).

NCEER-93-0015 "Proceedings from School Sites: Becoming Prepared for Earthquakes - Commemorating the Third Anniversary of the Loma Prieta Earthquake," Edited by F.E. Winslow and K.E.K. Ross, 8/16/93.

NCEER-93-0016 "Reconnaissance Report of Damage to Historic Monuments in Cairo, Egypt Following the October 12, 1992 Dahshur Earthquake," by D. Sykora, D. Look, G. Croci, E. Karaesmen and E. Karaesmen, 8/19/93, (PB94-142221, A08, MF-A02).

NCEER-93-0017 "The Island of Guam Earthquake of August 8, 1993," by S.W. Swan and S.K. Harris, 9/30/93, (PB94-141843, A04, MF-A01).

NCEER-93-0018 "Engineering Aspects of the October 12, 1992 Egyptian Earthquake," by A.W. Elgamal, M. Amer, K. Adalier and A. Abul-Fadl, 10/7/93, (PB94-141983, A05, MF-A01).

NCEER-93-0019 "Development of an Earthquake Motion Simulator and its Application in Dynamic Centrifuge Testing," by I. Krstelj, Supervised by J.H. Prevost, 10/23/93, (PB94-181773, A-10, MF-A03).

NCEER-93-0020 "NCEER-Taisei Corporation Research Program on Sliding Seismic Isolation Systems for Bridges: Experimental and Analytical Study of a Friction Pendulum System (FPS)," by M.C. Constantinou, P. Tsopelas, Y-S. Kim and S. Okamoto, 11/1/93, (PB94-142775, A08, MF-A02).

NCEER-93-0021 "Finite Element Modeling of Elastomeric Seismic Isolation Bearings," by L.J. Billings, Supervised by R. Shepherd, 11/8/93, to be published.

NCEER-93-0022 "Seismic Vulnerability of Equipment in Critical Facilities: Life-Safety and Operational Consequences," by K. Porter, G.S. Johnson, M.M. Zadeh, C. Scawthorn and S. Eder, 11/24/93, (PB94-181765, A16, MF-A03).

NCEER-93-0023 "Hokkaido Nansei-oki, Japan Earthquake of July 12, 1993, by P.I. Yanev and C.R. Scawthorn, 12/23/93, (PB94-181500, A07, MF-A01).

NCEER-94-0001 "An Evaluation of Seismic Serviceability of Water Supply Networks with Application to the San Francisco Auxiliary Water Supply System," by I. Markov, Supervised by M. Grigoriu and T. O'Rourke, 1/21/94.

NCEER-94-0002 "NCEER-Taisei Corporation Research Program on Sliding Seismic Isolation Systems for Bridges: Experimental and Analytical Study of Systems Consisting of Sliding Bearings, Rubber Restoring Force Devices and Fluid Dampers," Volumes I and II, by P. Tsopelas, S. Okamoto, M.C. Constantinou, D. Ozaki and S. Fujii, 2/4/94, (PB94-181740, A09, MF-A02 and PB94-181757, A12, MF-A03).

NCEER-94-0003 "A Markov Model for Local and Global Damage Indices in Seismic Analysis," by S. Rahman and M. Grigoriu, 2/18/94.

NCEER-94-0004 "Proceedings from the NCEER Workshop on Seismic Response of Masonry Infills," edited by D.P. Abrams, 3/1/94, (PB94-180783, A07, MF-A02).

NCEER-94-0005 "The Northridge, California Earthquake of January 17, 1994: General Reconnaissance Report," edited by J.D. Goltz, 3/11/94, (PB193943, A10, MF-A03).

NCEER-94-0006 "Seismic Energy Based Fatigue Damage Analysis of Bridge Columns: Part I - Evaluation of Seismic Capacity," by G.A. Chang and J.B. Mander, 3/14/94.

NCEER-94-0007 "Seismic Isolation of Multi-Story Frame Structures Using Spherical Sliding Isolation Systems," by T.M. Al-Hussaini, V.A. Zayas and M.C. Constantinou, 3/17/94, (PB193745, A09, MF-A02).

NCEER-94-0008 "The Northridge, California Earthquake of January 17, 1994: Performance of Highway Bridges," edited by I.G. Buckle, 3/24/94, (PB94-193851, A06, MF-A02).

NCEER-94-0009 "Proceedings of the Third U.S.-Japan Workshop on Earthquake Protective Systems for Bridges," edited by I.G. Buckle and I. Friedland, 3/31/94, (PB94-195815, A99, MF-MF).

NCEER-94-0010 "3D-BASIS-ME: Computer Program for Nonlinear Dynamic Analysis of Seismically Isolated Single and Multiple Structures and Liquid Storage Tanks," by P.C. Tsopelas, M.C. Constantinou and A.M. Reinhorn, 4/12/94.

NCEER-94-0011 "The Northridge, California Earthquake of January 17, 1994: Performance of Gas Transmission Pipelines," by T.D. O'Rourke and M.C. Palmer, 5/16/94.

NCEER-94-0012 "Feasibility Study of Replacement Procedures and Earthquake Performance Related to Gas Transmission Pipelines," by T.D. O'Rourke and M.C. Palmer, 5/25/94.

NCEER-94-0013 "Seismic Energy Based Fatigue Damage Analysis of Bridge Columns: Part II - Evaluation of Seismic Demand," by G.A. Chang and J.B. Mander, 6/1/94, to be published.

NCEER-94-0014 "NCEER-Taisei Corporation Research Program on Sliding Seismic Isolation Systems for Bridges: Experimental and Analytical Study of a System Consisting of Sliding Bearings and Fluid Restoring Force/Damping Devices," by P. Tsopelas and M.C. Constantinou, 6/13/94.

NCEER-94-0015 "Generation of Hazard-Consistent Fragility Curves for Seismic Loss Estimation Studies," by H. Hwang and J-R. Huo, 6/14/94.

NCEER-94-0016 "Seismic Study of Building Frames with Added Energy-Absorbing Devices," by W.S. Pong, C.S. Tsai and G.C. Lee, 6/20/94.

NCEER-94-0017 "Sliding Mode Control for Seismic-Excited Linear and Nonlinear Civil Engineering Structures," by J. Yang, J. Wu, A. Agrawal and Z. Li, 6/21/94.

NCEER-94-0018 "3D-BASIS-TABS Version 2.0: Computer Program for Nonlinear Dynamic Analysis of Three Dimensional Base Isolated Structures," by A.M. Reinhorn, S. Nagarajaiah, M.C. Constantinou, P. Tsopelas and R. Li, 6/22/94.

NCEER-94-0019 "Proceedings of the International Workshop on Civil Infrastructure Systems: Application of Intelligent Systems and Advanced Materials on Bridge Systems," Edited by G.C. Lee and K.C. Chang, 7/18/94, to be published.

NCEER-94-0020 "Study of Seismic Isolation Systems for Computer Floors," by V. Lambrou and M.C. Constantinou, 7/19/94.

NCEER-94-0021 "Proceedings of the U.S.-Italian Workshop on Guidelines for Seismic Evaluation and Rehabilitation of Unreinforced Masonry Buildings," Edited by D.P. Abrams and G.M. Calvi, 7/20/94.

NCEER-94-0022 "NCEER-Taisei Corporation Research Program on Sliding Seismic Isolation Systems for Bridges: Experimental and Analytical Study of a System Consisting of Lubricated PTFE Sliding Bearings and Mild Steel Dampers," by P. Tsopelas and M.C. Constantinou, 7/22/94.

NCEER-94-0023 "Development of Reliability-Based Design Criteria for Buildings Under Seismic Load," by Y.K. Wen, H. Hwang and M. Shinozuka, 8/1/94, to be published.

NCEER-94-0024 "Experimental Verification of Acceleration Feedback Control Strategies for an Active Tendon System," by S.J. Dyke, B.F. Spencer, Jr., P. Quast, M.K. Sain, D.C. Kaspari, Jr. and T.T. Soong, 8/29/94.